(12)

WT-1625(EX)
EXTRACTED VERSION

OPERATION HARDTACK—PROJECT 2.8

Fallout Measurements by Aircraft and Rocket Sampling

S. L. Whitcher
L. R. Bunney
R. R. Soule
U.S. Naval Radiological Defense Laboratory
San Francisco, CA

R. A. daRoza
Lawrence Radiation Laboratory
Livermore, CA

29 September 1961

NOTICE:
This is an extract of WT-1625, Operation HARDTACK, Project 2.8.

Approved for public release;
distribution is unlimited.

Extracted version prepared for
Director
DEFENSE NUCLEAR AGENCY
Washington, DC 20305-1000

1 September 1985

UNCLASSIFIED
SECURITY CLASSIFICATION OF THIS PAGE

AD-A225 345

REPORT DOCUMENTATION PAGE

Form Approved
OMB No. 0704-0188
Exp. Date: Jun 30, 1986

1a. REPORT SECURITY CLASSIFICATION UNCLASSIFIED	1b. RESTRICTIVE MARKINGS
2a. SECURITY CLASSIFICATION AUTHORITY N/A since Unclassified	3. DISTRIBUTION/AVAILABILITY OF REPORT Approved for public release; distribution is unlimited.
2b. DECLASSIFICATION/DOWNGRADING SCHEDULE N/A since Unclassified	
4. PERFORMING ORGANIZATION REPORT NUMBER(S)	5. MONITORING ORGANIZATION REPORT NUMBER(S) WT-1625(EX)
6a. NAME OF PERFORMING ORGANIZATION 1-Naval Radiological Defense Laboratory 6b. OFFICE SYMBOL (If applicable)	7a. NAME OF MONITORING ORGANIZATION Defense Atomic Support Agency
6c. ADDRESS (City, State, and ZIP Code) 1-San Francisco, CA	7b. ADDRESS (City, State, and ZIP Code) Washington, DC
8a. NAME OF FUNDING/SPONSORING ORGANIZATION 8b. OFFICE SYMBOL (If applicable)	9. PROCUREMENT INSTRUMENT IDENTIFICATION NUMBER
8c. ADDRESS (City, State, and ZIP Code)	10. SOURCE OF FUNDING NUMBERS PROGRAM ELEMENT NO / PROJECT NO / TASK NO. / WORK UNIT ACCESSION NO.

11. TITLE (Include Security Classification)
OPERATION HARDTACK—PROJECT 2.8
Fallout Measurements by Aircraft and Rocket Sampling, Extracted Version

12. PERSONAL AUTHOR(S)
Whitcher, S.L.; Bunney, L.R.; Soule, R.R.; and daRoza, R.A.

13a. TYPE OF REPORT	13b. TIME COVERED FROM ____ TO ____	14. DATE OF REPORT (Year, Month, Day)	15. PAGE COUNT
		610929	84

16. SUPPLEMENTARY NOTATION This report has had sensitive military information removed in order to provide an unclassified version for unlimited distribution. The work was performed by the Defense Nuclear Agency in support of the DoD Nuclear Test Personnel Review Program.

17. COSATI CODES			18. SUBJECT TERMS (Continue on reverse if necessary and identify by block number)
FIELD	GROUP	SUB-GROUP	
18	3		Hardtack
18	8		Fallout
			Aircraft Sampling

19. ABSTRACT (Continue on reverse if necessary and identify by block number)

The general objective of this project was to estimate, from analytical data on cloud samples, the relative distribution of certain radionuclides between the local and worldwide fallout formed by megaton-range detonations on land and water surfaces, with particular emphasis on the distribution of Sr^{90} and Cs^{137} between local and worldwide fallout.

Specific objectives were to: (1) obtain airborne particle and gas samples by rocket and aircraft sampling techniques; (2) determine the distribution of radionuclides between two groups of particles that differed from one another in their falling rates in air and that could be considered representative of local and worldwide fallout; (3) attempt to determine an early time distribution of radionuclides and particles between the upper and lower halves of the cloud and radially outward from the cloud axis; and (4) estimate the extent of separation of fallout from gaseous fission products by fission determinations on gas and particle samples collected coincidentally near the top of the cloud at various times following the shots.

20. DISTRIBUTION/AVAILABILITY OF ABSTRACT	21. ABSTRACT SECURITY CLASSIFICATION	
☒ UNCLASSIFIED/UNLIMITED ☐ SAME AS RPT ☐ DTIC USERS	UNCLASSIFIED	
22a. NAME OF RESPONSIBLE INDIVIDUAL Mark D. Flohr	22b. TELEPHONE (Include Area Code) (202) 325-7559	22c. OFFICE SYMBOL DNA/ISCM

DD FORM 1473, 84 MAR — 83 APR edition may be used until exhausted. All other editions are obsolete.

SECURITY CLASSIFICATION OF THIS PAGE
UNCLASSIFIED

6a. NAME OF PERFORMING ORGANIZATION (Continued)

2-Lawrence Radiation Laboratory

6c. ADDRESS (Continued)

2-Livermore, CA

FOREWORD

Classified material has been removed in order to make the information available on an unclassified, open publication basis, to any interested parties. The effort to declassify this report has been accomplished specifically to support the Department of Defense Nuclear Test Personnel Review (NTPR) Program. The objective is to facilitate studies of the low levels of radiation received by some individuals during the atmospheric nuclear test program by making as much information as possible available to all interested parties.

The material which has been deleted is either currently classified as Restricted Data or Formerly Restricted Data under the provisions of the Atomic Energy Act of 1954 (as amended), or is National Security Information, or has been determined to be critical military information which could reveal system or equipment vulnerabilities and is, therefore, not appropriate for open publication.

The Defense Nuclear Agency (DNA) believes that though all classified material has been deleted, the report accurately portrays the contents of the original. DNA also believes that the deleted material is of little or no significance to studies into the amounts, or types, of radiation received by any individuals during the atmospheric nuclear test program.

OPERATION HARDTACK—PROJECT 2.8

FALLOUT MEASUREMENTS BY AIRCRAFT AND ROCKET SAMPLING

S. L. Whitcher
L. R. Bunney
R. R. Soule, Project Officer

U. S. Naval Radiological Defense Laboratory
San Francisco 24, California

R. A. daRoza

Lawrence Radiation Laboratory
Livermore, California

Page 4 is Blank

ABSTRACT

The general objective was to estimate, from analytical data on cloud samples, the relative distribution of certain radionuclides between the local and worldwide fallout formed by megaton-range detonations on land and water surfaces, with particular emphasis on the distribution of Sr^{90} and Cs^{137} between local and worldwide fallout.

It was planned to achieve these objectives by radiochemical analyses and particle size measurements on the following types of samples: (1) particles and radioactive gases present in the upper portions of the clouds to be collected by high-flying aircraft, (2) particulate matter in the clouds to be collected along nearly vertical flight paths, at several different distances from the cloud axis, by rocket-propelled sampling devices, and (3) fallout to be collected at an altitude of 1,000 feet by low-flying aircraft.

The project participated in a 1.31-Mt shot (Koa) fired over a coral island, a shot (Walnut) fired from a barge in deep water, and a 9-Mt shot (Oak) fired over a coral reef in shallow water. The aircraft sampling program was generally successful, and fairly complete sets of both cloud and fallout samples were collected on each shot. The rocket program was unsuccessful because of a variety of equipment malfunctions.

The gas samples were analyzed for radioactive krypton, and the cloud and fallout samples were each analyzed for Sr^{90}, Cs^{137}, and several other nuclides to give information on fractionation. Fall rate and size distribution measurements were made on the particle samples from the land-surface shot. The combined analytical data was used to estimate the distribution of Sr^{90} and Cs^{137} between the local and long-range fallout.

There are no results to be reported on the spatial distribution of radioactivity in the clouds, because this part of the project was dependent on the rocket samples.

The results from Shot Koa indicate that, if the cloud layers sampled were representative of their respective clouds, about one-fifth of the Sr^{90} and about two-thirds of the Cs^{137} produced were dispersed over distances greater than 4,000 miles. Corresponding fractions for Walnut were about one-third for each of the two nuclides. For Oak, the fractions were about one-third and one-half, respectively. Radionuclide fractionation was pronounced in Koa and Oak, i.e., the radionuclide composition in the clouds varied with altitude. The local fallout was depleted, and the upper portions of the cloud were enriched in both Sr^{90} and Cs^{137}. Fractionation was much less evident in Walnut, the water-surface shot.

FOREWORD

This report presents the final results of one of the projects participating in the military-effect programs of Operation Hardtack. Overall information about this and the other military-effect projects can be obtained from ITR–1660, the "Summary Report of the Commander, Task Unit 3." This technical summary includes: (1) tables listing each detonation with its yield, type, environment, meteorological conditions, etc.; (2) maps showing shot locations; (3) discussions of results by programs; (4) summaries of objectives, procedures, results, etc., for all projects; and (5) a listing of project reports for the military-effect programs.

PREFACE

In the formulation of this project, several distinct parts were established: rocket fallout sampling, aircraft fallout sampling and sample analysis, data interpretation, and report preparation. Responsibility for the conduct of rocket sampling was assigned to the University of California Radiation Laboratory (UCRL); responsibility for the conduct of the aircraft sampling was assigned to the Los Alamos Scientific Laboratory (LASL); and responsibility for the conduct of sample analysis, report writing, and so forth, was assigned to the U.S. Naval Radiological Defense Laboratory (NRDL).

The Project Officer was supplied from the NRDL technical staff. H.F. Plank, as technical adviser to the project officer, was responsible for the conduct of the LASL portion; E.H. Fleming acted in a similar capacity for the UCRL portion; and N.E. Ballou and T. Triffet were responsible for the NRDL portion.

The authors acknowledge the vital contributions made to the project, in both the field and the laboratory, by members of the laboratories. The individuals included: G. Cowan, P. Guthals, and H. Plank, of LASL; R. Batzel, E. Fleming, R. Goeckerman, F. Momyer, W. Nervik, P. Stevenson, and K. Street of UCRL; and J. Abriam, N. Ballou, C. Carnahan, E. Freiling, M.G. Lai, D. Love, J. Mackin, M. Nuckolls, J. O'Connor, D. Sam, E. Scadden, F. Schuert, P. Strom, E.R. Tompkins, T. Triffet, H. Weiss, L. Werner and P. Zigman of NRDL.

CONTENTS

ABSTRACT ---- 5

FOREWORD ---- 6

PREFACE ---- 6

CHAPTER 1 INTRODUCTION ---- 11

1.1 Objectives ---- 11
1.2 Background and Theory ---- 11
1.2.1 Formation and Nature of Fallout Particles ---- 12
1.2.2 Cloud Development ---- 14
1.2.3 Transport and Distribution ---- 14
1.2.4 Procedures for the Determination of Fallout Partition ---- 15
1.2.5 Prior Estimates of Local Fallout ---- 16
1.2.6 Worldwide Fallout ---- 16
1.2.7 Fractionation Effects—Observations at Other Tests ---- 17
1.2.8 Fractionation Effects—Relations among the R-Values for Several Radionuclides ---- 18
1.3 Experimental Program ---- 18
1.3.1 Outline of the Program ---- 18
1.3.2 Rocket Sampling of Clouds ---- 19
1.3.3 Aircraft Sampling of Clouds ---- 20
1.3.4 Aircraft Sampling of Fallout ---- 20
1.3.5 Selection of Radionuclides ---- 21

CHAPTER 2 PROCEDURE ---- 22

2.1 Shot Participation ---- 22
2.2 Instrumentation ---- 22
2.2.1 Rocketborne Cloud Sampler ---- 22
2.2.2 Aircraftborne Samplers ---- 23
2.2.3 Possible Errors in Sampling ---- 23
2.3 Field Operations ---- 24
2.3.1 Meteorology ---- 24
2.3.2 Shot Koa ---- 24
2.3.3 Shot Walnut ---- 25
2.3.4 Shot Oak ---- 25
2.3.5 Rocket Development ---- 26
2.3.6 Aircraft Samples ---- 26
2.4 Particle Work ---- 27
2.5 Sample Analysis and Radiochemical Procedures ---- 27
2.6 Data Reduction ---- 28

CHAPTER 3 RESULTS AND DISCUSSION ---- 37

3.1 Discussion and Interpretation of the Data ---- 37
3.1.1 Cloud Data ---- 37
3.1.2 Fallout Data ---- 38

3.1.3 Combined Cloud and Fallout Data ---- 39
3.2 Data Reliability ---- 40
3.2.1 Cross-Contamination of Koa Samples ---- 40
3.2.2 Accuracy of Radiochemistry ---- 40
3.2.3 Reliability of Sampling ---- 40
3.2.4 Particle Fall Rates and Specific Activities ---- 40
3.3 Comparison with Results of Previous Tests ---- 41
3.4 Effectiveness of Instrumentation ---- 41

CHAPTER 4 CONCLUSIONS AND RECOMMENDATIONS ---- 52

4.1 Conclusions ---- 52
4.2 Recommendations ---- 53

APPENDIX A ROCKET DEVELOPMENT ---- 54

A.1 Hardtack Performance ---- 54
A.1.1 6 May Test ---- 54
A.1.2 9 May Test ---- 54
A.1.3 13 May Test ---- 54
A.1.4 26 May Test ---- 54
A.1.5 1 June Test ---- 55
A.1.6 15 June Test ---- 55
A.1.7 20 June Test ---- 55
A.1.8 23 June Test ---- 55
A.1.9 24 June Test ---- 55
A.2 Later Research ---- 56

APPENDIX B RADIOCHEMICAL DATA TABLES ---- 60

APPENDIX C PARTICLE DATA AND CHARACTERISTICS, SHOT KOA ---- 64

C.1 Size Distribution, Fall Rate, and Specific Activity Data ---- 64
C.2 Particle Characteristics ---- 64

APPENDIX D METEOROLOGICAL DATA TABLES ---- 79

APPENDIX E DERIVATION OF FORMULA FOR PERCENT MOLYBDENUM LEFT IN CLOUD ---- 83

REFERENCES ---- 85

TABLES

2.1 Device Information ---- 29
2.2 Cloud Altitude Data ---- 29
3.1 Particle-Gas Fission Ratios and R-Values for Samples from Light and Variable Wind Layer ---- 42
3.2 Percent of Nuclides Left in Cloud After 1 Day ---- 42
3.3 Sr^{90} and Cs^{137} R-Values versus Altitude ---- 43
3.4 Ratios of Mo^{99} to Kr^{85} and Kr^{88} to Kr^{85} for First 4 Hours ---- 44
3.5 Data on Nuclides in Fallout ---- 44
3.6 Enrichment Factors in Fallout ---- 45
3.7 Mo^{99} Fractions from Combined Data ---- 45
3.8 Fractions of Mo^{99}, Sr^{90}, and Cs^{137}, in Cloud ---- 46
3.9 Comparison of Airborne and Deposited Fractions ---- 46
3.10 Radiotungsten Analyses on Koa Cloud Samples ---- 47
3.11 Cloud Data, Operation Redwing ---- 47
3.12 R-Values, Operation Redwing ---- 47

B.1 Particulate Samples, Shot Koa ---------- 61
B.2 Gas Samples, Shot Koa ---------- 62
B.3 Particulate Samples, Shot Walnut ---------- 62
B.4 Gas Samples, Shot Walnut ---------- 62
B.5 Particulate Samples, Shot Oak ---------- 63
B.6 Gas Samples, Shot Oak ---------- 63
C.1 List of Samples Measured, Shot Koa ---------- 65
C.2 Particle Classification and Size Measurements, Shot Koa ---------- 65
D.1 Winds Aloft Data, 13 and 14 May 1958, Shot Koa ---------- 80
D.2 Winds Aloft Data, 15 June 1958, Shot Walnut ---------- 80
D.3 Winds Aloft Data, 29 June 1958, Shot Oak ---------- 81
D.4 Atmospheric Temperature Data, 13 May 1958, Shot Koa ---------- 81
D.5 Atmospheric Temperature Data, 15 June 1958, Shot Walnut ---------- 82
D.6 Atmospheric Temperature Data, 29 June 1958, Shot Oak ---------- 82

FIGURES

2.1 Air-Sampling rocket ---------- 30
2.2 Diffuser section of air-sampling rocket ---------- 30
2.3 Battery of rockets ready of firing ---------- 31
2.4 B-57 gross particulate sampler ---------- 31
2.5 Intake and filter section, B-57 gas sampler ---------- 32
2.6 Pumps and gas bottles, B-57 gas samplers ---------- 32
2.7 Filter foil installed on top of B-50 ---------- 33
2.8 B-50 filter screen ---------- 33
2.9 Plan view, wind velocity hodograph, Shot Koa ---------- 34
2.10 Plan view, wind velocity hodograph, Shot Walnut ---------- 35
2.11 Plan view, wind velocity hodograph, Shot Oak ---------- 36
3.1 Particle-gas fission ratios as a function of time for samples from the light and variable wind layer ---------- 48
3.2 Fraction of total Sr^{90} formed that remains aloft at various times ---------- 49
3.3 Fraction of total Cs^{137} formed that remains aloft at various times ---------- 50
3.4 Ratios of Mo^{99} to Kr^{88} for the first 4 hours as a function of altitude ---------- 51
A.1 Diagram to illustrate rocket programing ---------- 59
A.2 Schematic view of rocket nose section ---------- 59
C.1 Particle fall rate distribution curves for height line samples, Shot Koa: Samples Massive L1, L2, L3, and L4 ---------- 66
C.2 Particle fall rate distribution and specific activity curves for height line samples, Shot Koa: Sample Massive L5 ---------- 67
C.3 Particle fall rate distribution and specific activity curves for height line samples, Shot Koa: Wilson special sample ---------- 68
C.4 Particle fall rate distribution and specific activity curves for cloud samples, Shot Koa: Sample 502, coarse ---------- 69
C.5 Particle fall rate distribution and specific activity curves for cloud samples, Shot Koa: Sample 502, fine ---------- 70
C.6 Particle fall rate distribution and specific activity curves for cloud samples, Shot Koa: Sample 500, coarse ---------- 71
C.7 Particle fall rate distribution and specific activity curves for cloud samples, Shot Koa: Sample 500, fine ---------- 72
C.8 Particle fall rate distribution and specific activity curves for cloud samples, Shot Koa: Sample 977, coarse ---------- 73
C.9 Particle fall rate distribution and specific activity curves for cloud samples, Shot Koa: Sample 977, fine ---------- 74

C.10 Particle size distribution curves for heigh[illegible]amples,
Shot Koa: Samples Massive L1 and Mas[illegible]L4 ---------- 75
C.11 Particle size distribution curves for cloud [illegible]amples,
Shot Koa: Samples 502, coarse, and 502, fine ---------- 76
C.12 Particle size distribution curves for cloud samples,
Shot Koa: Samples 500, coarse, and 500 fine ---------- 77
C.13 Particle size distribution curves for cloud samples,
Shot Koa: Samples 977, coarse, and 977, fine ---------- 78

Chapter 1

INTRODUCTION

1.1 OBJECTIVES

The general objective was to estimate, from analytical data on cloud samples, the relative distribution of certain radionuclides between the local and worldwide fallout formed by megaton-range detonations on land and water surfaces, with particular emphasis on the distribution of Sr^{90} and Cs^{137} between local and worldwide fallout.

Specific objectives were to: (1) obtain airborne particle and gas samples by rocket and aircraft sampling techniques, (2) determine the distribution of radionuclides between two groups of particles that differed from one another in their falling rates in air and that could be considered representative of local and worldwide fallout, (3) attempt to determine an early time distribution of radionuclides and particles between the upper and lower halves of the cloud and radially outward from the cloud axis, and (4) estimate the extent of separation of fallout from gaseous fission products by fission determinations on gas and particle samples collected coincidentally near the top of the cloud at various times following the shots.

1.2 BACKGROUND AND THEORY

Data on the geographical distribution of fallout is particularly needed to assess the global hazards associated with the testing of nuclear devices, but the information is also important for an appraisal of the effects of nuclear weapons used in warfare.

It has been recognized since the earliest weapon tests that a substantial portion of the radionuclides formed in a nuclear detonation are deposited throughout the world, thereby becoming available for general biological assimilation. The total fallout is usually considered as being divided into two classes, designated as local and worldwide fallout. In a general way, local fallout is thought of as consisting of relatively large particles, which reach the earth's surface in a few hours, whereas worldwide fallout is composed of finely divided material, which may remain suspended in the atmosphere for months or years and be deposited at long distances from the source. A more precise differentiation is needed for specific situations—one of the most important considerations being the location of the detonation site in relation to world centers of population. For explosions at the Eniwetok Proving Ground (EPG), the boundary between the two classes has been chosen at a particle falling velocity of 3 inches per second; material settling out more slowly than this is likely to be transported beyond the ocean areas and deposited in inhabited regions, if it attains an altitude of 100,000 feet.

The ratio of local to worldwide fallout is also governed by the height attained by the nuclear cloud and the size distribution of the particles in the nuclear cloud, which act as collectors for the radioactive fission-product atoms. If many large particles with fast falling rates are present, as is the case for underground or surface shots where the fireball contacts the ground, the local fallout will be large. Local fallout can be expected to decrease as the detonation height increases and to become a negligible quantity for an airburst high above the ground.

Numerous estimates of local fallout have been prepared from previous operations, mainly from analyses of radiation intensity data obtained in aerial and surface monitoring surveys. However, the uncertainties in converting from dose rate measurements to fission products deposited per unit area are so great that the results cannot be regarded with a great deal of confidence. More reliable values are evidently needed, and in planning for Operation Hardtack, the Atomic Energy Commission examined possible ways of obtaining such information (Reference 1). After consideration of the difficulties inherent in additional refinement of surface measurement techniques, this approach was abandoned. An alternative program based on further development of existing cloud-sampling procedures was formulated (Reference 2), and this culminated in Project 2.8.

A knowledge of fallout partition and how it is influenced by shot environment may contribute to reduction in worldwide fallout during future tests and to a better understanding of the military implications of local fallout. It will also assist in extrapolation to previously untried shot conditions and yields.

1.2.1 Formation and Nature of Fallout Particles. When a surface burst is detonated, great quantities of the adjacent environment are swept up and mixed with the incandescent air in the fireball. There is sufficient thermal energy in the hot gas to completely vaporize all the material in the immediate vicinity, but the flow of heat into a massive object, such as a shot tower, shield, or coral rock, will be comparatively slow even with a high temperature gradient. Consequently, the interior portions of large structures in the neighborhood may not receive enough heat to evaporate and will be melted only. Later, when the fireball has risen above the surface, the material carried into it by the vertical air currents around ground zero will not be heated to the melting point. As a result, the fireball in its later stages will contain the environmental components as a mixture of solid particles, molten drops, and vapor. The extraneous material in the Pacific shots will consist of coral and ocean water salts plus the components of the device, shield, and tower or barge.

The preponderance of oxygen and of the environmental material in the fireball is of outstanding importance in the formation of the fallout particles. As the hot air cools through the range 3,500° to 1,000° K, it becomes saturated with respect to the vaporized constituents, and they condense out as an aggregate of liquid drops (Reference 3), most of which are very small (References 4 and 5). These are mixed with the larger drops formed by melting the environmental material and with the solid particles.

The radionuclide atoms present will collide frequently with oxygen atoms or molecules and, because the majority of them are electron donors, metallic oxide molecules will be formed, which become thermodynamically stable as the temperature falls. The oxide molecules, or free radionuclide atoms, also have frequent collisions with the liquid drops of environmental material (silica, alumina, iron oxide or calcium oxide), and these collisions may be inelastic, because in some cases the incoming molecules will be held by strong attractive forces. The radioactive oxide molecules that condense at the liquid surface will spread into the interior of the drops and become more or less uniformly distributed throughout. Later, after the liquid drops have frozen, the incoming radionuclide molecules may be held by surface forces. Because of the very low concentrations of the radionuclide oxide molecules, collisions with one another will be relatively infrequent, and it appears that the aggregation of enough molecules of this type to form a drop or crystal will be a rare event, if it occurs at all.

Another way in which the radionuclide molecules may become associated with the environmental material is by participation in the structure of the cluster embryos, which are the precursors of the liquid drops (References 4 and 6).

The isobaric radionuclide chains formed in the explosion are known to be distributed on a mass scale in a way generally similar to the products of asymmetric fission of U^{235} by thermal neutrons, but with some important differences. The experimental yield curve for slow neutron fission has a broad minimum for mass numbers approximately half that of the original nucleus and maxima on either side at mass numbers in the neighborhood of 95 and 139 (Reference 7). Comparing the chain yields for megaton-range detonations with this curve, it is noted that there

is a small drop in the peak yields accompanied by an increase in the symmetric fission probability. The same nuclide distribution might be expected in the fallout material, and this is found to be roughly true under certain conditions. In other cases, the elements formed initially partially separate with respect to one another so that samples of fallout may differ in composition among themselves and also from the distribution curve characteristic for the event.

Fractionation is a term that has been applied to this phenomenon. It is used to signify an alteration in nuclide composition of some portion of the debris that renders it nonrepresentative of the products as a whole. The R-values, which are commonly used for reporting radiochemical data on cloud and fallout samples, are useful indices of fractionation. The R-value for any nuclide is defined as the ratio of the number of atoms of this nuclide to the number of atoms of a reference substance (usually Mo^{99}) in the sample divided by the same ratio for the products of thermal neutron fission of U^{235}. Atoms that do not separate from the reference substance have R-values appropriate for the type of detonation, while enrichment or depletion are manifested by positive or negative deviations from the characteristic value.

Knowledge of the causes and mechanism of fractionation is still largely incomplete at the present time. One effect that seems to be indicated by the available data may occur in the isobaric chains near mass numbers 90 and 140, which contain rare gas nuclides as prominent chain members. Because of their half-lives and independent fission yields, they comprise a considerable fraction of the total chain yield during the period when the environmental material is condensing. If the rare gas atoms that collide with the liquid drops of environmental material are not held by strong forces, as appears probable, the particles formed at this stage will be depleted in the nuclide chains in question.

A variety of types of particles have been observed in the local fallout at previous test series (References 8 through 13). For land surface shots in the Pacific they have been mainly of three kinds: irregular grains, spherical solids, and fragile agglomerated flakes. The grains were not, in general, uniform throughout but consisted of layers or shells of calcium oxide, calcium hydroxide, and calcium carbonate formed by the decarbonation, hydration, and recarbonation processes going on in the fireball and subsequently. The majority of them were white or transparent, but some were yellow or brown. Many of the flaky aggregates were observed to disintegrate spontaneously into smaller particles within a few hours after collection. In addition to these primary types, a fourth kind was noted consisting of small black spheres of calcium iron oxide ($2CaO \cdot Fe_2O_3$). These were usually observed adhering to the surfaces of the large grains but occasionally were found isolated (Reference 12).

For detonations over ocean surfaces, the fallout collected consisted of droplets of salt slurry 50 to 300 microns in diameter. These contained about 80-percent salt, 18-percent water and 2-percent insoluble solids by volume. The major part of the radioactivity was found in the insoluble solids portion. The fallout deposited at more distant points has not been as well characterized but is believed to be composed of minute spheres formed by condensation of the environmental material from the vapor plus a very fine, unfused dust swept up into the cloud from the area around the shot point (Reference 14).

The availability of the radioactivity in the fallout for assimilation into the biosphere depends to a large extent on its solubility in aqueous or slightly acid media. Determination of the soluble fraction is therefore an important problem, and solubility studies have been reported on fallout from several of the shots during Operations Castle and Redwing. For Castle fallout, it was found that the soluble fraction was strongly dependent on the detonation environment, being around 0.05 for land shots and 0.58 to 0.73 for shots fired from a barge (Reference 15). The solubility in seawater of the fallout from the reef shot (Tewa) during Operation Redwing was investigated in two ways: by leaching of particles placed on top of a glass wool column and by centrifuging a suspension of the fallout material (Reference 13). The soluble fractions found by these two methods were 0.08 and 0.18, respectively. An ultrafiltration method was used for determining the solubility of fallout from the land shot (Zuni). About 25 percent of the total gamma activity and Np^{239} were soluble in seawater, and 5 percent of the total gamma activity was soluble in rainwater.

Recent investigations (Reference 10) have shown that biological availability is analogous to solubility in 1 N HCl. Debris from megaton-range bursts is 99 percent soluble in 1 N HCl, independent of shot environment.

1.2.2 Cloud Development. During the later stages of existence of the fireball, it is transformed into a vortex ring whose rotational velocity persists up to the maximum cloud altitude, at least for the larger shots. The vortex contains the fission products, environmental material, and bomb components that were present in the fireball and is the site where the radioactive fallout particles are generated. The cloud continues to rise until its buoyancy is reduced to zero by adiabatic expansion, entraining of cold air, and loss of energy in overcoming atmospheric drag (References 17 through 19). The diameter of the ring increases rapidly during the ascent, and the cloud spreads out laterally to a large area as its upward velocity decreases. For smaller yields the cloud stops at the tropopause or below, but for megaton-range yields the top may penetrate several thousand feet into the stratosphere. The time to maximum altitude is somewhat less than 10 minutes.

A knowledge of the distribution of activity and particles within the stabilized cloud is needed for the establishment of a rational fallout model; however, the collection of a suitable set of samples that could be used to determine these quantities experimentally presents a formidable operational problem that has not yet been solved. Several distributions have been assumed in an effort to match the fallout patterns on the ground, but it is not known how closely these models correspond to the actual structure of the cloud. Considering the method of formation, it might be anticipated that the activity would be greatest in an anchor ring centered on the axis of the cloud. Some evidence for this structure was obtained during Operation Redwing with rockets with telemetering ionization chambers (Reference 20).

1.2.3 Transport and Distribution. During the ascent of the nuclear cloud, the particles are acted on by body forces and by the vertical currents in the rising air. Some of the large particles will be heavy enough so that they will have a net downward velocity even though the cloud as a whole is moving upward. They will contribute to the fallout in the immediate vicinity of ground zero (Reference 21). During this time, volatile fission products may be fractionated from less volatile fission products by a kind of fractional distillation process within the hot cloud.

Once the upward motion has ceased, the particles in the cloud will begin to settle out at rates determined by their density, dimensions, and shapes and by the viscosity and density of the air (Reference 22). The terminal velocities for small spheres can be accurately calculated when the dependence of the drag coefficient on Reynold's number is known. Irregular or angular particles will fall more slowly than spheres of the same weight, but their velocities cannot be estimated as well because of uncertainty in the shape factors (Reference 23).

The particles that make up the local fallout follow trajectories to the surface governed by their fall rates and by the mean wind vector between their points of origin in the cloud and the ground level. Locations can be specified by reference to a surface coordinate system made up of height lines and size lines. The height lines are the loci of the points of arrival of all particles originating at given heights on the axis of the cloud. The size lines connect the arrival points of particles of the same size from different altitudes. Time and space variation of the winds will change the magnitude and direction of the mean wind vector, and vertical motions in the atmosphere will alter the falling rates of the particles. Corrections for these effects can be made when adequate meteorological data is available.

The local fallout, as defined here, will be down in 4.5 days or less, leaving aloft an aggregate of particles ranging from about 25-micron diameter down to submicron size. For small shots the majority of this will be in the troposphere, but for megaton-range yields a large proportion will be deposited in the stratosphere. Hence, in discussing worldwide fallout, it is desirable to consider it as subdivided into two classes identified as tropospheric (or intermediate) fallout and stratospheric (or delayed) fallout (Reference 24).

The material left in the troposphere is thought to remain aloft up to 40 days and to circle the earth a few times before reaching ground level. It deposits in relatively narrow bands, centered on the detonation latitude, with little evidence of diffusion across the stable air barrier located in the troposphere north of the equator. It is probably brought down largely by the scavenging effect of rainfall or other precipitation (Reference 24).

Those particles which do not fall out within the first few weeks will remain suspended in the atmosphere for a prolonged period, which is frequently described by the term "half-residence time." This is the time during which the amount of material so suspended will be depleted by one-half. The half-residence times for the stratosphere vary from 6 months to 5 years depending on the latitude and altitude of injection. Polar shots like those of the USSR in October 1958 gave about a 6-month half-residence time. The equatorial shots similar to those of Hardtack, which stabilized in the lower stratosphere, have a half-residence time of about 1 year. Clouds that stabilize in the higher stratosphere like those from Shot Bravo during Operation Castle and Shot Orange during Operation Hardtack may have a half-residence time of up to 5 years. The particle size of the material in the stratosphere is extremely small, much of it being less than 0.1 micron (Reference 25). It is distributed by the stratospheric winds in the east-west or west-east direction, and there is also thought to be a slow circulation toward the poles. Movement into the troposphere can take place by slow settling or by seasonal changes in the altitude of the tropopause. The exchange may be most prevalent at the break in the tropopause near the middle latitudes. Once transfer from the stratosphere is completed, the material will be deposited relatively quickly in the same manner as intermediate fallout (Reference 24).

1.2.4 Procedures for the Determination of Fallout Partition. The hazards of nuclear testing are associated primarily with worldwide fallout, inasmuch as local fallout can be controlled by selection of the test site and the proper winds aloft so that its area of deposition will be of minor consequence to the population of the world. However, local fallout has regional ecological consequences that are not negligible. It may spread over considerable areas of as much as a million square miles (Reference 26). Introduction of radionuclides, such as Sr^{90}, into the human environment via worldwide fallout has a potential effect on the whole population, and the significance of such nuclides has been studied in great detail (Reference 27). These studies led to the conclusion that certain radionuclide levels at the earth's surface can be tolerated and that these levels can be maintained within acceptable limits by restrictions on the rate of nuclear testing. This is based on the concept that a condition of equilibrium is reached in the stratosphere at which the rate of injection of radioactive debris will be equal to the decay plus deposition rate.

The fraction of the device appearing in global fallout has usually been estimated indirectly by measuring the fallout in the local area and subtracting from unity. The methods used for the determination of local fallout have involved measurement of gamma ray field contours or representative sampling of the material arriving at the surface of the earth (References 28 and 29). The total amount of radioactive debris in the fallout area may be calculated if the relation between dose rate and surface density of radioactive material is known. Similarly, samples representing a known area of the fallout field may be analyzed for amount of weapon debris, and all such areas summed to give the total local fallout. A combination of fallout sampling and analysis plus gamma radiation measurements has also been used (Reference 29).

These procedures are subject to a number of difficulties and uncertainties, not only with regard to making adequate sample collections and radiation field measurements but also in data interpretation. The establishment of accurate gamma contours requires an extensive and costly field program, because radiation intensity measurements must be made over areas up to tens of thousands of square miles. When the fallout is deposited mainly over the surface of the ocean, the original patterns are distorted continuously by settling of the particles and by ocean currents. The collection of samples at the earth's surface, which are truly representative of the area sampled and free from collector bias, presents problems that have not been fully solved to date.

Conversion of gamma intensity contour data to fraction of device requires knowledge of the relation of dose rate to fissions per unit area of the fallout field at 1 hour and of the gross radioactive decay rate. The decay rate varies with the device composition, environment, and fractionation in a way that is not well understood. Some uncertainty will always be present in local fallout determinations by this method when fractionation exists to an unknown degree, even though all the other quantities are known accurately.

Another procedure for the determination of fallout partition was originated by the University of California Radiation Laboratory (UCRL) based on the supposition that certain of the rare-gas fission products remain throughout their lifetimes as free atoms unattached to surfaces (Reference 29). If this is true, they will not be removed from the cloud by the falling particles and may be considered as representative of the number of fissions remaining aloft for long periods.

In the application of this method, coincident samples of gas and particles are taken by an isokinetic collector during the first few hours of existence of the clouds. The nuclear aerosol is sucked through a filter to remove the suspended material and the particle-free gas is then pumped into a storage bottle. The number of fissions in the two samples is determined by analyzing the gas for 2.8-hour Kr^{83} and the solid for a representative nuclide such as Mo^{99}.

The ratio of sample fissions calculated from a bound nuclide to those from an unattached rare-gas nuclide will give the fraction of the reference substance that is in the sampled portion of the cloud at the time of sampling. At a very early time, if no separation of gas and particles occurs, this ratio should be 1. Later it would be expected to decrease as the falling particles remove the bound fission products. Hence, if the early ratio is 1, the fraction of the material in worldwide fallout may be determined if the time is known at which particles having a falling velocity of 3 in/sec leave the sampling region, or if the ratio approaches a constant with time.

1.2.5 Prior Estimates of Local Fallout. Determinations of local fallout have been made at virtually all the nuclear tests conducted by the United States. Estimates of the fraction of the radioactivity deposited locally have been made for Operations Jangle (References 17, 24, 28, 30, and 31), Tumbler-Snapper (References 17 and 30), Upshot-Knothole (References 17 and 30), Castle (References 32 through 36), Wigwam (Reference 37), Teapot (Reference 38), and Redwing (References 24 and 39). A summary of fraction of radioactivity deposited, computed from gamma contours and/or area sampling, covered a range from 0.2 to 0.6 (References 28 and 29). Reexamination of the preliminary Redwing data (Reference 40) gave higher figures in the range 0.65 to 0.70 for barge (water-surface) shots and up to 0.85 for land-surface shots.

Results by the UCRL cloud-sampling method are also available from Operation Redwing (Reference 29) for the ground shots, Lacrosse, Mohawk, Zuni, and Tewa (part land, part water); for the water-surface shots, Huron and Navajo; and the high-altitude airburst, Shot Cherokee. In the first three events the ratio of solid-to-gas fissions was as low as 0.04. Values for Tewa were not much less than 1, but this was probably due to the low sampling altitudes relative to cloud height. The ratios for the barge shots were greater than 0.6 in all cases. For Shot Cherokee the only sample taken from the main body of the cloud gave a ratio of 1. From the assumption that the ratio at early times in all cases is 1, interpretation of these figures in terms of fallout distribution indicates that 90 to 95 percent of the activity came down locally for the land shots, 15 to 50 percent for the water shots, and essentially none for the high-altitude airburst.

On 5 to 7 March 1957, a symposium was held at The RAND Corporation to summarize and evaluate work done on fallout partition up to that time (Reference 29). The conferees concluded that the best generalization that could be reached on the basis of the data presented was an equal distribution of radioactivity between worldwide and local fallout for both land and water detonations in the megaton range.

1.2.6 Worldwide Fallout. Worldwide fallout has been of great concern to persons responsible for the conduct of nuclear tests because of the possible consequences attendant upon the global dispersal of radioactive substances (References 41 and 42). The dangers from external irradiation are generally believed to be of a minor nature because of the low levels of activity

involved, but the incorporation of nuclides into the human system through the usual biological channels introduces the possibility of long-term effects whose seriousness is not easily determined.

The local fallout from the tests at Eniwetok, as defined earlier, will settle out in the Pacific Ocean and hence will be of only indirect concern. However, the tropospheric and stratospheric fallout will come down over land areas. Careful consideration of the nuclides present in global fallout has indicated that Sr^{90} is the one to be most feared because of its possible accumulation in the human skeleton and subsequent long-term irradiation of the hematopoetic tissues (Reference 27). Consequently, a major part of the work done on worldwide fallout has been directed toward the estimation of Sr^{90}. Measurements have been made to determine the existing levels at the earth's surface, the quantity stored in the stratosphere, and the deposition rate. Samples of fallout have been taken from the soil and vegetation, by gummed tape and pot-type collectors on the ground and by air-filter samplers at the surface and in the troposphere and stratosphere (References 8, 24, 25, and 43 through 56).

Based on this work, it was estimated that in the fall of 1956 the Sr^{90} levels were about 22 mc/mi^2 in the midwestern section of the United States, 15 to 17 mc/mi^2 for similar latitudes elsewhere, and perhaps 3 to 4 mc/mi^2 for the rest of the world (References 43 and 57). The total amount in the stratospheric reservoir, if uniformly distributed over the area of the globe, would increase these figures by about 12 mc/mi^2. The deposition rate of the stored material was considered to be around 10 percent per annum. It was further estimated that, if these levels were maintained for 15 years, the concentration in the human skeleton would be about 1 percent of the maximum permissible (Reference 27).

The quantity of radioactivity in the stratospheric reservoir was estimated by summation of the contributions of all the bursts through Operation Redwing that have deposited debris in the stratosphere. The available fraction of the device was determined by subtracting the local and intermediate fallout from the total. The intermediate fallout is thought to contain 1 to 5 percent of the weapon for megaton-range detonations (References 17, 58, and 59). Determinations of this quantity by a worldwide network of stations for Shots Mike and King of Operation Ivy gave a figure of 2 percent (Reference 59).

Much information on Sr^{90} concentrations in the stratosphere has been obtained by the extensive high-altitude sampling program (HASP) of the Defense Atomic Support Agency. In addition, other data was gathered from filter samples collected on high-altitude balloons. The latter work was part of a continuing program for sampling the stratosphere along the 80th meridian (References 50 through 54, and 60).

1.2.7 Fractionation Effects — Observations at Other Tests. The occurrence of fractionation is manifested by differences in radiochemical composition, decay rate, or energy spectra among various samples of fallout taken at different times or locations in the contaminated region. Observations of some degree of fractionation have been made at many different detonations. As expected, fission product nuclides such as Sr^{89}, Sr^{90}, Cs^{137}, or Ba^{140}, which have rare-gas ancestors with half-lives of a fraction of a minute or longer, are frequently found among the products that are most severely fractionated with respect to the bulk matrix material (always a refractory substance). The location of the burst is also an important factor. Separation of the nuclides from one another appears to be most pronounced in underground or surface shots (References 61 and 62), generally less for a water surface (Reference 63) and still smaller for balloon, high tower, and air detonations (References 63 and 64). Relatively little fractionation was found in water samples for one device detonated in deep water (Reference 37).

During Operation Greenhouse, it was noted that the exponent of the beta decay curve increased from 0.95 to 1.3 with median particle size for samples taken from the clouds of Shots Dog, Easy, and Able. This indicated that the close-in particles were enriched in fast-decaying components with respect to the more distant fallout (Reference 65).

For surface shots during Operation Jangle, pronounced depletion of chains 89, 115, 111, and 140 referred to Mo^{99} was observed in comparing long-range with local fallout samples.

Chains 144 and 95 were not fractionated. Still more extensive nuclide separation was found for the underground shot, with all the above chains showing depletion in the crater area (Reference 65).

From Shot 6 of Operation Tumbler-Snapper, the gross decay exponent decreased steadily with distance up to 70 miles from ground zero (Reference 65).

Radiochemical data from Shot Bravo of Operation Castle showed fractionation of Sr^{89} and Ba^{140} with respect to Mo^{99}, but none for Ce^{144} (Reference 65).

In the land shots, Zuni and Tewa, of Operation Redwing, depletion of Cs^{137}, Sr^{90}, and Te^{132} was found in the close-in fallout with maximum factors of 100, 13, and 7 (Reference 66). These depletion factors became smaller with increasing distance from the shot point. Fractionation of the fallout from the barge shots, Flathead and Navajo, was much less, and variations in abundance were not greater than a factor of 2 (Reference 66). Analytical data on cloud samples from these four events corroborated the fallout results (References 62 and 63).

Some radiochemical analyses have been performed on particles of different sizes from certain balloon shots (Reference 64). For Shot Boltzmann of Operation Plumbbob, both the Sr^{89}/Mo^{99} and Sr^{90}/Mo^{99} ratios were a factor of 2 greater in 22-micron particles than in 137-micron particles. Enrichment of Sr^{89} in smaller particles was also found in two other balloon shots, Hood and Wilson.

1.2.8 Fractionation Effects — Relations among the R-Values for Several Radionuclides. As noted above, some scattered observations on fractionation were reported from the earlier tests, but it was not until Operation Redwing that enough data became available to investigate the separation of various nuclides from one another in any detail. During Shot Tewa of Operation Redwing, six particle samples were collected from different locations in the cloud and subsequently analyzed for about 30 nuclides. From this work, relations among the R-values for the products became apparent, which seem to be of significance for understanding the fallout formation process (Reference 67). The R-values for the substances studied (normalized to give unit intercept on the axis of ordinates) were plotted against the R-value for Eu^{156}, and a series of straight lines resulted with slopes ranging from positive to negative values. Positive slopes indicated a simultaneous enrichment of the cloud particles in europium and the product nuclide, whereas negative slopes showed that as the particles became richer in europium they were more and more depleted in the product nuclide. Products having rare-gas and alkali metal precursors had the steepest negative slopes, whereas U, Np and Pb had small negative slopes. The more refractory oxide elements — neodymium, beryllium, zirconium, and niobium — had positive slopes, and those elements such as calcium, which showed no fractionation with respected to europium, had infinite positive slopes. The results are consistent with the view that those products having rare-gas or alkali metal ancestors at the time of condensation will concentrate in the smaller particles, which have a larger surface-to-volume ratio.

Similar relationships have been found for several high-yield airbursts, using Ba^{140} as the secondary reference nuclide and Mo^{99} as the primary reference nuclide (the primary reference nuclide is the substance used as reference in calculating the R-values; the secondary reference nuclide is the substance used as abscissa in the R-value plots). In this reference system, Ag^{111}, U^{237}, Cd^{115}, Cs^{136}, Np^{239}, Y^{91}, and Sr^{89} had approximately unit positive slopes, whereas Zr^{97}, Ce^{144}, Pu^{239} and the rare earths had average negative slopes of 1.5. For these shots, there was evidence that the nuclides in the larger particles (3 to 12 μ) were fractionated, but those in particles smaller than 1 μ were not (Reference 68).

This method of data analysis has been shown to be valid regardless of the secondary reference nuclide, the primary reference nuclide, and the reference event (Reference 6).

1.3 EXPERIMENTAL PROGRAM

1.3.1 Outline of the Program. The foregoing discussion indicates that further progress in the development of a realistic fallout model will require an improved knowledge of the structure of nuclear clouds with respect to the vertical and radial distribution of particle size and

radioactivity within the mushroom. Quantitative data on the activity associated with particles in different size groups is also needed for estimation of the partition of the weapon between local and worldwide fallout. Project 2.8 was established to attempt to obtain such information from certain shots during Operation Hardtack. It was planned to explore the cloud structure by means of air sampling rockets and to use both the rocket samples and aircraft samples collected from the cloud with the UCRL coincident sampler for determination of the fallout partition. Other aircraft flying at 1,000 feet were scheduled to collect fallout samples to be used for the determination of the effect of particle size on fractionation and for corroboration of the radionuclide composition of local fallout as determined from the rocket samples. The influence of the environment on fallout partition was to be investigated by participation in events over land and water surfaces.

The basic hypothesis on which the determination of fallout partition by the measurement of relative enrichment is based is that the increase of a volatile material with respect to a refractory material, e.g., Kr^{88} with respect to Mo^{99}, occurs principally as a result of fallout of the refractory material, i.e., the only force producing separation is gravitation. If this hypothesis is correct, then the Mo^{99} left in the cloud region sampled compared to the Kr^{88} may be interpreted as the fraction of refractory debris that will be distributed in worldwide fallout. This fraction (y) is given by

$$y = \frac{[R^{99}(88)]_E}{[R^{99}(88)]_C}$$

where the subscripts E and C refer to the explosion and the cloud, respectively.

If, however, other forces operate on the particles (particularly centrifugal forces that exist during the initial phase of cloud rise or turbulent forces that may exist for several hours as a result of temperature inequalities), the possibility exists that separation of gasses or small particles from large particles may occur without requiring real fallout of refractory material. It is also possible that separation of the more volatile products from the less volatile may occur in that gas phase as a function of altitude in the cloud without requiring separation of large particles from small particles or particles from permanent gasses. If these processes occur, even a large enrichment of volatile material near the top of the cloud would not necessarily be attributable principally to fallout.

To help determine whether these alternative processes are important, it is considered necessary to obtain very early data for R-values of relatively volatile fission products in the cloud. If it can be established that the very early distribution is normal and then departs from the normal pattern at a rate consistent with the fallout interpretation, other separative forces might be considered unimportant.

1.3.2 Rocket Sampling of Clouds. Experimental determination of the distribution of activity within the cloud required the collection of a group of samples at different vertical distances along paths nearly parallel to the axis and at various radial distances. The almost-vertical flight path requirement necessitated the use of sample collectors that were propelled by rockets.

The rockets used by the project had a rather complex structure (Chapter 2), but from the standpoint of particle collection their important features were the sampling head and the electronic programer. The sampling head was designed to separate the particles collected into two groups having falling rates corresponding to local and worldwide fallout as already defined. The separation was to be attained by the action of aerodynamic forces in the sampler similar in effect to those experienced by particles falling through the atmosphere in the gravitational field of the earth. The function of the electronic programer was to open the head at predetermined positions in the flight path so that samples could be collected from different portions of the cloud.

It was planned to fire 18 rockets on each shot at about H + 10 minutes from launching platforms spaced at various distances from ground zero. Two rockets were to be fired along each trajectory, one programmed to collect a sample from the base to the top of the debris and the other to collect from the top half of the cloud only.

1.3.3 Aircraft Sampling of Clouds. A condition necessary for use of the gas-particle sampling technique for the determination of device partition is that the samples be collected from a region that is losing material by fallout but not receiving particles from any other section of the cloud. The portions of the cloud that are suitable for this type of sampling are dependent on the wind structure existing at the time of burst. For one type of structure that occurs fairly frequently at EPG, the top and bottom parts of the cloud are blown off rapidly in different directions, leaving a layer approximately 1 mile thick that experiences only light and variable winds. Hence this stratum, which is located between 50,000 and 60,000 feet, will soon be isolated from the rest of the cloud and may remain fairly stationary above ground zero for a day or more. It is called the light and variable wind layer and is satisfactory for coincident sampling, because it can not receive fallout from higher cloud levels.

In cases where the stratum is not well defined, sample collections can be made from the top of the cloud (provided it can be reached and followed by the sampling aircraft) or from a location selected to minimize the feed-in of fallout from higher altitudes.

The theory of this technique has been discussed under Section 1.2.4, and the sampling equipment is described in Chapter 2. The operation plan was to fly through the light and variable layer at several intervals between H+2 and H+24 hours with B-57D aircraft, equipped both with the coincident samplers and with wing tank particle collectors. The coincident samples were to be analyzed for Kr^{85} and Mo^{99} to determine the fallout partition (Section 1.2.4), and the wing tank samples for 10 radionuclides to investigate fractionation with particle size.

1.3.4 Aircraft Sampling of Fallout. The fallout sampling part of the program was intended to provide information supplementary to that obtained from the rocket and aircraft cloud-sampling experiments. WB-50 aircraft were scheduled to fly at an altitude of 1,000 feet and to collect fallout at various times between H+4 and H+24 hours along height lines that would correspond to the cloud level (about 55,000 feet) sampled by the B-57D's. Because the cloud is an extended source of fallout, the term "height-line sampling," as used here, signifies the sampling of a band of material centered on the geometrical height line and having a bandwidth approximately equal to the diameter of the cloud.

The wind structure described in the preceding section on the formation of the light and variable layer also leads to isolation of the 55,000-foot height line along the eastern periphery of the fallout curtain. This situation is advantageous for height-line sampling, because the aircraft may proceed westward from a position east of the fallout area and collect the first fallout encountered. The samples should contain 55,000-foot fallout alone, uncontaminated by material from the rest of the cloud.

Other types of wind structure would probably not be as favorable for height-line sampling, and the fallout collected likely would contain particles originating from different levels in the cloud.

Outward from ground zero along a height line, the particle size of the fallout decreases and the time of arrival increases. However, low-altitude sampling at a given location should provide a sample containing particles of relatively uniform size (used synonomously with falling rate). Hence, by making a series of collections along a height line at different distances from the shot point, advantage can be taken of particle size separation by natural fallout processes. The WB-50 operations were arranged to utilize this situation to obtain a set of samples suitable for an investigation of size-dependent properties.

It was planned to use the radiochemical data from these samples to corroborate the composition of local fallout as determined from the rocket experiments, to investigate fractionation with particle size, and to compare the composition of local fallout with worldwide fallout. The data can also be used for determination of device partition if the fallout is shown to be highly depleted in a particular fission product. The enrichment of the debris remaining aloft in this fission product will then be related to the fraction of the debris that has fallen out, in much the same way as has already been described for interpretation of the enrichment of a gaseous fission product in the cloud with respect to particulate debris.

1.3.5 Selection of Radionuclides. The radionuclides chosen for determination from the particle samples were those of greatest concern in worldwide fallout, namely, Sr^{90} and Cs^{137}, plus a sufficient number of others to provide basic data for further investigation of fractionation. In the latter category were Sr^{89}, Y^{91}, Mo^{99}, Cs^{136}, Ce^{144}, Eu^{156}, and U^{237}. The members of this group existed in a variety of forms, ranging from gaseous to relatively nonvolatile species, during the period of condensation from the fireball. Ca^{45} was determined in conjunction with elemental analyses for calcium and sodium to help in tracing the behavior of the environmental material that forms the major part of the fallout particles.

Analyses for I^{131}, which were tentatively planned originally, were not carried out because of the limited analytical personnel available, the uncertainties of sample collection for this nuclide, and the relatively lesser interest in its ultimate fate.

Chapter 2

PROCEDURE

2.1 SHOT PARTICIPATION

The project initially planned to participate in Shot Koa, a megaton-range land-surface burst, and Shot Walnut, a megaton-range water-surface burst. Because of apparent contamination of the Koa cloud samples by debris from Shot Fir, participation was later extended to include Shot Oak, a high-yield water-land burst fired over the lagoon reef. Device information is given in Table 2.1.

The project rockets participated during Shots Koa and Walnut and were also fired during Cactus and Yellowwood for system check and nose cone recovery practice. Aircraft were flown during Koa, Walnut, and Oak.

2.2 INSTRUMENTATION

The instrumentation for this project fell into two general classes: rocketborne and aircraft-borne cloud samplers. Two types of aircraft, B-57D's and WB-50's, were used.

2.2.1 Rocketborne Cloud Sampler. The rocket, a 20-foot unit, consisted of an air-sampling nose section, a two-stage propulsion unit and various items of auxiliary equipment (Reference 69).

Figure 2.1 shows a complete rocket on a launcher. Part A is the primary motor, Part B the sustainer motor, Part C the parachute compartment, Part D the electronics compartment, and Part E the air-sampling nose section.

The air-sampling diffuser of the nose section was 36 inches long, as measured from the intake orifice to the filter (Figure 2.2). An additional 32 inches of length behind the filter was occupied by exhaust ports and auxiliary equipment. The extreme forward part of the rocket was a conical section 5 inches long, which sealed the intake orifice prior to the time when sampling was begun. The orifice of the diffuser was 2 inches in diameter, and the filter was 8 ½ inches in diameter. An expansion from 2 to 8 ½ inches in diameter in a length of 36 inches gave an expansion angle of 10°, the maximum at which the flow would not separate from the diffuser walls. The filter was an 8-inch circle of matted cellulose fiber coated with stearic acid to help retain the particles. It was supported by a wire retaining screen. The inside wall of the diffuser was in the form of a revolved segment of a circle 250 inches in radius and was parallel to the axis of the rocket at the orifice.

Particles entering the sampling section were decelerated from about twice the sonic velocity to subsonic by passage through a shock front that formed near the throat of the diffuser. Following this, they were subjected to a force field that caused the smaller particles to be impelled toward peripheral areas of the collecting filter to a greater extent than the larger particles. The diffuser was designed to effect a resolution of particles having average settling rates greater or less than 3 in/sec in the normal atmosphere (Reference 69). A light skin was wrapped around the outside of the diffuser to fair up the external shape of the nose cone.

The propulsion section contained primary and sustainer motors, both of which were solid-fuel units about 6 inches in diameter with burning times of 6 seconds. The sustainer motor was ignited shortly before the start of sampling and provided sufficient thrust to maintain the rocket speed at about Mach 2 during passage through the cloud.

Items of auxiliary equipment included explosive squibs, electronic timing circuitry, a parachute system, a closure system for the sampling section, a radio beacon, and a dye marker. Foamed plastic inserts were fitted to the nose sections to provide additional buoyancy.

The explosive squibs were used to remove the conical nose tip, thereby opening the sampling orifice, and to jettison the propulsion unit. The electronic timing circuitry initiated the opening of the orifice, disconnected the propulsion unit, ejected the parachute, closed the sampling section and activated the radio beacon. The parachute system consisted of a pilot chute, a pilot chute shroud cutter, and the main canopy. The pilot chute was withdrawn from its compartment when the propulsion section was jettisoned but remained attached by shrouds to the nose section until the latter had slowed down to a speed that would not cause damage to the main canopy. At this time, the pilot chute shrouds were cut free from the nose cone, and the main canopy was withdrawn from the nose section by the pilot chute shrouds, which were still attached to a bag containing the large parachute. The front closure of the sampling unit, made by a ball joint, and the aft closure, consisting of a cone and O-ring seal, were closed after sampling. The radio beacon was activated at launch time so that search craft equipped with radio direction finders could locate the nose sections.

Figure 2.3 is a view of a battery of six rockets assembled for firing.

2.2.2 Aircraftborne Samplers. Three different types of equipment were utilized to obtain the samples discussed in Sections 1.3.3 and 1.3.4. Units of the kind illustrated in Figure 2.4 were used for collection of the cloud particle samples needed for the radiochemical work. These samplers were stainless steel shells of parabolic shape fitted with intake butterfly valves, which were open only during the sampling runs. They were installed at the forward end of both the right and left wing fuel tanks of the B-57D's. The particles were collected on a 24-inch-diameter filter paper, which was supported by a retaining screen located near the aft end of the unit.

The coincident sampler was designed so that both the gas and particle samples would be taken from the same volume of the cloud. Air was drawn through a desiccant section and a filter section by a circulating pump and then forced under pressure into a sample bottle. Figure 2.5 shows the intake and desiccant-filter sections, and Figure 2.6 is a photograph of the compressor pumps and gas bottles. These samplers were mounted on both sides of the B-57D fuselage toward the rear of the aircraft.

The WB-50's used for the fallout sampling were equipped with Air Force Office of Atomic Energy (AFOAT-1) standard E-1 filter assembly. Figure 2.7 is a view of a WB-50 with the filter foil installed on top, nearly over the rear scanner's position. Figure 2.8 shows the filter screen removed from the foil with a filter paper in one side. The foil was sealed by sliding doors in front and back of the filter screen except during the sampling periods.

2.2.3 Possible Errors in Sampling. Polydisperse aerosols contain an aggregate of particles whose sizes are arranged in accordance with a characteristic frequency distribution. When the aerosol is sampled under ideal conditions, the ratios of the numbers of particles in the various size ranges will be preserved unchanged in the collector. However, a departure from the initial size distribution may be encountered if the collecting device has a dimensional bias (non-isokinetic condition) or if some of the particles are broken up during the sampling operation.

Isokinetic sampling conditions will be achieved with a filtering device moving through the aerosol at subsonic speeds, if the air velocity into the intake of the filter is identical with the flow rate past the outside. As used in Project 2.8, both the wing tank and coincident samplers were close to isokinetic, because the velocity ratios were respectively 0.8 (or greater) and 0.7 to 0.9. However, in a few cases, the calculated velocity ratios for the coincident units were much less because of malfunction of the sampling equipment (Appendix B). The E-1 sampler used on the WB-50's was poor isokinetically, but this was considered to be immaterial for height line sampling where the particles in a given region should be fairly uniform in size. Samplers, such as the project rockets, which move at supersonic speed with respect to the aerosol, are expected from aerodynamic theory to be unbiased.

In the rocket samplers, some breakup of the fallout particles was thought to be likely during passage through the shock front in the diffuser throat. A series of the experiments carried out by the Naval Radiological Defense Laboratory (NRDL) in the shock tube at the University of California Engineering Experiment Station indicated that coral fallout grains were not fractured by Mach-2 shock waves (Reference 70). Impact with the filter is another possible cause of particle breakup in all the sampling devices, but little or nothing is known about this effect.

2.3 FIELD OPERATIONS

2.3.1 Meteorology. It was indicated in Section 1.3.3 that samples to be used for the determination of fallout partition by the UCRL method should be collected from the light and variable layer, if well defined, or from higher locations in the cloud. The cloud heights and wind structure in the upper atmosphere were therefore important characteristics to consider in devising operational plans. It was known from previous work that the clouds rise to a maximum altitude in the first few minutes and then settle back to a stabilized level. Based on height-yield curves derived from photographic data on earlier shots (Reference 22), it was estimated that the stabilized altitudes would be around 72,000 feet for Shots Koa and Walnut and 99,000 feet for Shot Oak (Reference 71). The altitudes observed by project aircraft were considerably lower (Reference 16). A radar record for Shot Koa indicated that the cloud rose to 72,000 feet at 5 minutes and then settled rapidly (Reference 72).

The light and variable layer existed for all the shots, being possibly best defined for Koa where it circulated over the atoll for at least a day. For Koa and Walnut, the altitude of the layer coincided quite closely with the top of the cloud, whereas for Oak it was some 20,000 feet below the top, which was blown off rapidly by the strong easterly winds. Because the B-57D samples were taken from this stratum in each case, the criterion of sampling from a region that would not be receiving fallout from any other source was easily satisfied.

Some altitude data taken in part from the wind and temperature tables in Appendix D is given in Table 2.2.

The suitability of the wind structures for fallout sampling along height lines can be most readily visualized by reference to the plan view, wind velocity hodographs at shot time (Figures 2.9 through 2.11). The hodograph for Koa shows that the winds were ideal for height line sampling, because material falling from the light and variable layer would be clearly isolated from the rest of the fallout. For Walnut, an overlap of particles originating in the cloud at 40,000 feet and at higher levels would be anticipated. For Oak, the samples collected at 1,000 feet would contain material that came from several different elevations in the cloud.

2.3.2 Shot Koa. No rocket samples were collected from Shot Koa. In preshot planning it was intended that a salvo of 18 rockets would be fired into the cloud, 6 each from Sites Wilma, Sally, and Mary. The firing line to Site Wilma failed on the day before the shot and could not be repaired before evacuation. Firing circuits to Sites Sally and Mary were intact at shot time, and a firing signal was transmitted to these sites at H+7 minutes, but no rockets fired. Evidently, the heavy current drain by several launcher orienting motors caused the main power supply voltage to drop to a point where it was insufficient to operate critical relays in the local launch-programing equipment. Thereafter, launching operations were programed so that only a single launcher motor would be operating at one time.

Five samples were taken from the cloud by B-57D aircraft at 4½, 6½, 8, 11, and 29 hours postshot time (Table B.1). A flight scheduled for 13 to 14 hours had to be canceled because of rain and atmoshperic turbulence. The first four samples were collected in about ½ hour each, and the last sample required 2½ hours. The wing tank samplers functioned on each flight, but there were no gas samples on the last three runs because of a failure of the compressor pumps on the coincident sampling units.

Samples of material falling from the 60,000-foot layer were collected at an altitude of 1,000 feet at 4, 6, 8, 10, and 12 hours after shot time by a WB-50 aircraft. The fallout was encountered on a bearing of 50° to 60° at 28, 59, 88, 109, and 131 miles from ground zero. A second

WB-50 collected one 1,000-foot sample at H+6 hours on a bearing of 20° at 42 miles from ground zero. It is thought that this material came from about 45,000 feet. A third WB-50 mission was flown at 0700 the next day to 300 miles on a bearing of 58° based on an extrapolation of the previous contacts. From there, the aircraft was directed to 225 miles, bearing 55°, then to 200 miles, bearing 40°, and finally to 400 miles, bearing 60°, but no fallout was encountered. The aircraft was released after 6 hours for a weather mission.

Shot Fir was fired at Bikini on the day preceding Koa, On the day following Koa, there was a deposition of fallout in the Eniwetok area, and in the afternoon the gamma radiation background on Site Elmer rose to 25 to 30 mr/hr. The Fallout Prediction Unit (FOPU) was not able to establish definitely the origin of this material but felt that there was some reason to think that it had come from Shot Fir. After arrival of the Koa samples at Los Alamos Scientific Laboratory (LASL), a dispatch was received in the field indicating that the cloud, and possibly the fallout samples, were heavily contaminated with Fir debris. The nature of the evidence was not known at the time.

Examination of the wind structures existing during the period of the Fir and Koa detonations indicated a possibility of some contamination of Koa fallout by Fir debris, but no mechanism was apparent that could lead to heavy contamination.

When the radiochemical data became available, it was found that all the Koa cloud samples contained some material from Fir but not enough to appreciably alter the significance of the results (Chapter 3).

2.3.3 Shot Walnut. It was planned to project a total of 10 rockets into the cloud, four each from Sites Mary and Sally and two from Site Wilma. The launchers on Mary were set for automatic positioning by blue-box signal, whereas on Sally and Wilma the quadrant elevations and azimuths were preset. After the shot, the firing circuits to Sally and Wilma were intact, but the line to Mary was open. A firing signal was sent at H+10 minutes, and the rockets on Sally and Wilma were launched, but the obscuring cloud cover prevented observation of their trajectories. The rockets on Mary did not launch, and later inspection showed that one launcher was inoperative, one elevated without rotating, and two elevated and rotated. Two nose sections from the Sally rockets were recovered by boat, but the others were lost. The closures on the nose sections recovered were intact, but water had leaked in. There was a small amount of activity in the water and on the filter, and the filter sample was returned to the NRDL for analysis. It was identified by the name Whiskey 6 (Table B.3).

Six samples were taken from the cloud at times between 1 1/2 and 28 hours postshot time (Table B.3). Both the wing tank and the coincident samplers were operative on each flight.

In preparing the height line flight program for this shot, it was intended that one WB-50 would collect 1,000-foot samples at 4, 6, 8, 10, and 12 hours with a second WB-50 standing by on the ground to take over the mission, if necessary. No sampling flight was scheduled for D+1 day. The first aircraft encountered fallout at H+4 hours on a bearing of 320° at a distance of 42 miles from surface zero, and a sample was collected. Because of deposition of damp fallout material on the nose of the aircraft, a dose of 1.5 r (read on an electronic integrating dosimeter) was accumulated at the bombardier's position during the sampling run. The dose was continuing to rise at the rate of 50 mr/min, and the radiological adviser aboard decided to discontinue the mission and return to base. The standby aircraft took off and was flown to a point on a bearing of 330° at a distance of 120 miles from surface zero. At H+8 hours, the aircraft searched on a course of 225°, but no fallout was encountered. At H+10 hours, the active fallout area was reentered at bearing 283°, 140 miles from surface zero, and a sample taken. At H+13 hours, a third sample was collected at bearing 278°, 150 miles from surface zero.

2.3.4 Shot Oak. There was no rocket participation during Shot Oak. Circumstances leading to the discontinuation of the rocket sampling portion of the project are outlined in Section 2.3.5 and Appendix A.

Five samples were taken from the cloud by B-57D aircraft between 2 and 23 hours postshot time (Tables B.5 and B.6). Both the wing tank and coincident samplers were operative on all flights.

A WB-50 aircraft collected samples from the northeastern edge of the fallout pattern at 4, 6, 8, 10, and 11½ hours after the detonation. The fallout was encountered on a bearing of 300° to 310° at 65, 93, 125, 160, and 187 miles from surface zero. The operation progressed without incident, mainly because of the experience gained by the participating personnel on the first two shots.

2.3.5 Rocket Development. The project cloud sampling rocket (Section 2.2.1) was a new one of complex design. The main motor had been used previously on the ASP (atmospheric sounding projectile) and the sustainer motor on the RTV (reentry test vehicle), but the nose section and associated equipment had not been used as a component of a rocket before. Development work on a similar sampling device had been done during Operation Plumbbob, and at the end of the operation a satisfactory unit for land recovery had evolved. After Plumbbob, Project 21.3 was set up for the purpose of developing a sea recovery version of the rocket for Operation Hardtack. When Project 2.8 was established, the existing rocket contracts were extended to provide additional units for use on this program. Because of the experimental nature of the rocket, the sponsors of this work, UCRL, assessed the probability of obtaining any rocket data as being of the order of 50 percent.

The development problems were the responsibility of Project 21.3, but a review of their work at EPG is of interest, because a large portion of Project 2.8 was directly dependent on the availability of a suitable rocketborne cloud sampler. This review will also serve to provide an explanation of the circumstances that led to the cancellation of the rocket experiment prior to Shot Oak.

Notes on the developmental rocket firings and tests are outlined in Appendix A. Details of the firings on Koa and Walnut (Sections 2.3.2 and 2.3.3) are not repeated.

2.3.6 Aircraft Samples. The B-57D aircraft used for the cloud sampling work were under the control of a LASL representative. The person responsible for these collections communicated with the aircraft by normal voice radio from the Air Operation Center on Site Fred. The fallout samples were taken by WB-50 aircraft controlled by an NRDL representative. They were directed from the Air Weather Central on Site Elmer using CW radio communication. The transmitters used by the Air Weather Central operated on a long wavelength, thereby making it possible to maintain radio contact with the WB-50's at long ranges and low altitudes.

Estimated coordinates for each sampling position on the height line flights were furnished by the FOPU. The initial 4-hour position prediction was based solely on the wind data available at shot time, but contacts made by the sampling aircraft, plus additional wind data, assisted in preparing the later estimates. Interchange of information between FOPU and the Air Weather Central was maintained throughout the sampling flights.

The FOPU predictions were generally quite accurate with respect to radial distance from ground zero, but the wind information was not always adequate to determine the angular position. For example, on Koa the estimated height line bearing was 0°, but the sampling aircraft encountered fallout at a polar angle of 50°. For Walnut the 4-hour sampling position given was quite accurate, but the later curving of the height line toward the west could not be predicted. Sampling position estimates were the best of all on Oak, and even the most distant points were predicted within 2° in bearing and 3 miles in distance.

Tables B.1 through B.6 give a summary of all the samples collected by aircraft for the project. It will be noted that in addition to the cloud samples taken from the light and variable layer, there were several samples on each shot from lower altitudes. Analytical data for these samples are included, inasmuch as it gives information on the variation of cloud composition with altitude (Appendix D).

2.4 PARTICLE WORK

Some investigation of particle characteristics was carried out for all the cloud and height line samples from Shot Koa that were large enough to work with. Approximately a quarter of each filter paper from the cloud samples and one section from the E-1 sampler were shipped to UCRL by the first flyaway following the shot. On each sample, the filter paper was removed by burning off in a stream of atomic oxygen from a gas discharge generator. The maximum temperature reached during burnoff was around 200° C. The weight of material recovered varied from 50 mg to about 4.5 gm.

At UCRL, some of the cloud samples were separated into coarse and fine fractions using a Bahco centrifuge, and fall rate distribution curves were determined for the two fractions with the micromerograph. Fall rate data was also obtained for all the height line samples, and in several cases the specific activity-fall rate curves were determined for cloud and fallout samples. In operating the micromerograph, the weight could either be recorded continuously or in 16 increments by means of individual pans on a rotating turntable.

Two of the height line samples and three cloud samples, separated into coarse and fine fractions with the Bahco, were transmitted from UCRL to NRDL for examination. The chemical substances present in these samples were identified with the polarizing microscope and by X-ray diffraction, and the particle size distributions determined by microscopic observation. A binocular microscope fitted with ocular micrometers containing a linear scale was used for the particle work. Each scale division of the micrometer represented 15 microns for the magnification used (100X). A portion of the sample was placed on a microscope slide and tapped gently to disperse the particles. Traverses were made along the slide from one extreme edge of the dispersion to the other and every particle within the micrometer scale was sized and typed. Generally, several appropriately spaced traverses were taken. The particles were sized in terms of maximum diameter and typed by the conventional classification of irregular, spherical, or agglomerated. Diameters were measured to the nearest half scale division, and particles less than a half unit were ignored. Particles adhering to each other were sized individually, if possible, or otherwise not taken into account.

Particle characteristics and fall rate and size distribution curves are given in Appendix C. No particle work was done on the samples from Oak and Walnut.

2.5 SAMPLE ANALYSIS AND RADIOCHEMICAL PROCEDURES

Radiochemical analyses were carried out on the gross particulate cloud samples from the wing tank collectors, on size-separated cloud samples, on gas-particulate samples from the coincident units, and on fallout samples. The major part of the analytical work on the cloud and fallout particle samples was done by NRDL (some by LASL), whereas the gas-particulate samples for the determination of fission ratios (Section 1.2.4) were analyzed at UCRL.

The gross particulate and fallout samples were shipped to NRDL on filter papers as collected in the field. The size-separated samples were prepared at UCRL by the oxygen burnoff and centrifuge technique described in Section 2.4, and were then transmitted to NRDL. Two particle groups were separated for the Koa and Oak samples and three for Walnut (Appendix B).

At NRDL the samples were prepared for analysis by wet ashing with fuming HNO_3 and $HClO_4$ to destroy organic material, then fuming with HF to remove silica. The HF was expelled by again fuming with $HClO_4$, and the resulting solution was transferred to a volumetric flask and diluted to volume with 4N HCl. Aliquots of the HCl solutions were taken for the analyses. A total of 1,040 radionuclide determinations and 41 elemental analyses (Section 1.3.5) were performed at NRDL using the following procedures:

1. Elemental sodium and calcium were determined with the flame photometer using a matrix very similar to the constituents of coral.
2. Mo^{99} was determined by either of two methods, depending on the age of the sample. A carrier-free anion exchange method (Reference 73) was used for fresh samples, whereas a modified precipitation method (Reference 74) was used for older samples.

3. Ba^{140}, Y^{91}, and Ce^{144} were measured by a cation exchange procedure after preliminary separation of the rare-earth group by precipitation reactions and anion exchange (Reference 75).

4. Ca^{45} was separated by a procedure using precipitation reactions. Barium and strontium were removed by precipitation as the nitrates, using fuming HNO_3 under controlled conditions. The calcium was recovered from the nitric acid solution by precipitation as the sulfate. The sulfate was then dissolved, scavenged twice with zirconium, tellurium, iron and lanthanum hydroxides, once with basic molybdenum and cadmium sulfides and once with acidic molybdenum and cadmium sulfides. Calcium was precipitated as the oxalate for mounting and counting.

5. Sr^{89} and Sr^{90} were originally separated by precipitation procedures (References 76 and 77). For the determination of Sr^{90}, the Y^{90} was allowed to grow into equilibrium, the $SrCO_3$ precipitate dissolved in HNO_3 containing Y carrier, $Y(OH)_3$ precipitated with ammonia gas, and the Sr removed as the nitrate in fuming nitric acid. The Y was precipitated as the oxalate from an acetic acid solution in the pH range 3 to 5 and ignited to the oxide for mounting and counting.

6. The cesium procedure used for the determination of Cs^{136} and Cs^{137} was a modification by the original author of a precipitation and ion exchange procedure (Reference 78). The modification consisted mainly of a cesium tetraphenyl boron precipitation in the presence of EDTA, the use of Dowex-50 in place of Duolite C-3 in the cation exchange step, and the addition of an anion exchange step.

The radiochemical work reported as being done at LASL was performed in conjunction with diagnostic measurements on the events. The methods used were those reported in the LASL compilation of radiochemical procedures (Reference 79).

The gas samples were analyzed for Kr^{85}, Kr^{85}, Kr^{85m}, and in some cases for Xe^{133}. The rare-gas radionuclides were separated from the constituents of the atmosphere and then counted in a gas counter. The separation procedure used was developed at UCRL, under the direction of Dr. Floyd Momyer. Carrier amounts of inactive krypton and xenon were added to the air sample, and the mixture was pumped through a series of traps for purification purposes. Water and carbon dioxide were condensed out in the first trap, which was filled with inert packing and held at liquid nitrogen temperature. The krypton and xenon were absorbed on activated charcoal in a second trap, also immersed in liquid nitrogen, but the major part of the nitrogen molecules, oxygen molecules and argon passed through the trap and were removed. Residual air was desorbed at −80°C and the krypton desorbed by subsequent warming to 10°C. Further purification was effected by two more absorption-desorption cycles on charcoal. After determination of the pure krypton yield, it was transferred to the gas counter.

This was the procedure used when krypton alone was the desired product; additional purification steps were necessary when xenon was also determined.

2.6 DATA REDUCTION

The analytical results were computed in the normal manner for the elemental analyses done for the project. However, the first and more time-consuming phases of the data reduction were carried out on the IBM 650 computer at UCRL. The radiochemical data was manually transcribed to IBM cards in the proper form for use by the computer, which was coded to apply a least-squares fit to the decay data and to make corrections for chemical yield, radioactive decay, and the aliquot of the sample used. The output of the computer gave the counting rates for the individual radionuclides at zero time of the shots.

Further computation was performed by hand to obtain the number of fissions, product-to-fission ratios, or R-values. Determination of the R-values, defined in Section 1.2.1, required calibration values on fission products from the thermal neutron fission of U^{235}. When these were not available, or only recently obtained, comparison analyses between LASL and NRDL provided the necessary factors.

TABLE 2.1 DEVICE INFORMATION

	Koa	Walnut	Oak
Total yield, Mt	1.31 ± 0.08		9 ± 0.6
Fission yield, Mt			
Location	Site Gene	Near Site Janet	4 miles south of Site Alice
Shot time and date	0630 M 13 May 1958	0630 M 15 June 1958	0730 M 29 June 1958
Shot type	Land-surface	Water-surface, fired from a barge in deep water	Water-land surface, fired from an LCU anchored in 15 feet of water over the lagoon reef

TABLE 2.2 CLOUD ALTITUDE DATA

Approximate altitude in feet.

	Koa	Walnut	Oak
Tropopause	57,000	54,000	50,000
Light and variable layer	60,000+	55,000	55,000
Cloud top, expected*	72,000	72,000	99,000
Cloud top, observed	65,000	61,000	70,000 to 75,000
Sampling flights	60,300	56,500	56,300

* Reference 71.

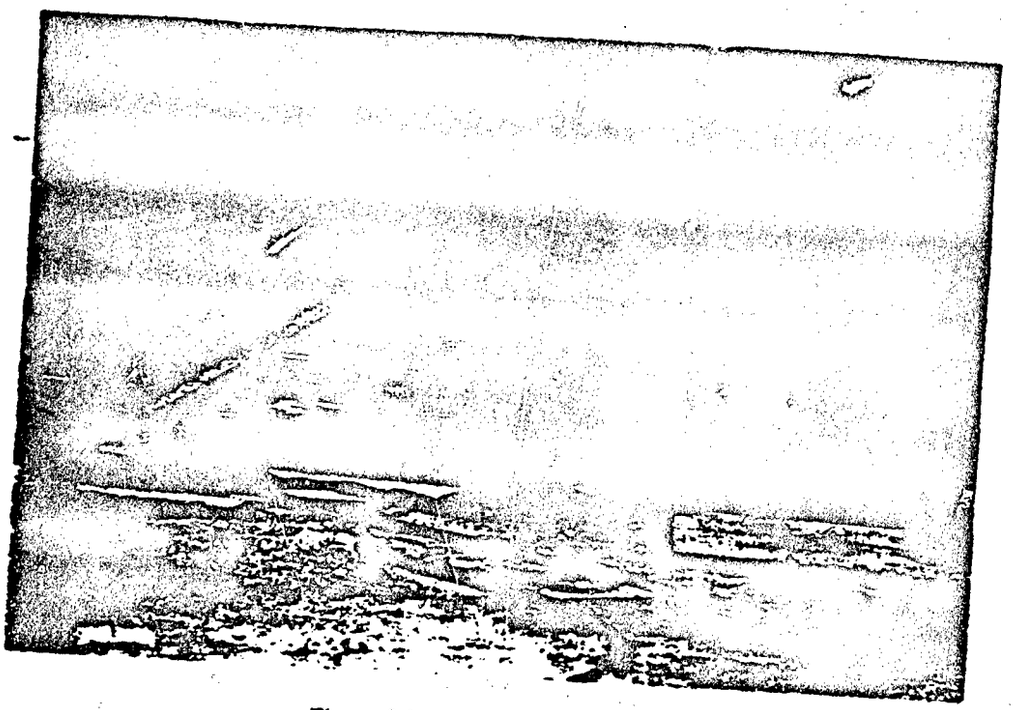

Figure 2.1 Air-sampling rocket.

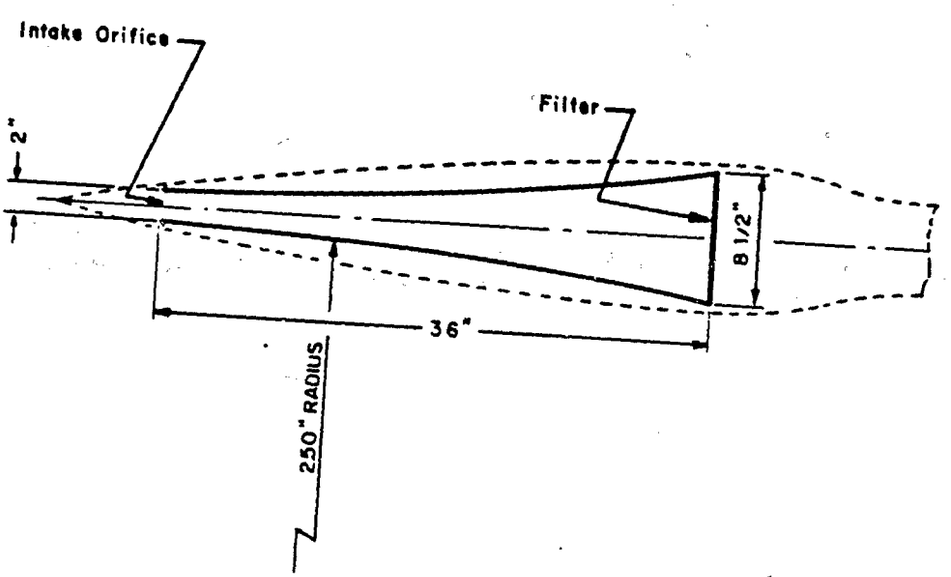

Figure 2.2 Diffuser section of air-sampling rocket.

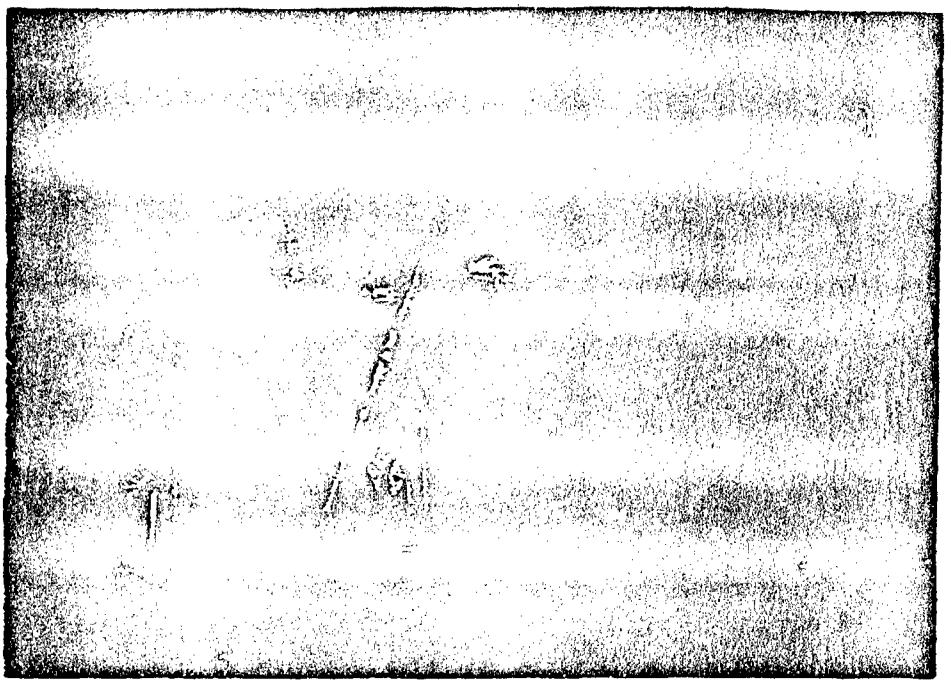

Figure 2.3 Battery of rockets ready for firing.

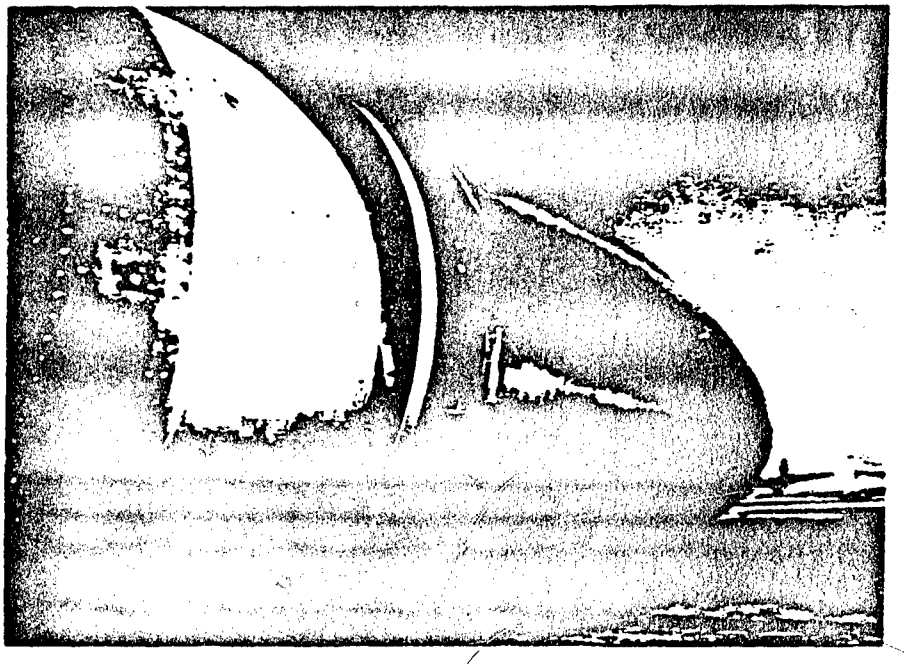

Figure 2.4 B-57 gross particulate sampler.

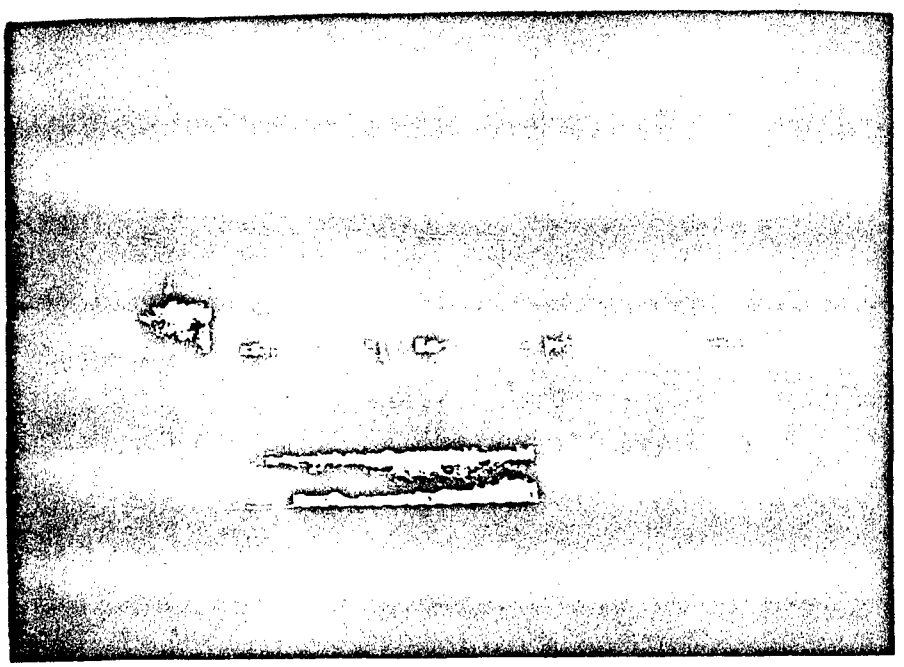

Figure 2.5 Intake and filter section, B-57 gas sampler.

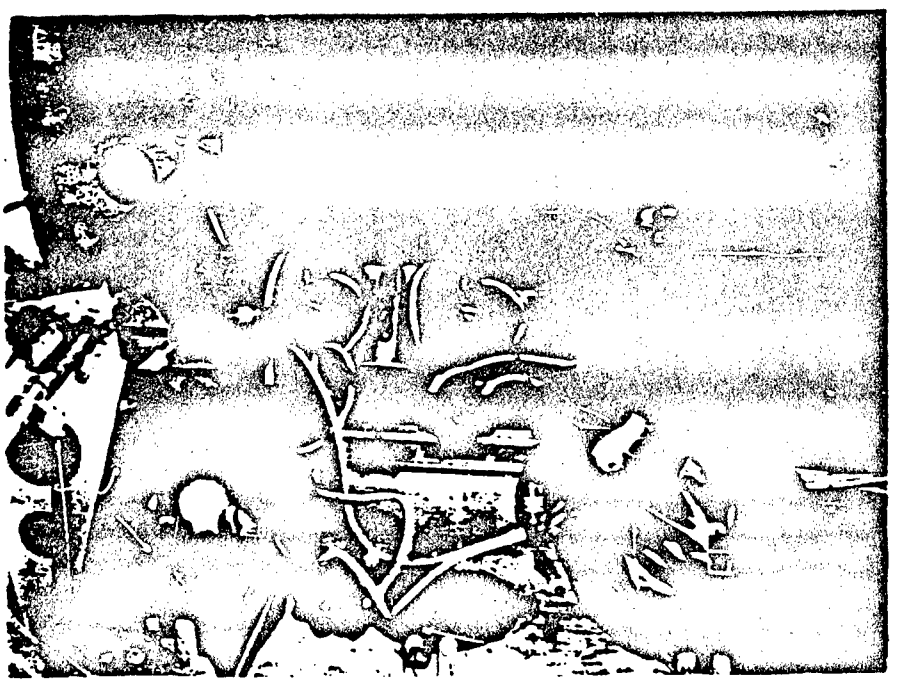

Figure 2.6 Pumps and gas bottles, B-57 gas samplers.

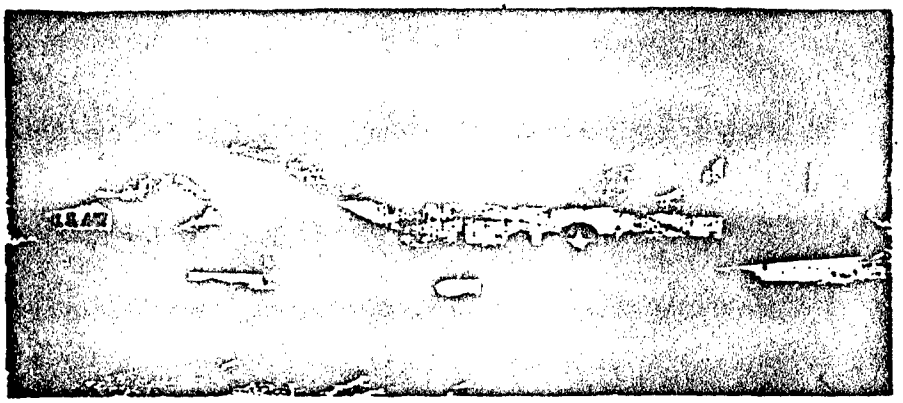

Figure 2.7 Filter foil installed on top of B-50.

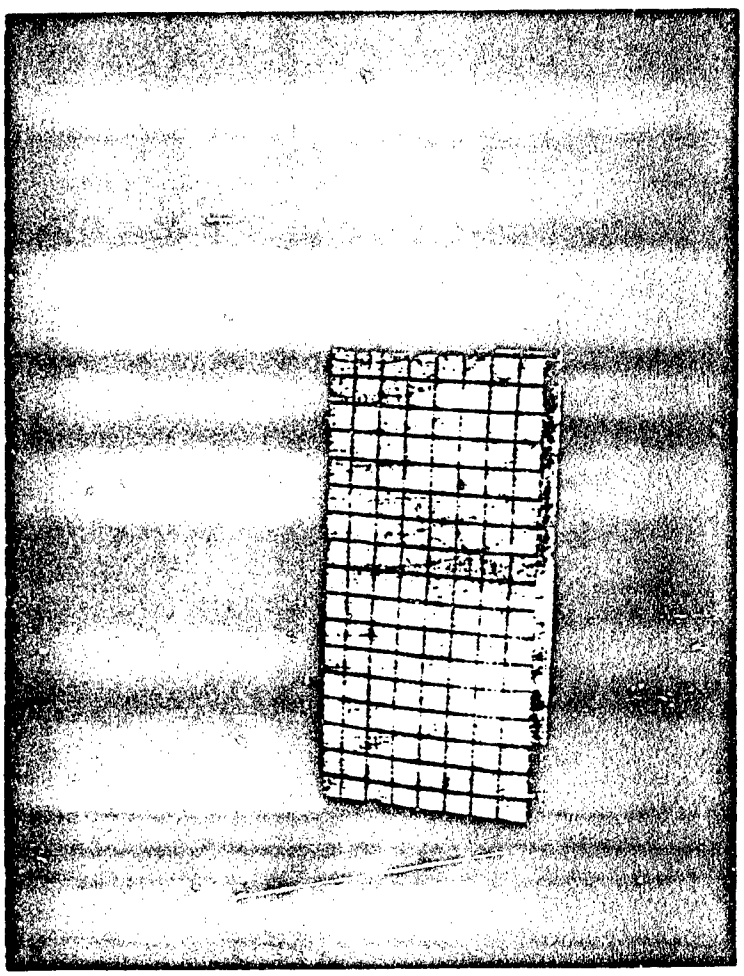

Figure 2.8 B-50 filter screen.

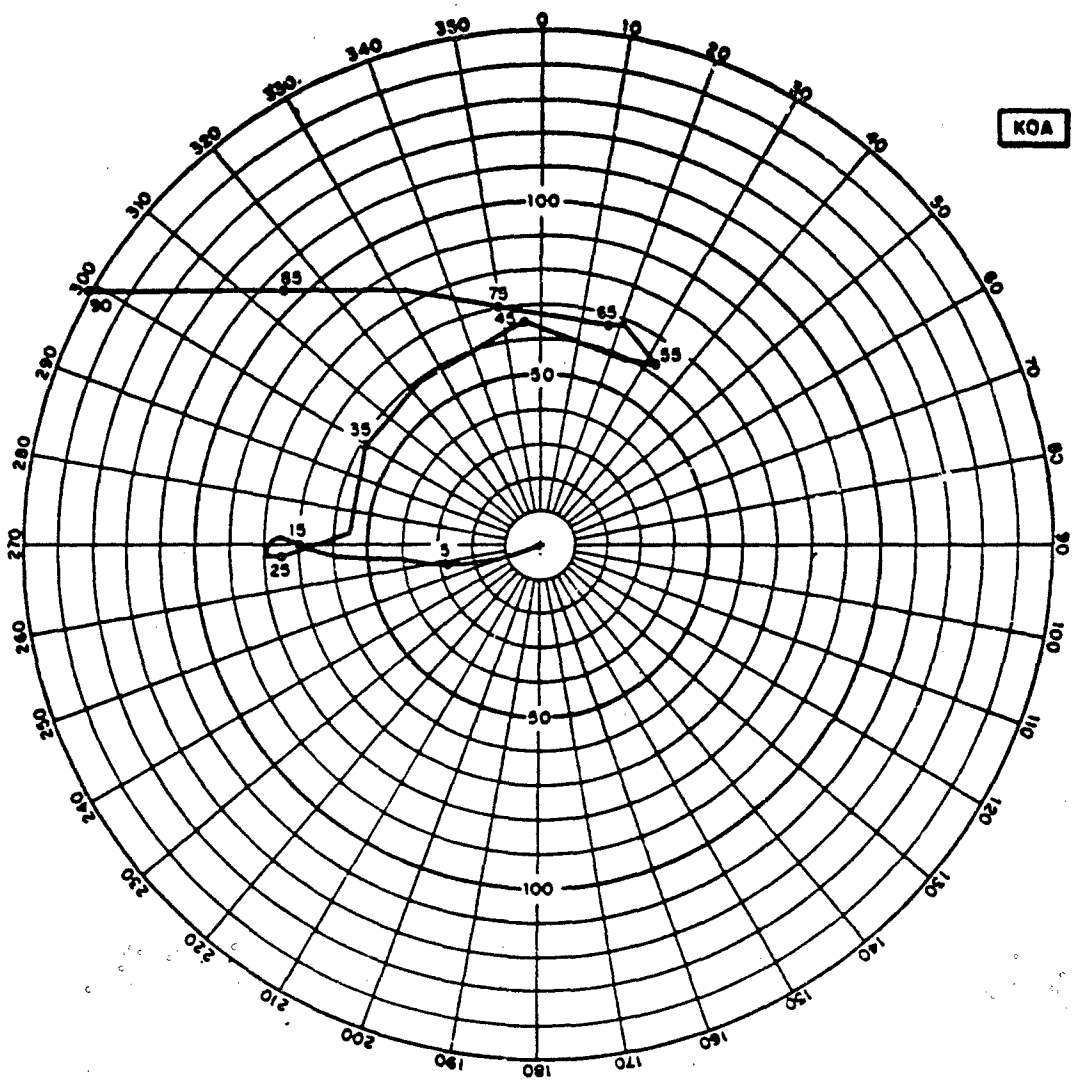

Figure 2.9 Plan view, wind velocity hodograph, Shot Koa.

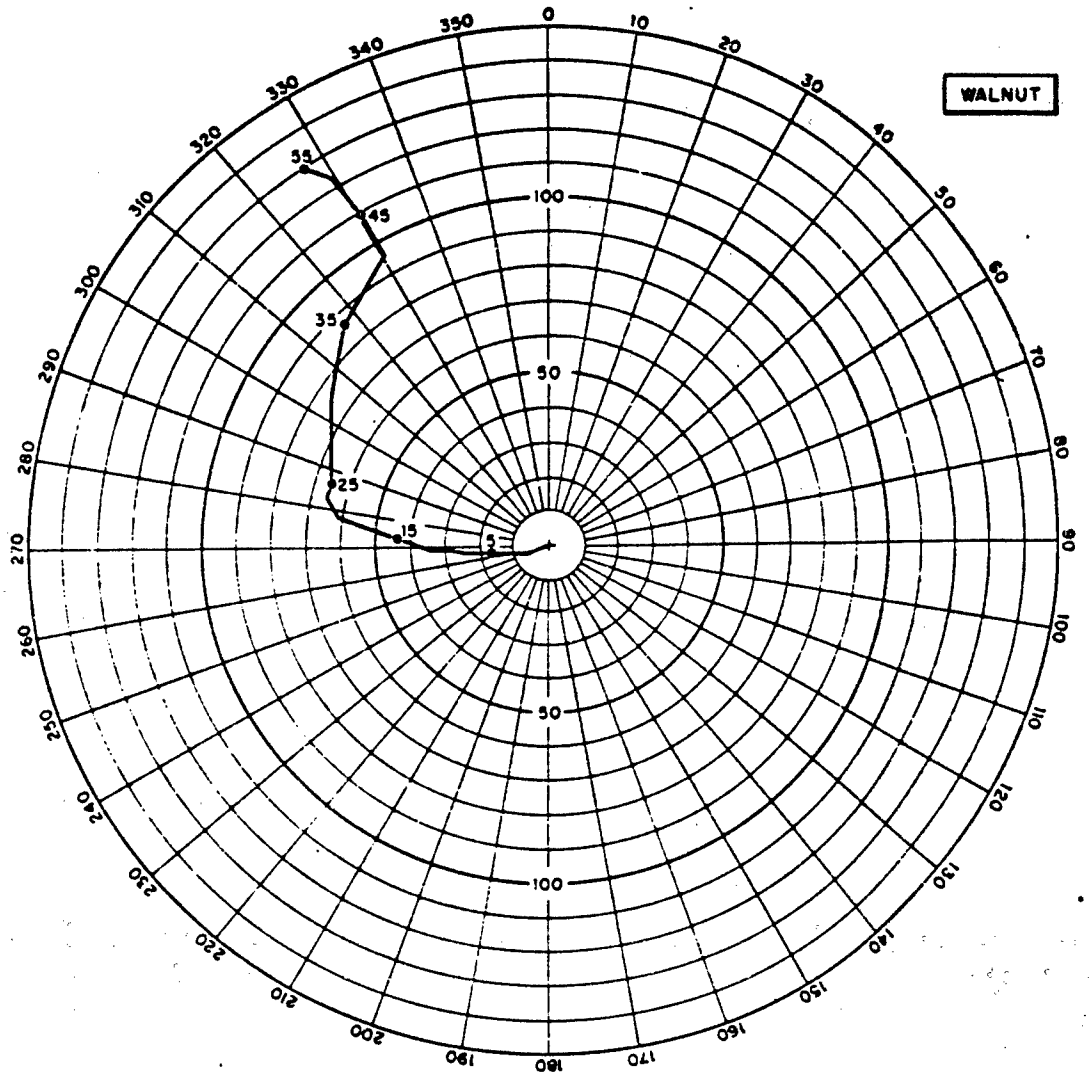

Figure 2.10 Plan view, wind velocity hodograph, Shot Walnut.

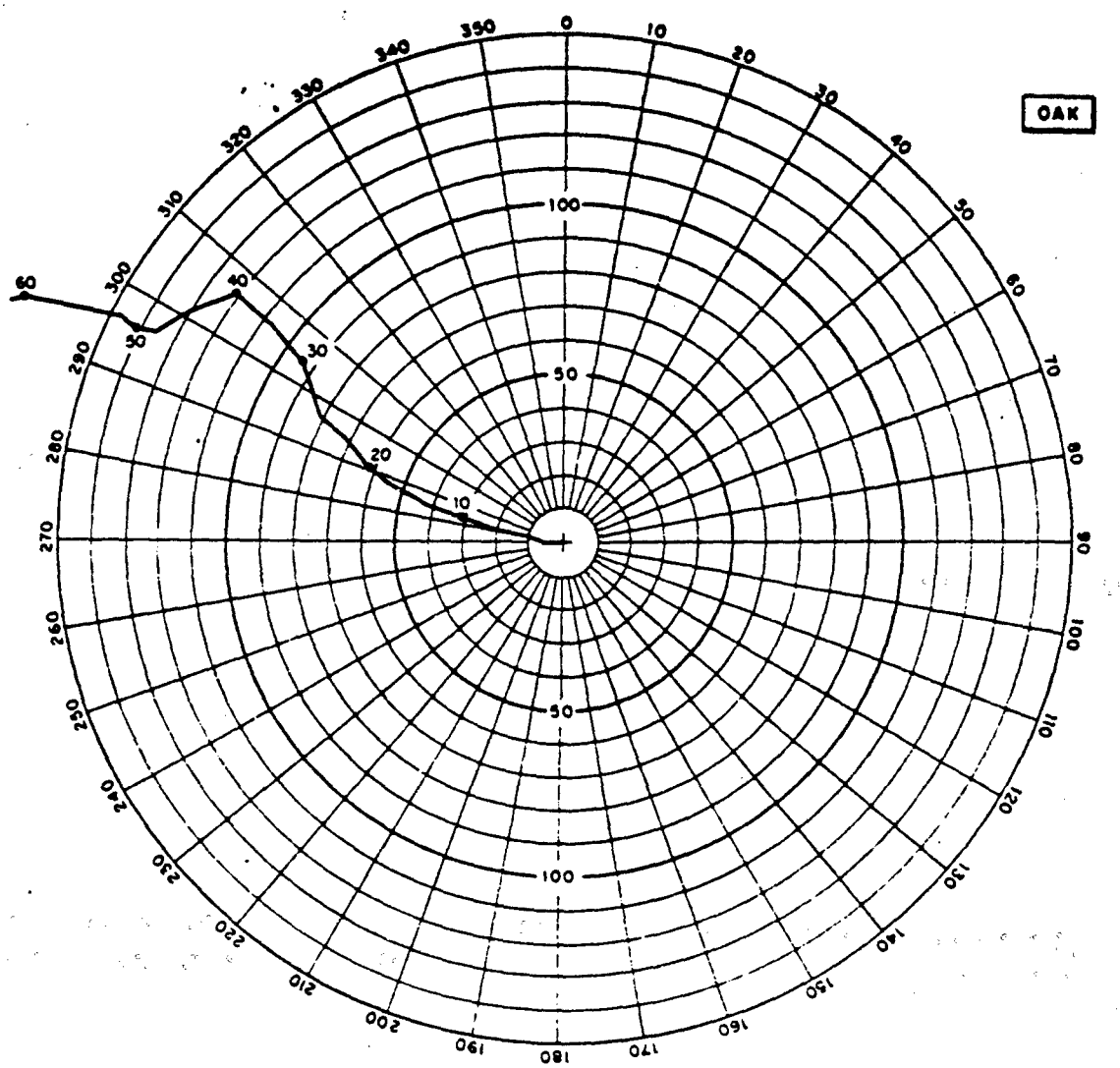

Figure 2.11 Plan view, wind velocity hodograph, Shot Oak.

Chapter 3

RESULTS AND DISCUSSION

3.1 DISCUSSION AND INTERPRETATION OF THE DATA

It is noted that the achievement of Objectives 1, 2, and 3 depended wholly or in part on the proper functioning of the rocket samplers. Because of their failure, there are no results to be reported on the vertical and radial distribution of particles in the clouds, which was Objective 3. However, Objectives 1 and 2 were partially met, and 4 was fully met by the aircraft samples.

Referring to the nuclides listed in Section 1.3.5, it is to be observed that a number of them were included for the purpose of developing a general background of information on nuclide fractionation. Although this material could serve as the basis for a separate report, it is not being considered here, because it was not a primary concern of Project 2.8. Only the data that has a bearing on the distribution of Sr^{90} and Cs^{137} in the fallout will be covered in this chapter. The radiochemical results for each of the different types of samples collected contribute something to the overall evaluation.

3.1.1 Cloud Data. For the coincident samples from the light and variable wind layer, there are two sets available for Shot Koa, five for Shot Walnut, and six for Shot Oak. The ratio of total fissions, as calculated from the sample analytical data for Mo^{99}, Kr^{85} and Kr^{88} are given in Table 3.1. Also listed are the R-values for Sr^{90} and Cs^{137} from the gross particulate samples collected from the cloud at the same time. The measured Sr^{90} and Cs^{137} R-values for the devices are listed in Tables B.1, B.3, and B.5. Subject to the assumptions inherent in the method, which include among others that the ratio of Mo^{99} to Kr^{85} in the sampled portion is representative of the entire cloud, the ratio of Mo^{99} fissions to Kr^{85} fissions gives directly that fraction of the total Mo^{99} formed in the explosion which was left in the cloud at the time of sampling (Appendix E). Multiplication of these ratios by the cloud R-values and division by the device R-values convert them to the fractions of the nuclides remaining in the clouds, e.g.,

$$\left(\frac{Mo^{99}}{Kr^{85}}\right)_{cloud} \times \frac{R(Sr^{90})_{cloud}}{R(Sr^{90})_{device}} = \text{fraction of } Sr^{90} \text{ remaining in cloud.}$$

The last step is necessary to correct for the difference in fission yields between device neutrons and thermal neutrons (Section 1.2.1). The assumption is made here that the ratios of Mo^{99} to Sr^{90} and Cs^{137} are constant throughout the cloud. The samples in the table are identified by aircraft numbers, as in Appendix B to which reference should be made for further details.

The calculated fractions of Mo^{99}, Sr^{90}, and Cs^{137} in the cloud, based on the Kr^{85} fission product ratios, are plotted as a function of time in Figures 3.1 through 3.3. Kr^{85} was not determined on the 27-hour samples from Walnut and Oak because of its low counting rate at that time. The points on the curves for these shots at 27 hours are based on the fission ratios of Mo^{99} to Kr^{85}, corrected by the ratio of Kr^{88} to Kr^{85} at 12 hours. On Koa the late-time fission ratio is extrapolated, and the Sr^{90} and Cs^{137} fractions are calculated from R-values averaged from the particulate samples taken in the main cloud on the same aircraft as the gas samples. The fractions for Oak are also from averages, here in the light and variable stratum, whereas for Walnut the stabilized condition shown in Figure 3.1 is used. Sample 980 L for Oak is not included because of the poor sampling conditions.

The fractions of these nuclides remaining in the cloud after 1 day are given in Table 3.2.

These numbers are to be interpreted as the quantity of material that does not come down in the local area. The limits assigned are derived from the variability in the data.

Of the curves for the fraction of Mo^{99} left in the clouds, the one for the water-surface burst (Shot Walnut) shows to a considerable degree the behavior anticipated when the project was planned. On the reef shot, the points appear to be fluctuating around a fraction of 0.11, whereas for the land-surface detonation, there is insufficient data to do anything but extrapolate beyond 6.5 hours. Because it is likely that the fission ratios would be around 1 initially, the curves shown for Oak and Koa may be only the relatively flat part, which appears for Walnut at a later time. This seems to be consistent with what is surmised about the cloud particle size distribution for land and water shots.

In addition to the samples from the light and variable wind layer, there were also a number of collections made on each shot at lower altitudes. Although not of direct application to the project objectives, the radiochemical data for these samples is instructive, because it shows how the nuclide composition of the particulate matter varied with altitude. Some of the samples came from the bottom portions of the clouds, but those collected at the lowest altitudes may have been below the base of the mushroom and would perhaps be considered as fallout. Table 3.3 gives a summary of the Sr^{90} and Cs^{137} R-values for the three shots as related to altitude and time of collection. The R-values for the samples marked with an asterisk were calculated as gross figures from the R-values for the size-separated fractions. For the land-surface shot, the R-values showed a general increase with altitude, attaining values at 60,000 feet which were 10 (Sr^{90}) to 40 (Cs^{137}) times those expected for the detonation. The water-surface shot R-values were relatively insensitive to altitude, and the enrichment factor was not more than 2 for either nuclide. Samples collected below 45,000 feet may be from the fallout.

On the reef shot, it appears that the sampling aircraft were just entering the base of the cloud at the 55,000-foot level, because there was a sudden jump in the R-values at this point. The material collected at lower altitudes was depleted in both Sr^{90} and Cs^{137} and was not greatly different in composition from the fallout at 1,000 feet. It is also noted that the enrichment factors for both nuclides went through a maximum with time for the samples from the light and variable stratum. Several conjectures might be offered in explanation of this unexpected behavior with time. One of these is that some sampling might have been done at the lower boundary of the light and variable stratum where some of the particles collected had fallen below the stratum where the rare gases were present. This could also be offered as a possible explanation for the late time rise in the ratio of molybdenum to krypton in Shot Oak.

Somewhat similar data for the ratios of Mo^{99} to Kr^{85} and Kr^{85} to Kr^{85} for the first 4 hours following detonation is given in Table 3.4. The ratios of Mo^{99} to Kr^{85} are also shown graphically in Figure 3.4. At the lower altitudes, the Mo^{99} was enriched and the Kr^{85} depleted with respect to Kr^{85}.

3.1.2 Fallout Data. The radiochemical data on the fallout samples may be used to obtain results for the distribution of Sr^{90} and Cs^{137}, which are complementary to those found from the cloud analyses. The fraction of the total Mo^{99} formed in the explosion, which has left the cloud, is found by difference from the numbers given in Table 3.2. Multiplication of these figures by the Sr^{90} and Cs^{137} R-values for the fallout and division by the device R-values convert them to fractions of the two nuclides in the fallout. Table 3.5 lists results obtained in this way based on the averaged composition for the fallout.

All the fallout samples from the land and reef shots show depletion of both Sr^{90} and Cs^{137} as compared to the detonation yields. This is most pronounced in the earliest samples. Material coming down at times later than 4 hours for the land shot and 6 hours for the reef shot is quite uniform in composition and exhibits little evidence of fall rate-dependent fractionation.

The 4-hour fallout from the water-surface shot is depleted in both Sr^{90} and Cs^{137}, but the 10- and 13-hour samples show an enrichment. The two latter samples have nearly the same composition. The failure of the 6- and 8-hour flight missions makes the data rather scanty in this case.

These effects are brought out clearly by the listings in Table 3.6.

3.1.3 Combined Cloud and Fallout Data. If alternative processes to fallout are not important, fission products with volatile predecessors can be as useful as gaseous fission products for measuring the extent of fallout. Because it is incorrect to assume that the content of a volatile fission product in fallout is zero, the R-value in fallout must be measured.

Then:

$$y = \frac{[R^{99}(Y)]_F - [R^{99}(Y)]_{FO}}{[R^{99}(Y)]_C - [R^{99}(Y)]_{FO}}$$

This formula can be derived by algebraic operations from the definitions of the R-values (Appendix E). If, despite the fact that it is incorrect, the R-value for Y in fallout is assumed to be zero, the above equation reduces to the expression for a gas, and y becomes the upper limiting value for the fraction of Mo^{99} (or refractory debris) left in the region sampled.

Fission products such as Sr^{89}, Cs^{137}, and to a somewhat lesser extent Sr^{90} appear to behave very much like Kr^{85} in Shots Koa, Walnut, and Oak and may be used to estimate fractional fallout of refractory debris or upper limits to the fraction remaining aloft.

The disadvantage of using Sr^{89} or Cs^{137} for this purpose is that R-values must be measured in fallout and are necessarily constant. The chief advantage is that the analyses may be extended to longer times, because the half-lives are long and a sufficient sample may be obtained by simply filtering more air.

Values have been calculated in the above manner and are given in Table 3.7.

In calculating the values for fraction of Mo^{99} in the cloud, the data must be picked from Tables B.1 through B.6 with care. Only cloud samples taken in the light and variable layers are used, and these are matched on an individual basis with height line samples taken at a later time, wherever possible.

The half-lives of the noble-gas precursors of the nuclides used above are: Cs^{137}, 3.8 minutes; Sr^{89}, 3.2 minutes; Sr^{90}, 33 seconds; Y^{91}, 10 seconds; Ce^{141}, ~1 second; Cs^{138}, none. The fraction of Mo^{99} remaining in the cloud as calculated by each of these nuclides generally increases inversely as the half-life of the nuclide's noble-gas precursor. If it is assumed that the R-values in the height line samples are representative of the material that has fallen from the light and variable layer, the results of the calculation of the fraction of Mo^{99} remaining in the cloud may be interpreted to mean that the original R-values in the light and variable layer were not representative of the device. This is due to the fact that if the original R-values were representative and if the average R-value is used for all the fallout, the fraction of Mo^{99} calculated to remain in the cloud (y) should be the same no matter which radionuclide is used in the calculation.

However, the same experimental data could have been obtained if the sampled region originally had representative R-values, provided the R-values from the height line samples were not representative of all the fallout from the light and variable layer. The assumption here is that the unsampled portion of the fallout, i.e., the portion between 1,000 and 50,000 feet, had R-values between those found in the fallout and in the cloud. The explanation of such behavior might be that nuclides that condense shortly after the explosion occur in larger particles than nuclides that condense later, e.g., those with noble-gas precursors. The larger particles fall faster, are depleted in the cloud samples, and are enriched in the height line samples. The opposite situation would exist for small particles. The actual explanation of the variation in the calculated fraction of Mo^{99} remaining in the cloud may well be a combination of the two given above.

Small variations, such as those due to experimental uncertainties in the R-values, have large effects on the calculation when the differences between the device R-values and those observed in the cloud and fallout are small. The Mo^{99} fractions calculated from Cs^{137} and Sr^{89}, the two nuclides having the longest-lived noble-gas precursors and showing the greatest fractionation, are given in Table 3.8. They are compared to the Mo^{99} fractions calculated from Kr^{85}.

The sum of the nuclide fractions from the cloud and fallout should be 1 in each case, provided that the R-values used are representative of the cloud and fallout as a whole. This seems to be likely for the fallout where the R-values change only relatively slightly with time but more doubtful in the cloud as a result of the scatter of the analytical results. Table 3.9 gives a comparison between the deposited fractions (from Table 3.5) and airborne fractions (from Tables 3.2 and 3.8). The agreement is generally as good as could be expected, considering the nature of the data.

In Shot Koa, the gas sample data is very meager. The gas and particulate samples are not matched well in time and altitude. It is believed that the Mo^{99} fractions, and consequently the Sr^{89} and Cs^{137} fractions, as calculated from the Sr^{89} and Cs^{137} in the cloud and fallout are better values than those calculated from Kr^{85}.

For Shot Walnut, the late fallout results are limited and not interpretable in obtaining the fraction airborne; hence, only the gas sample data has been used. This fallout data also leads to unreasonably large fractions deposited.

In Shot Oak, both fallout and gas samples gave similar values for the fractions deposited and airborne. The averages have been used.

3.2 DATA RELIABILITY

3.2.1 Cross-Contamination of Koa Samples. As discussed in Section 2.3.2, a preliminary examination of the samples from Shot Koa, shortly after their receipt at LASL, indicated that they might be badly contaminated with debris from Shot Fir. If this were the case, the fission ratios from the Koa cloud data could not be used for the determination of fallout partition, because they would not be representative of the detonation. To investigate the extent of cross-contamination, the Koa samples were analyzed

Table 3.10 gives a summary of the results of this work.

It is evident that the Koa samples contained at most a little over 1 percent of material from the Fir cloud, and generally much less. Hence, the quantities of molybdenum and krypton introduced into the Koa cloud from Fir were small enough so that they would have a negligible effect on the fission ratios.

3.2.2 Accuracy of Radiochemistry. Radionuclide analyses on the particle samples were accurate to 5 percent on a relative basis, and the gas counting had an accuracy better than 10 percent.

3.2.3 Reliability of Sampling. Certain points on the curves of Figure 3.1 are to be attributed somewhat less significance than the others because of uncertainties regarding the samples. On Koa, the fission ratio for Sample 981 R may be off by a factor of 2 as a result of the small sample size and high counter background from fallout, which would decrease the counting accuracy. On Walnut, Sample 978 L (27.5 hour) the probe velocity was low, and Kr^{85} only was determined. (Probe velocity refers to the pumping speed in the gas particle coincident sampler.) Sample 980 L for Oak has been disregarded because of the very low probe velocity, which would tend to make the Mo^{99} to Kr^{85} ratio too high.

3.2.4 Particle Fall Rates and Specific Activities. The particle size distributions (and hence the specific activity as a function of particle size) could have been altered in a number of ways before the fall rate studies were made. Among these are breakup of particles by impaction on the filter, loss of fine particles in handling, spontaneous breakup of particles in the fallout process itself due to atmospheric moisture (see Appendix C regarding the behavior of particles in liquids), and several other possible means of alteration.

It is possible to calculate what fall rate a particle would need to fall 59,000 feet in four hours, i.e., to be collected in Koa Massive L1. This fall rate is 125 cm/sec. The diameter of a

spherical particle with a fall rate of 125 cm/sec is about 120 microns. Figure C.1 gives essentially no particles with fall rates as great as 125 cm/sec. However, Figure C.10 gives about 30 percent of the particles with diameters greater than 120 microns. This disagreement is possibly due to the effect of the micromerograph on weakly constructed particles, and the effect may not be uniform on all types of particles.

The above example illustrates the inconsistencies in the data and points out the need for caution in making interpretations based on them.

3.3 COMPARISON WITH RESULTS OF PREVIOUS TESTS

Shots were fired during Operation Redwing under conditions similar to those of the Hardtack series, and some results are available from published reports, which may be used for comparison purposes. Results on the ratios of Mo^{99} to Kr^{85} and on the Sr^{90} R-values as a function of altitude in the cloud for the first 4 hours are reproduced in Table 3.11 from Reference 29. It is noted that for the land and reef shots the Sr^{90} R-values increase and the Mo^{99} to Kr^{85} ratios decrease in a manner generally comparable to the similar Hardtack events. On the water shots, the Sr^{90} R-values are nearly constant with altitude, as with Walnut, but the ratios of Mo^{99} to Kr^{85} are not comparable.

The fallout R-values for the Hardtack shots are generally not inconsistent with those arrived at for the Redwing shots by Project 2.63. The latter gave radionuclide compositions which generated computed decay curves in good agreement with those actually measured on several different types of instruments. The R-values from Redwing are listed in Table 3.12. Fallout R-values for Sr^{90} amd Cs^{137} collected in different locations from Tewa and Zuni (land and reef shots) showed variations of up to an order of magnitude. The fallout collections from those stations closest to the zero point were most depleted in these nuclides. Flathead and Navajo (water surface shots) gave much less change in the R-values with distance from the zero point—at most a factor of 2.

3.4 EFFECTIVENESS OF INSTRUMENTATION

The aircraftborne sampling equipment performed in a generally satisfactory manner throughout the entire operation with the exception of some malfunctioning of the gas compressor pumps after the first shot. This was due primarily to the shortage of time for checkout prior to actual operational use. As the participating personnel gained experience, communications improved and the sampling flights progressed more smoothly. Each of the three types of aircraft sampling equipment is considered to be well suited for its intended use.

Difficulties experienced with the rocket samplers are fully described in Chapter 2 and Appendix A.

TABLE 3.2 PERCENT OF NUCLIDES LEFT IN CLOUD AFTER 1 DAY

Shot	Mo^{99}	Sr^{89}	Cs^{137}
Koa	2 ± 2	11 ± 11	36 ± 36
Walnut	20 ± 5	30 ± 8	36 ± 9
Oak	11 ± 5	38 ± 15	51 ± 25

pages 43 and 44 are deleted

TABLE 3.6 ENRICHMENT FACTORS IN FALLOUT

Sample Number	Sampling Time hr	R_1	R_2
Shot Koa:			
Massive L1	4	0.66	0.34
Massive R2	6	0.73	0.50
Massive R3	8	0.73	0.50
Massive R4	10	0.73	0.48
Massive R5	12	0.75	0.46
Wilson Sp. R	6	0.74	0.45
Shot Walnut:			
Massive 1 R1	4	0.70	0.58
Massive 2 R1	10	1.28	1.46
Massive 2 R2	13	1.16	1.46
Shot Oak:			
Massive R1	4	0.76	0.19
Massive R2	6	0.64	0.23
Massive R3	8	0.82	0.56
Massive R4	10	0.82	0.58
Massive R5	12	0.78	0.55

$$R_1 = \left[R^{90}(90)\right]_{FO} : \left[R^{90}(90)\right]_E$$

$$= \frac{\text{Ratio of } Sr^{90} \text{ to } Mo^{99} \text{ observed in fallout}}{\text{Ratio of } Sr^{90} \text{ to } Mo^{99} \text{ expected from the device}}$$

$$R_2 = \left[R^{90}(137)\right]_{FO} : \left[R^{90}(137)\right]_E$$

$$= \frac{\text{Ratio of } Cs^{137} \text{ to } Mo^{99} \text{ observed in fallout}}{\text{Ratio of } Cs^{137} \text{ to } Mo^{99} \text{ expected from the device}}$$

TABLE 3.7 Mo^{99} FRACTIONS FROM COMBINED DATA

	Time of Collection (Hours)		Fraction of Mo^{99} in Cloud Calculated From:					
	Cloud	Fallout	Cs^{137}	Sr^{89}	Sr^{90}	Y^{91}	Ce^{144}	Cs^{136}
Koa	4.5	6	0.015	0.024	0.039	0.26	0.33	0.24
	7.3	8	0.012	0.018	0.026	0.20	0.33	0.17
	8	10	0.015	0.021	0.033	0.28	0.36	0.22
	11	12	0.011	0.017	0.02[illegible]	0.22	0.55	0.19
Walnut	1.6	4	0.34	0.36	0.42	0.90	1.0	0.68
	3.4	4	0.53	0.56	0.55	1.04	1.0	0.65
	6.8	13	—	—	—	0.93	1.1	0.51
Oak	2.1	4	0.22	0.18	0.12	0.43	0.61	0.14
	2.1	6	0.21	0.15	0.16	0.51	0.44	0.42
	6	8	0.06	0.05	0.04	0.17	0.24	0.07
	6	10	0.06	0.06	0.04	0.20	0.19	0.06

TABLE 3.9 COMPARISON OF AIRBORNE AND DEPOSITED FRACTIONS

Shot	Sr^{89}			Cs^{137}		
	Fraction Deposited	Fraction Airborne	Total	Fraction Deposited	Fraction Airborne	Total
Koa	0.71	0.18	0.89	0.44	0.67	1.11
Walnut	0.83	0.30	1.13	0.95	0.36	1.31
Oak	0.68	0.35	1.03	0.37	0.48	0.86

TABLE 3.11 CLOUD DATA, OPERATION REDWING

This information is taken from Reference 29.

Altitude	$R^{90}(90)$	$Mo^{99}:Kr^{88}$
Land-Surface Shot (Zuni):		
41,000	0.51	50.0
51,000	0.64	2.5
55,000	2.0	0.11
Reef Shot (Tewa):		
32,000	0.44	16.6
48,000	0.47	14.3
51,000	0.86	0.77
53,000	1.5	0.59
Water-Surface Shot (Navajo):		
39,000	0.75	14.3
43,000	0.64	~100*
43,000	0.64	0.97†
46,000	0.68	~100*
50,000	—	0.54

* Note similarity to ratios for Shots Koa and Oak at lot altitude.

† $Mo^{99}:Kr^{85m}$.

TABLE 3.12 R-VALUES, OPERATION REDWING

Shot	$R^{90}(90)$		$R^{90}(137)$	
	Cloud	Average Fallout	Cloud	Average Fallout
Flathead	~1.1	0.34	~2.3	0.32
Navajo	–	0.8	–	0.7
Tewa	~1.0	0.29	~1.5	0.14
Zuni	~2.0	0.25	~2.8	0.08

page 48 is blanked

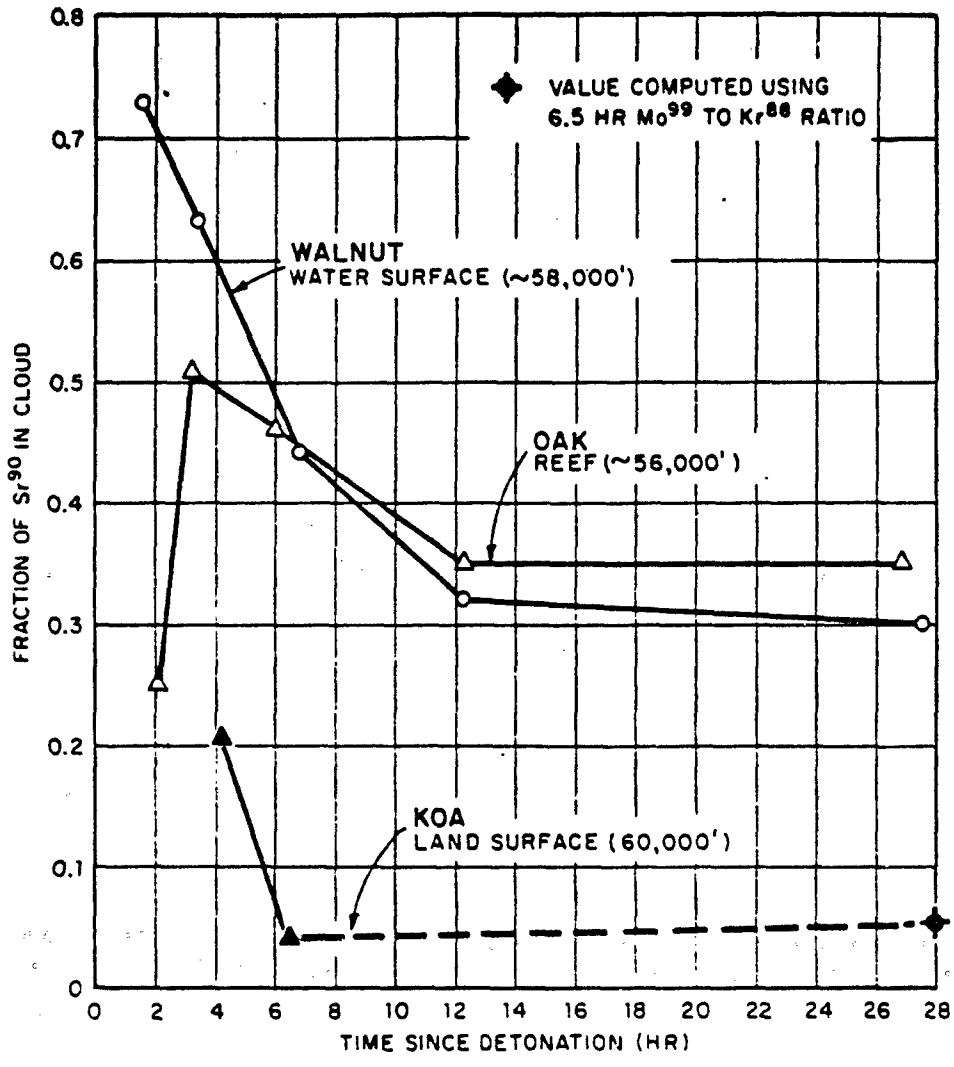

Figure 3.2 Fraction of total Sr^{90} formed that remains aloft at various times.

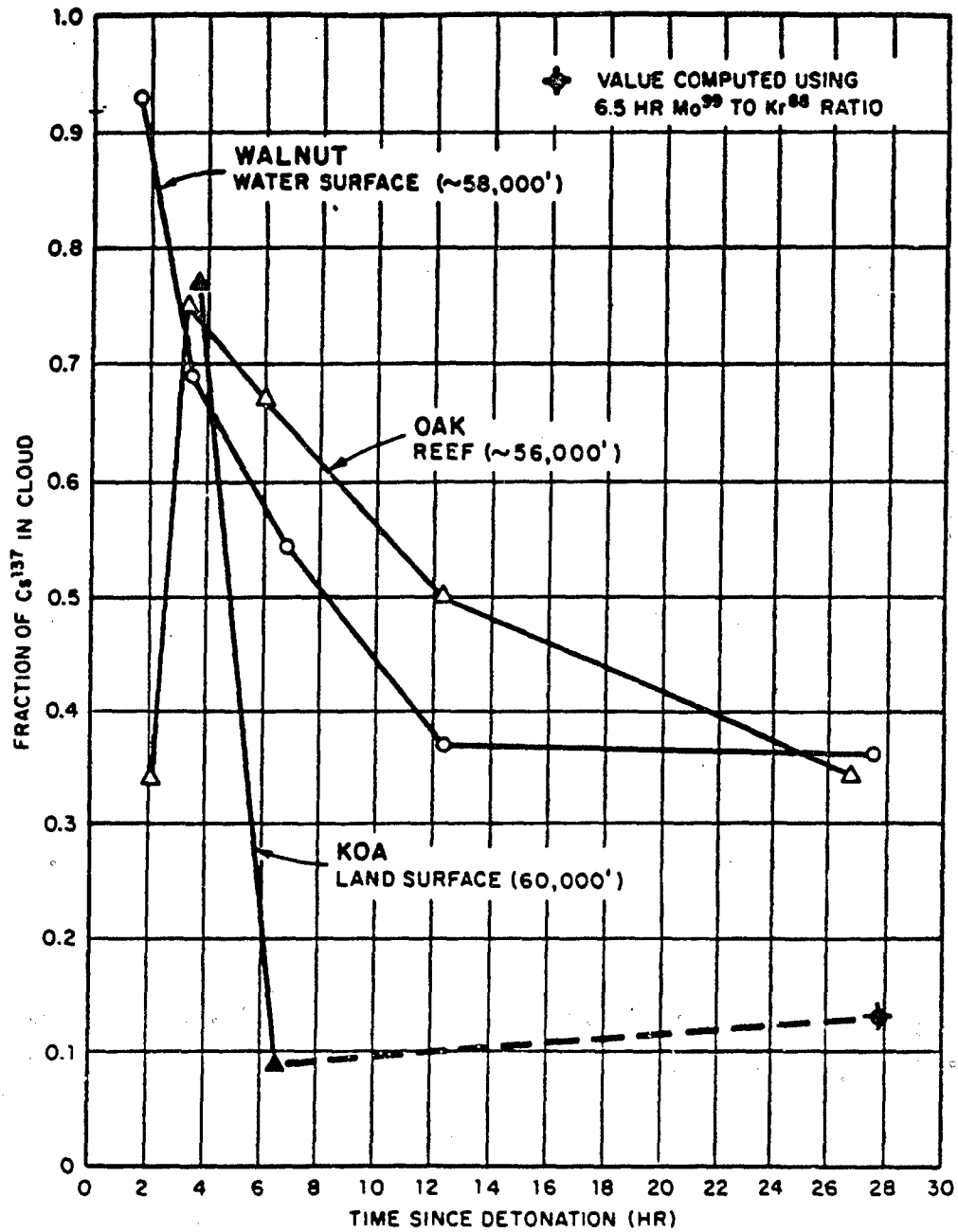

Figure 3.3 Fraction of total Cs^{137} formed that remains aloft at various times.

Page 51 is missing

Chapter 4

CONCLUSIONS AND RECOMMENDATIONS

4.1 CONCLUSIONS

The failure of the rocket sampling program made it necessary to rely almost exclusively upon the techniques of relative enrichment of volatile material in an isolated portion of the cloud for the measurement of fallout partition. This technique is an unproved one that includes some rather bold assumptions and a number of experimental difficulties.

It was not possible to sample at altitudes as high as desirable, and differences in cloud height with energy release and their subsequent effects upon fallo partition were not clearly defined. However, with these reservations, it is concluded that the technique generated a reasonably consistent body of data that was interpretable in the fashion expected.

The pattern of progressive enrichment of volatile material in an isolated portion of the cloud was displayed in Shot Walnut on a rather long time scale. However, if progressive enrichment occurred in Shots Koa and Oak, it was on a time scale short compared to 2 hours. Because the program for early sampling by rockets was not successful, no information was obtained on a time-dependent effect in the direction of enrichment.

1. The results suggest that, for a 1.31-Mt device (Koa) detonated on a coral surface, about one-fifth of the Sr^{90} formed is dispersed over distances greater than 4,000 miles. For a device detonated on a modified ocean surface (sand-filled barge), the fraction increases to about one-third. A device with a 9-Mt yield (Oak) in shallow water over a coral reef also disperses about one-third of the Sr^{90} produced at distances greater than 4,000 miles.

2. Fractions of Cs^{137} corresponding to those given above for Sr^{90} are about two-thirds dispersed for Koa, about one-third for Walnut, and about one-half for Oak.

Beside the obvious environmental differences in these detonations, the following are some of the factors that may have an effect on the fractions of various radionuclides that are widely dispersed: (a) An 8.9-Mt device produces a concentration of debris in the cloud volume lower by about a factor of 2 than the smaller devices studied here. (b) The time it takes the fireball to cool to 1,000° C was about three times as long for Oak as for Koa and Walnut. (c) The size distributions of the fallout particles may well be different for devices of different yield even though shot environment is similar. (d) The largest yield device had an appreciably larger fraction of its resulting cloud in the stratosphere where high-velocity winds could effect greater dispersion. (e) The different chemical and physical nature of the fallout particles may make for different distributions of various radionuclides between local and worldwide fallout.

3. Radionuclide fractionation is pronounced in shots over a coral land surface. The local fallout is depleted in both Sr^{90} and Cs^{137}, while the upper portion of the clouds are enriched. Fractionation is much less for water-surface shots.

4. Nuclear clouds are nonuniform in composition, and certain nuclide ratios vary by rather large amounts from top to bottom. Again, this is much larger for detonations on land than on water surfaces.

5. The radiochemical studies of fine and coarse particles indicate that the fission products with rare-gas precursors—Sr^{89}, Sr^{90}, Y^{91}, and Cs^{137}—are in general more concentrated in the fine particles in the land and reef shots. In the water-surface shot, they appear to be more evenly distributed among the particle groups.

6. Sr^{90} and Cs^{137} distributions computed from cloud and fallout data are roughly in agreement with one another.

4.2 RECOMMENDATIONS

The ratio of local to worldwide fallout is essentially governed by the distribution of particles with respect to size and altitude in the cloud at stabilization, i.e., at an early time before appreciable fallout has occurred, and by the specific activity of radionuclides of interest as a function of particle size. The latter function may vary with altitude in the cloud at stabilization.

The basic types of information necessary to calculate the fractions of a given radionuclide in local and worldwide fallout from particulate samples are: (1) the particle size at which division into local and worldwide fallout occurs for each sample, (2) the fraction of the volume of the cloud swept out in obtaining each sample, (3) the mass of each of the two groups of particles in each sample, and (4) the R-values of the radionuclide of interest in each of the two groups of particles in each sample.

The first of these can be calculated in advance from the criteria for worldwide fallout from the altitude of sample collection. The second can be calculated from the area of the sampling system by obtaining the total volume of the cloud and the cloud dimensions at various altitudes from cloud photography. The third can be obtained by separating the particles into the necessary two fractions during sampling and subsequently weighing each group. The fourth can be obtained by radiochemical analyses of each of the two particle groups.

It is recommended that such a program be carried out if the opportunity is presented by future nuclear tests.

Appendix A

ROCKET DEVELOPMENT

A.1 HARDTACK PERFORMANCE

A.1.1 6 May Test. Four rockets were set up on Site Yvonne for testing during Shot Cactus, an 18-kt detonation; two were located at 3,200 feet from ground zero, and two were placed at a position some 5,000 feet farther down-island. It was planned to fire both of the down-island rockets and one of those situated at 3,200 feet to check out the performance of the array prior to operational use on Shot Koa. The remaining rocket was to be left unfired on its launcher so that the results of exposure to the detonation could be observed.

The launching equipment for the close-in rocket that was to have been fired was rendered inoperative by the blast, but neither of the rockets at the close-in site were damaged. Both of the down-island rockets fired, and one penetrated the cloud and was recovered from the lagoon. However, it collected no activity, because the cloud height was less than predicted and the sampler head was programed to open at an altitude higher than the resultant cloud top. The second rocket flew in an erratic manner, missed the cloud and sank. Its nose section was recovered from the bottom of the lagoon, and a post-mortem examination indicated that the rocket had probably been damaged by a flying object prior to launching.

A.1.2 9 May Test. Two rockets were fired from Site Wilma for system check and nose section recovery practice, but both nose sections were leaky and sank soon after striking the water. The cause of the leakage was not known, but it was thought that a contributing factor might have been the existence of a partial vacuum inside the sampling heads, because they were sealed at an altitude of about 80,000 feet where the ambient pressure is much below that at sea level. To correct this situation, small holes of about 0.040-inch diameter were drilled in the nose sections and coated with a hydrophobic grease, thereby allowing air pressure equalization without permitting the entry of water. Static tests showed that no water entered the sampler heads by this route.

A.1.3 13 May Test. Eighteen rockets were set up for firing at the Koa cloud, but, as described previously, none was launched (Section 2.3.2).

A.1.4 26 May Test. After modification and testing of the launching equipment subsequent to Shot Koa, it was believed that the system was fully operational. It was desired at this time to test the complete array with a full complement of rockets. Four rockets were set up on Site Mary, eight on Site Sally, and six on Site Wilma for firing at the Yellowwood cloud. The cloud from Shot Yellowwood did not develop to the extent predicted, and launching signals were sent only to the launchers on Mary and Sally at H + 13½ minutes. All rockets launched successfully. The rockets on Wilma were intentionally not launched, because it was apparent that their trajectories would not intersect the cloud. Even of those fired, four were seen to have missed the cloud.

Three nose sections were recovered. The cap on the first nose section was still intact, probably as a result of a short in the circuit that fired the nose cap removal squib; therefore, no sample was collected. The second nose section was from a rocket programed to open at 30,000 feet. When recovered, the nose section contained about 60 ml of water. At H + 9 hours the filter of this nose section read about 1 mr/hr at the surface. The third nose section was from a rocket programed to open at 55,000 feet. About 100 ml of water had leaked into it, and the surface reading of its filter was 25 mr/hr at H + 9½ hours.

After this shot, an intensive effort was made to determine the cause of leakage of water into the nose sections. It was found that the ball joint sealing the forward end of the nose section after sampling could bounce back a small amount after closure, thereby permitting water to enter. A latching mechanism was designed to lock the ball joint in its totally closed position. This modification was then applied to all nose sections.

A.1.5 1 June Test. Three rockets were fired from Site Wilma to test the modified ball-joint closure mechanism. The sustainer motor on the first rocket did not ignite, causing the nose section to remain attached to this unit, which fell into the lagoon and sank. The second rocket was damaged by impact with a coral head. The third nose section was recovered intact and was dry inside. This represented a completely successful performance of the system. It appeared that the problem of water leakage into the nose section had been solved.

A.1.6 15 June Test. Ten rockets were set up for firing at the Walnut cloud. Of these, six were successfully launched (Section 2.3.3).

A.1.7 20 June Test. Because of the presence of water in the nose sections after Shot Walnut, two rockets were fired from Wilma to further investigate the cause of leakage. The nose section of the first rocket failed to separate from the sustainer motor and was destroyed when it hit the reef. The second nose section was recovered in the lagoon, and 50 ml of water was found to have leaked into it. It was conjectured at this time that the low ambient temperature (−100° F) encountered by the rocket at altitude might be freezing and causing distortion of the O-ring seals.

A.1.8 23 June Test. A nose section with parachute was dropped from a helicopter at an altitude of about 1,500 feet. It was recovered within 2½ minutes after striking the lagoon, and again, 50 ml of water was found inside. The possibility that the impact with the water caused the large rear conical seal to open momentarily was suspected. This was suggested by the rather large volume of water that had entered in a relatively short time.

A.1.9 24 June Test. Two nose sections with parachutes were dropped from an altitude of 1,500 feet in an effort to determine the exact point of water leakage. In the first nose section, the filter was replaced by a rubber membrane; and both the fore and aft spaces of the nose section were stuffed with absorbent paper tissue, so any water leaking in would be retained near the point of entry. After recovery, it was found that no water had leaked into this unit. The second nose section, which was the same one used in the 23 June test, was also stuffed with tissue. However, a normal filter unit was used to separate the sections rather than a rubber membrane. When recovered, this nose section was found to be dry inside. There was no difference between recovery conditions on the 23 and 24 June tests, except that the lagoon surface was rough 23 June and calm 24 June.

A.2 LATER RESEARCH

It is seen in Figures A.1 and A.2, illustrating the programing of the rocket and of the nose section, that the system is a complex one.

In the early stages of work on the rocket, prior to the field operation, it had been recognized that the chance of having a completely operational system ready for sampling the Hardtack clouds was small, because of the short length of time available for development and test firing. Nevertheless, it seemed possible that the remaining defects of a minor nature could be rectified in the field. The operational flights and tests already described show that significant progress was made toward this objective.

However, after the tests of 24 June, it became apparent that the cause of nose section leakage and other malfunctions could not be determined and corrected with facilities available at EPG. Further work, utilizing range and test installations in the United States, was essential to the attainment of a completely successful sampling system. Accordingly, the rocket portion of Project 2.8 was terminated 27 June with the concurrence of the Chief, AFSWP, and the Division of Military Application, AEC. All unfired rounds were shipped to California.

From July to December 1958, the Cooper Development Corp. tested the rockets from the EPG to investigate possible modes of entry of water into the sampling heads (Reference 69).

Three nose sections identical to those flown in the final EPG rounds were subjected to environmental tests at North American Aviation Co. during July. The tests included low-temperature cycle, vibration, and acceleration.

For the low-temperature tests, the forward and aft seals were closed, and the programer and its container were removed. Thermocouples were placed on the O-rings of the forward and aft seals. The assembly was brought to room temperature (75° F), and the cold chamber was stabilized at −65° F. The nose section was placed in the cold chamber and allowed to stand for 5 minutes. At the end of that time, the forward seal O-ring temperature was −10° F. The nose section was removed from the cold chamber and allowed to remain at room temperature for 4 minutes, then completely submerged in water for 1 minute and allowed to float at its normal level for 4 minutes. When the section was removed from the water and disassembled, it was found that no leakage had occurred.

The nose section used for the vibration test was a complete flight-ready assembly except that the skin around the diffuser had been removed. The acceleration load was maintained at 5 g's while the vibration frequency was varied from 3 to 2,000 cps. The dwell time at each resonant frequency was 1 minute. The vibration was applied first in the plane parallel to the longitudinal centerline of the assembly, then in the plane perpendicular to the centerline. No failures occurred.

For the acceleration tests, a flight-ready nose section assembly was separated into two sections at the filter joint. Both sections were placed on a spin table in the deceleration plane, and the load was raised to 50 g's and held there for 1 minute. No failures occurred. The sections were then placed in the acceleration plane, and the load was again increased to 50 g's and maintained at that level for 1 minute. The programer started its functions at approximately 15 g's, continued to operate properly, and no failures occurred. The test was then repeated using the nose section that had been vibration tested, and the results were the same. The four tests showed that the sampling cone design was entirely compatible with the anticipated environmental conditions.

Beginning 17 July, further testing of possible sources of leakage in the nose sections was conducted at the Morris Dam Small Caliber Range, Azusa, California, which is a

facility of the U.S. Naval Ordnance Test Station, Pasadena, California. Ten assemblies were dropped into the water at various angles and with various modifications. The first eight tests were carried out by dropping the assemblies from a height of approximately 32 feet at angles of 75° and 90° with the breathe hole left open. Other tests included drops of nose sections attached to parachutes from 100 feet, free-fall drops with the breathe hole closed, and parachute drops with a neoprene boot on the forward seal of the nose sections. The last six tests used sections in which a vacuum (23 inches of mercury), similar to the near-vacuum of the upper atmosphere, had been induced. Examination of these assemblies after recovery showed that the vacuum remained when the breathe hole was sealed.

Twenty-seven tests using ten nose section assemblies were conducted over a 5-day period. This work, plus further testing at the Cooper Development Corporation plant, indicated that certain points around the forward ball-seal joint and the operating mechanism were susceptible to small leaks when the pressure difference between the interior and exterior of the diffuser-filter section increased. The neoprene boot, which covered the operating mechanism, had proved to be particularly vulnerable during the EPG firings and later tests. The reliability of the seal was increased a great deal by redesign of the boot, and only infrequent minute leaks were observed after installation of the improved boots. These leaks were repaired as they occurred, until the seal was tight enough to hold a pressure difference of 23 inches of mercury for 10 minutes.

Following the successful drop tests, two flight test rounds were fired at the Naval Missile Center (NMC), Point Mugu, California, 24 July. The nose sections for these rounds were modified to incorporate the improvements which had been made during the tests at Morris Dam. All programer function times were as planned, and both rounds were judged to be successful. Their trajectories were followed throughout the flights by range radar, enabling the impact points to be quickly located by radars on the search aircraft. The nose sections were then recovered by a rescue craft. One of them was completely dry, and the second contained only a few milliliters of water. When the sections were disassembled, it was observed that the dry one had maintained a partial vacuum, while the other had apparently leaked air to equalize the pressure.

In spite of the success of the flight tests, it was felt that still further improvements could be made in sealing the diffuser-filter assembly. A conference was held in August between Cooper and UCRL personnel to investigate new approaches to the problem. After study of the design, it was concluded that moving the forward ball-seal O-ring from the forward to aft side of the ball would eliminate several possible sources of leakage, although there would be some sacrifice of performance. Slight leakage had been observed during some of the tests at the rubber boot on the push-puli rod, around the nose cap cable entries, and at the forward nose cap blowoff joint. Relocation of the O-ring to a position aft of these areas was expected to prevent any water that might enter from reaching the filter. All changes in design that had been made at the EPG and later, including the relocation of the O-ring, were incorporated in a new set of drawings, and two new nose sections were manufactured to the revised drawings.

A new antenna system, consisting of two bent dipoles located on opposite sides of the nose section and positioned as far forward as possible so that they would be above the surface of the water, was devised for the recovery transmitter. This system was tested at Puddingstone Dam near Pomona, California, 20 November. The antenna was first submerged, then the nose section was allowed to float during the test. Readable signals were received as far as 5 miles away with both ground and aircraft receivers. The signal was both stronger and steadier than that produced by the antennas used on the EPG rounds.

Drop tests using the two redesigned nose sections were conducted at Morris Dam, 22 November. The assemblies were dropped five times each from a height of 35 feet. No parachutes were used, and the angle of impact was not controlled. Both assemblies remained completely dry on the inside throughout the tests. One section was slightly damaged when it came to the surface under a steel barge, but this was quickly repaired.

The two new nose sections were assembled into flight rounds for tests at NMC, 2 December. Both rounds were launched at an elevation of 75° and azimuth of 217°. The second stage of the first round either failed to ignite or ignited only partially, as evidenced by the lack of a contrail and the horizontal range of only 14,200 yards. Nose section separation and parachute deployment were achieved satisfactorily. The nose section was located after impact by a very strong, steady, directional signal from the recovery transmitter and by sighting the dye marker. The nose section was completely dry inside, and a vacuum seal had been maintained for 2½ hours. On the next round, second-stage ignition was observed, and the range radar showed nose section separation at approximately 105,000 feet. The payload descended very rapidly and could not be located by the search craft. The radar plots gave no indication as to the nature of the malfunction that evidently occurred. It is possible that the main parachute failed to deploy or that the pilot chute was fouled by the motor.

These were the final tests carried out in the development of an ocean recovery version of the cloud sampling rocket. The results indicated that the improvements in design made subsequent to the field operation resulted in a more practical system than the one available in April 1958. However, further flight testing would be desirable if the rocket is to be used in a future cloud sampling program.

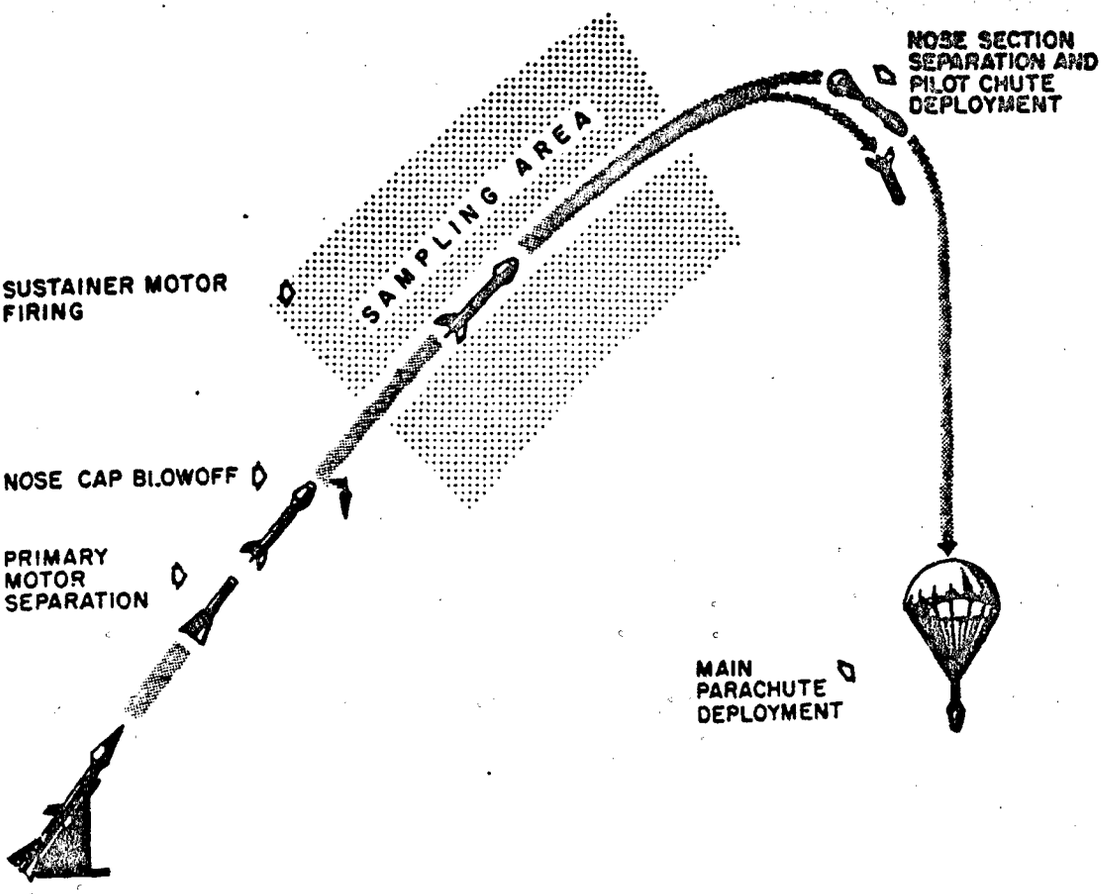

Figure A.1 Diagram to illustrate rocket programing.

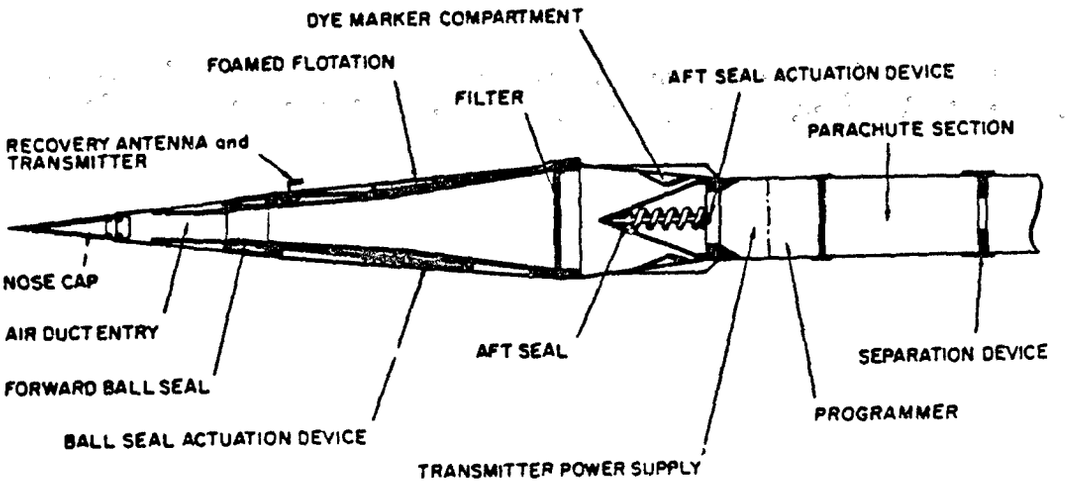

Figure A.2 Schematic view of rocket nose section.

Appendix B

RADIOCHEMICAL DATA TABLES

Tables B.1 through B.6 contain a compilation of radiochemical data for all the samples collected by project aircraft. The samplers are identified by the aircraft number. The letters R or L placed next to the aircraft number indicate that sampling units toward the right or left side of the aircraft were used. The single rocket sample obtained is also included. The analytical results are tabulated separately for the gas and particulate samples from the three shots. Data on the particulate material is divided into three groups, namely, gross cloud samples, size-separated cloud samples, and fallout samples. In each table, the results are arranged in the order of increasing time of collection.

The following general remarks will serve to clarify certain entries in the tables:

1. All fission values based on Mo^{99} in the particulate sample tabulations have been normalized to a LASL K-factor of 2.50×10^5. This factor gave approximately the correct number of fissions in samples from all three shots and facilitated comparison of the results from different laboratories.

6. All Sr^{89} and Sr^{90} R-values have been normalized to the LASL values by means of the Koa samples analyzed at both LASL and NRDL.

7. All Y^{91} R-values have been normalized to the NRDL values by means of the Koa samples analyzed at both LASL and NRDL.

8. The term "probe velocity" refers to the pumping speed in the gas-particle coincident sampler. Samples collected at a low probe velocity are very likely nonrepresentative of the cloud.

9. On Koa, the massive samples were collected on the 60,000-foot height line; the Wilson special sample was from the general fallout.

10. The fine and coarse fractions for the Koa and Oak size-separated samples were separated at a nominal fall rate of 1 cm/sec. Nominal fall rates for the Walnut fractions were: fine fraction, less than 0.1 cm/sec; medium fraction, 0.1 to 1.0 cm/sec; and coarse fraction, greater than 1 cm/sec.

11. The sampling altitudes given for Aircraft 978 on Walnut and 981 on Oak are thought to be too high, but more reliable figures are not available.

papers ... [illegible]
... are listed

Appendix C

PARTICLE DATA AND CHARACTERISTICS, SHOT KOA

C.1 SIZE DISTRIBUTION, FALL RATE, AND SPECIFIC ACTIVITY DATA

Fall rate distribution data, particle size data, and specific-activity fall-rate data are presented in graphical form in Figures C.1 through C.13, for the cloud and fallout samples listed in Table C.1. Samples, 500, 502, and 977 from the cloud were separated into coarse and fine fractions with the Bahco centrifuge before determination of the distribution curves. The boundary between the centrifuge fractions is as given in Appendix B. No fall rate work was done on samples taken from the cloud at times later than 4 hours because of the small quantity of material collected. These results are being reported primarily for record purposes.

C.2 PARTICLE CHARACTERISTICS

Most of the particles were translucent white and had an irregular shape. Some flaky aggregates—small spheres apparently formed by condensation—and clusters of varying sizes were also present. Many of the larger particles were discolored with a reddish-brown stain, presumably due to iron oxide.

The main constituents were identified as $Ca(OH)_2$ and $CaCO_3$ (both calcite and aragonite) by examination with polarized light and by X-ray diffraction. Small quantities of ocean water salts were observed in all the samples.

The particles disintegrated spontaneously into many small fragments when brought into contact with liquids. The disintegration was most rapid with water but also occurred at a slower rate with hydrocarbons and other fluids. Because of this effect, their density could not be determined by the bromobenzene-bromoform method.

Size measurement and type classification were described in Section 2.4; this investigation is summarized in Table C.2.

TABLE C.1 LIST OF SAMPLES MEASURED, SHOT KOA

Fall Rate Distribution	Particle Size Distribution	Specific Activity
Massive L1	Massive L1	Massive L5
Massive L2	Massive L4	Wilson Special
Massive L3	502 Coarse	502 Coarse
Massive L4	502 Fine	502 Fine
Massive L5	500 Coarse	500 Coarse
Wilson Special	500 Fine	500 Fine
502 Coarse	977 Coarse	977 Coarse
502 Fine	977 Fine	977 Fine
500 Coarse		
500 Fine		
977 Coarse		
977 Fine		

TABLE C.2 PARTICLE CLASSIFICATION AND SIZE MEASUREMENTS, SHOT KOA

Sample	Number of Particles Measured	Mean Size	Particle Type		
			Irregular	Aggregates	Spheres
		microns	pct	pct	pct
Massive L1	115	155	67.3	18.5	14.1
Massive L4	216	65	51.4	16.2	32.4
502 Coarse	255	48	82.0	11.0	7.0
502 Fine	287	19	93.7	3.5	2.8
500 Coarse	331	46	63.7	2.3	29.0
500 Fine	619	24	94.0	3.1	2.9
977 Coarse	264	47	76.1	9.5	14.4
977 Fine	299	21	94.6	2.3	3.1

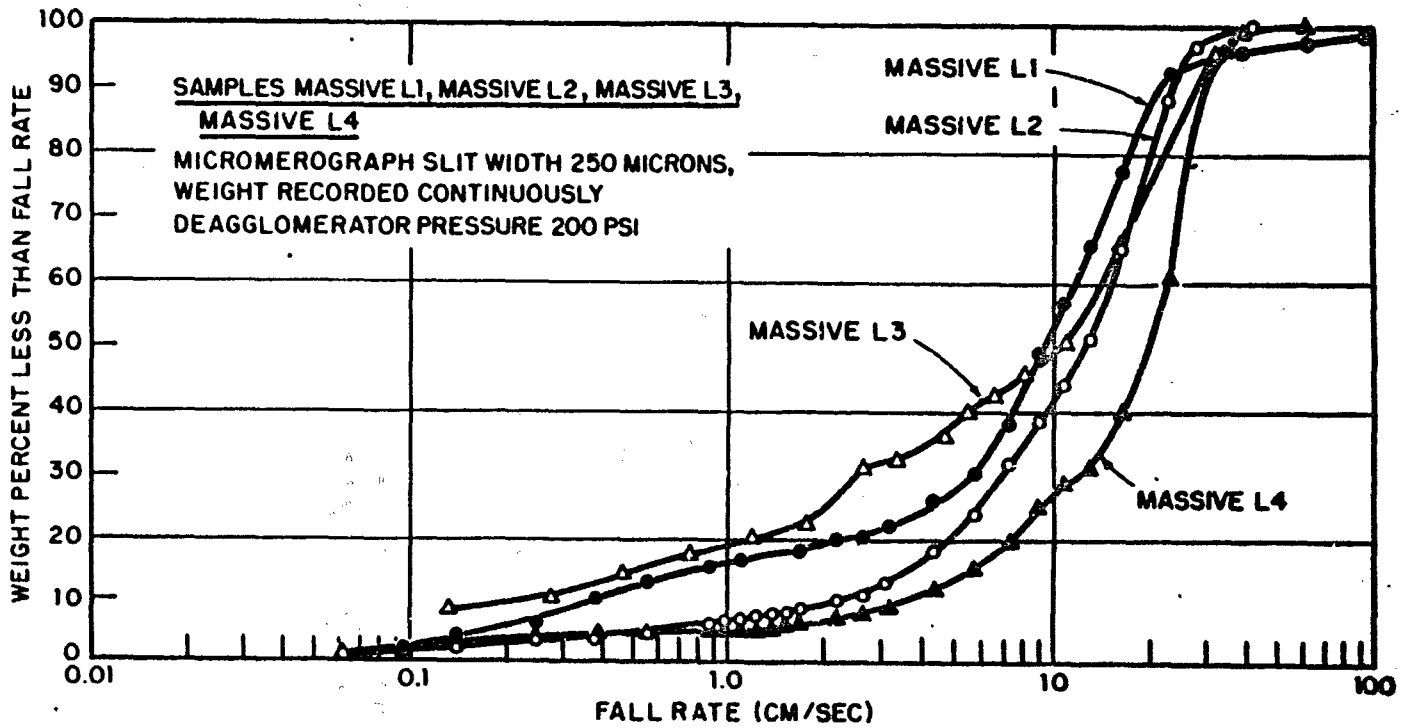

Figure C.1 Particle fall rate distribution curves for height line samples, Shot Koa: Samples Massive L1, L2, L3, and L4.

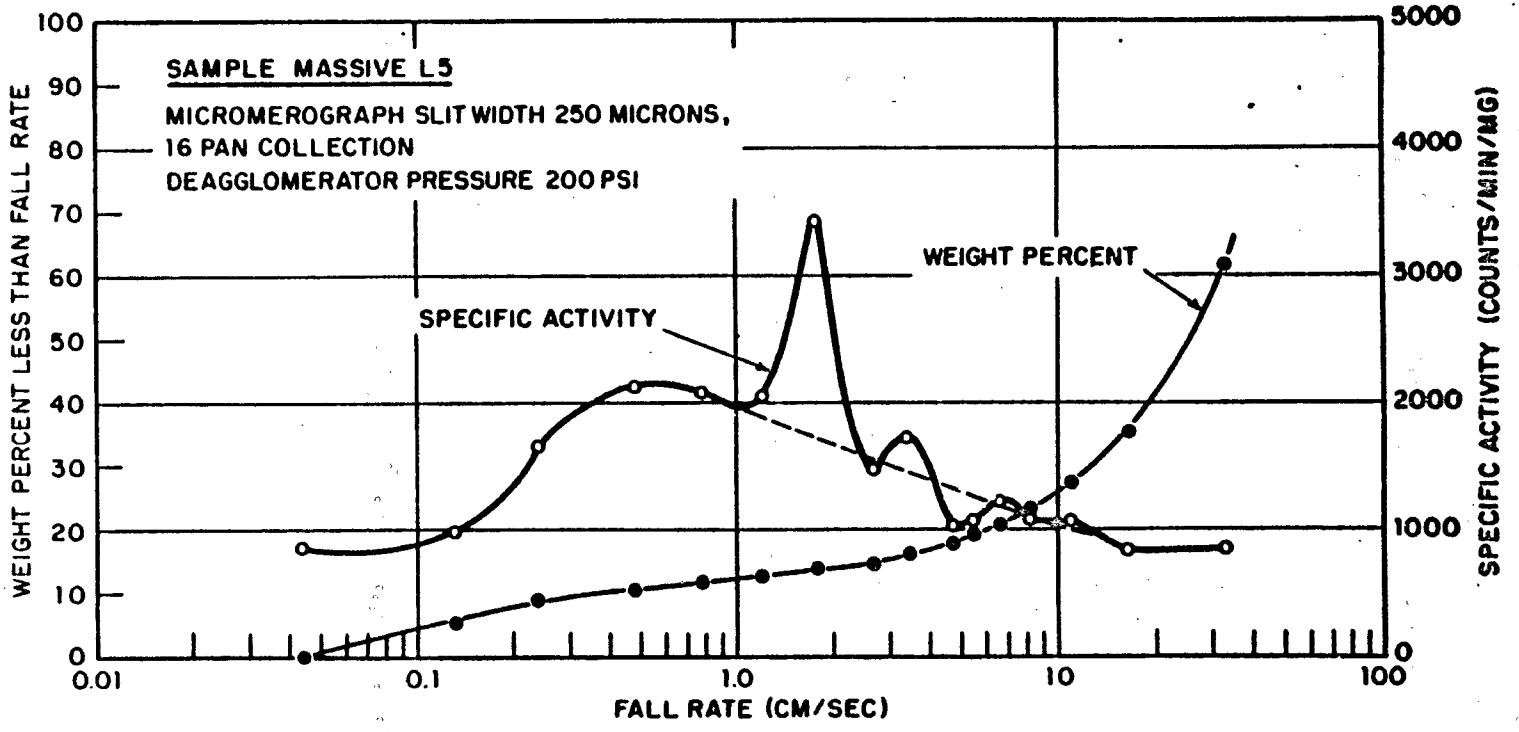

Figure C.2 Particle fall rate distribution and specific activity curves for height line samples, Shot Koa: Sample Massive L5.

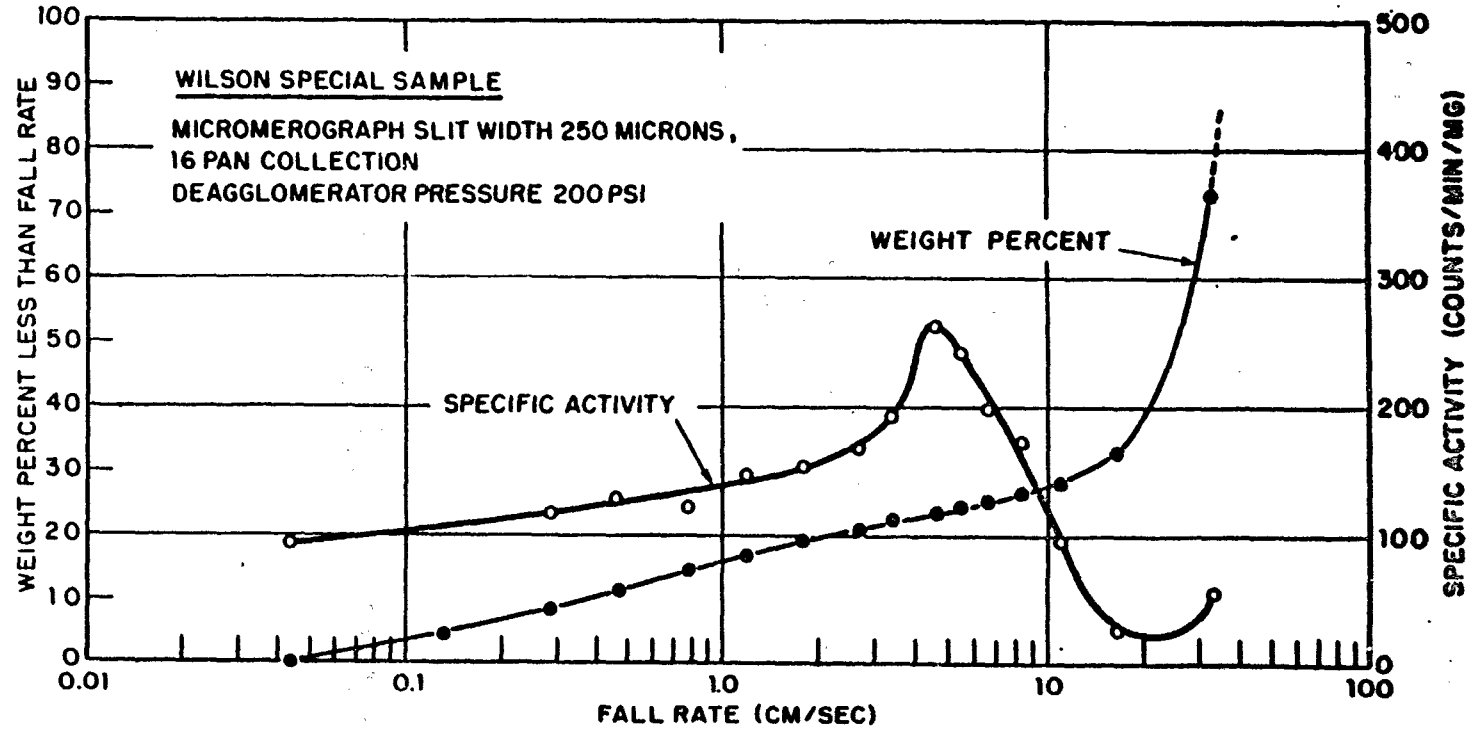

Figure C.3 Particle fall rate distribution and specific activity curves for height line samples, Shot Koa: Wilson special sample.

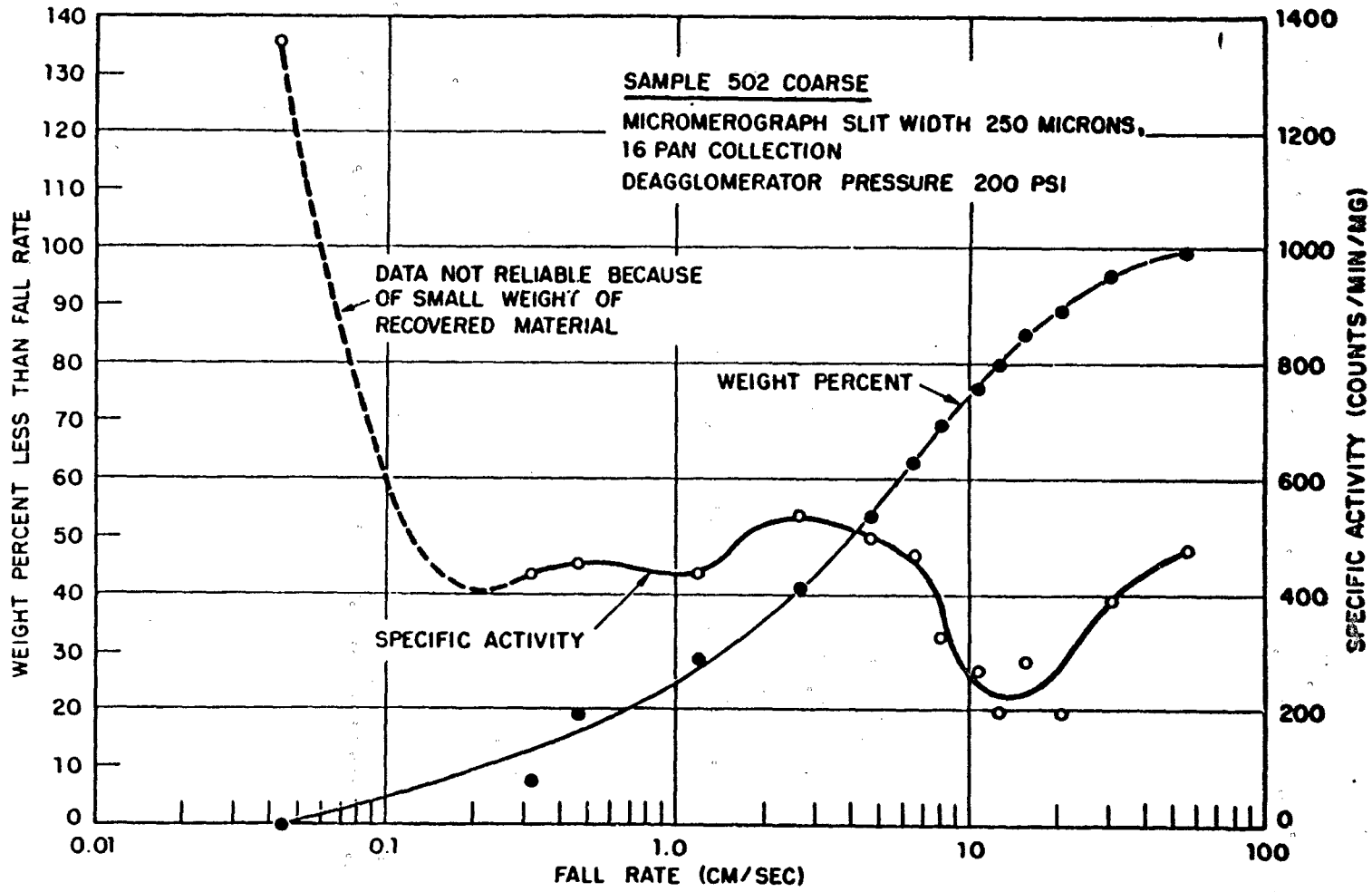

Figure C.4 Particle fall rate distribution and specific activity curves for cloud samples, Shot Koa: Sample 502, coarse.

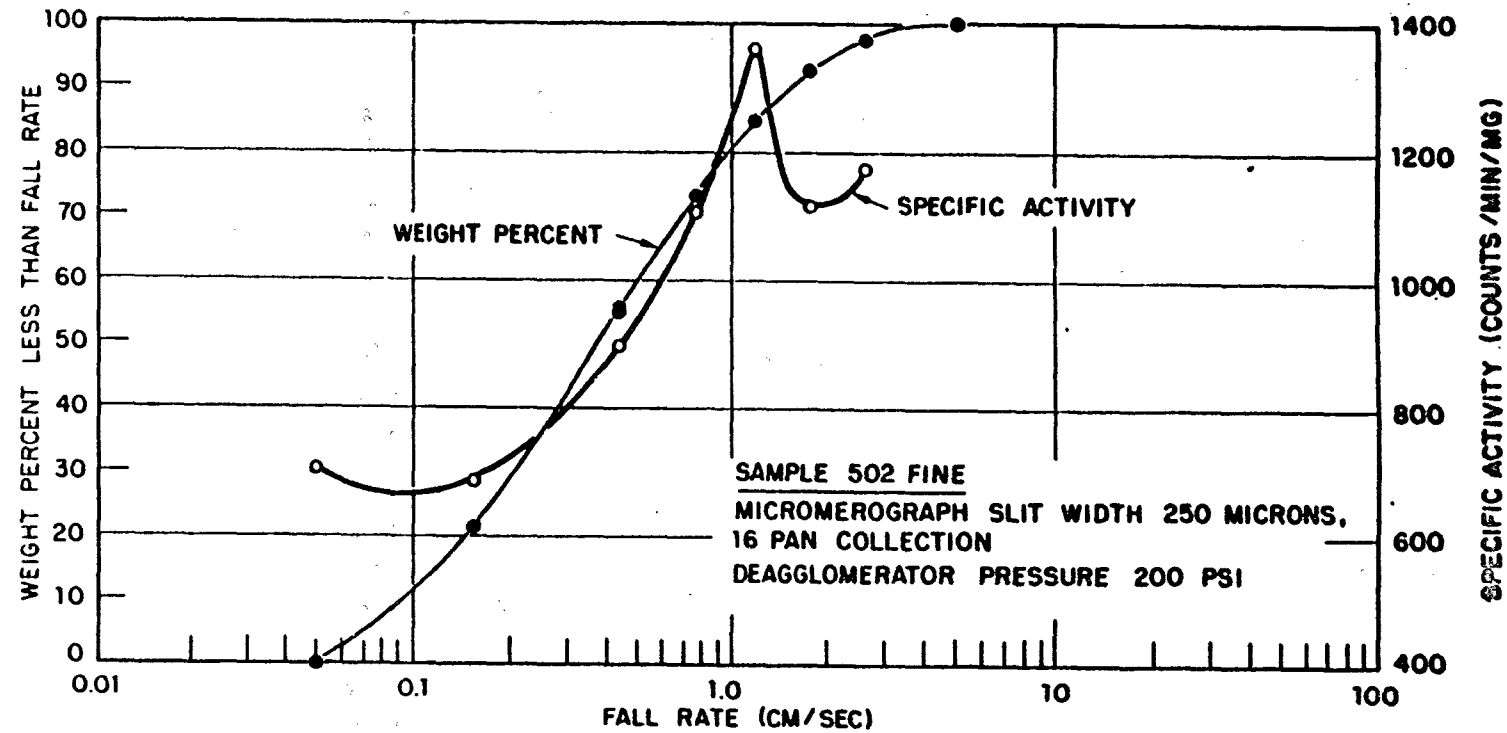

Figure C.5 Particle fall rate distribution and specific activity curves for cloud samples, Shot Koa: Sample 502, fine.

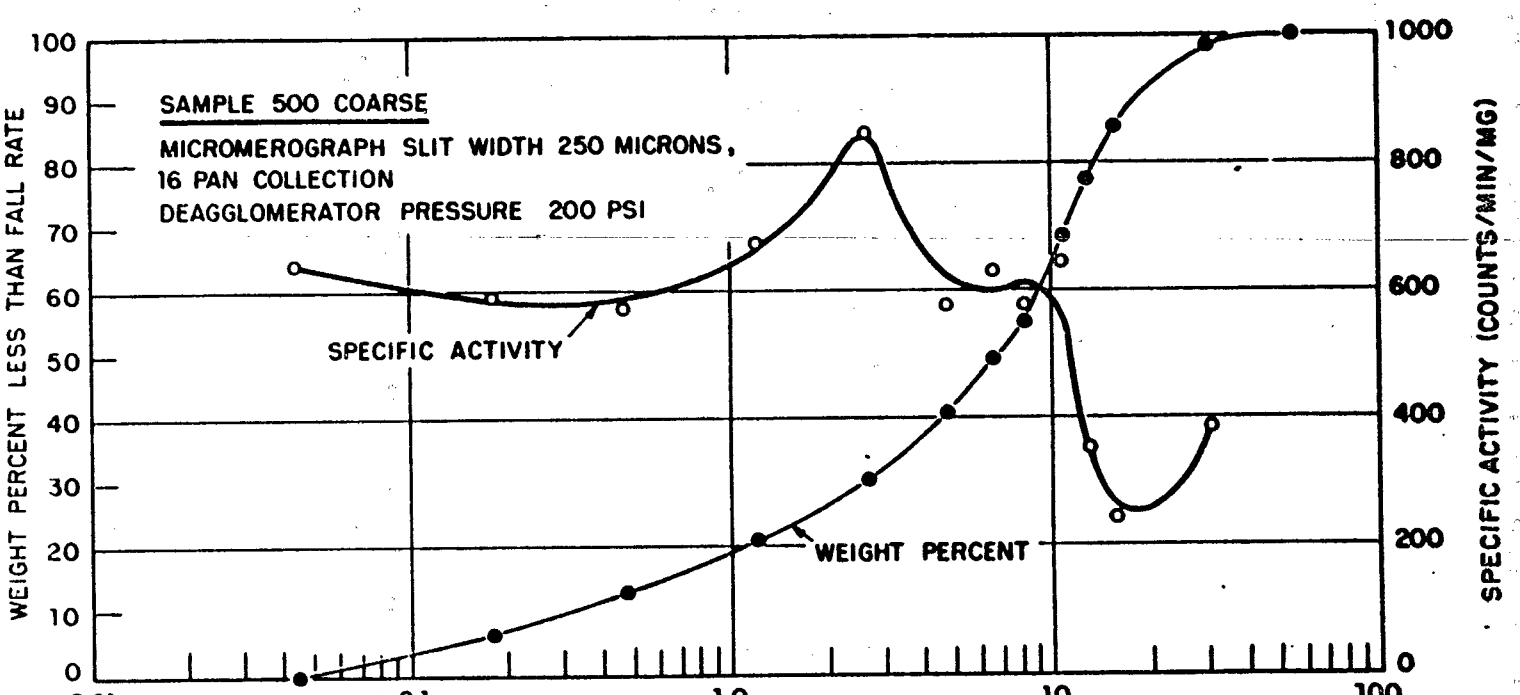

Figure C.6 Particle fall rate distribution and specific activity curves for cloud samples, Shot Koa: Sample 500, coarse.

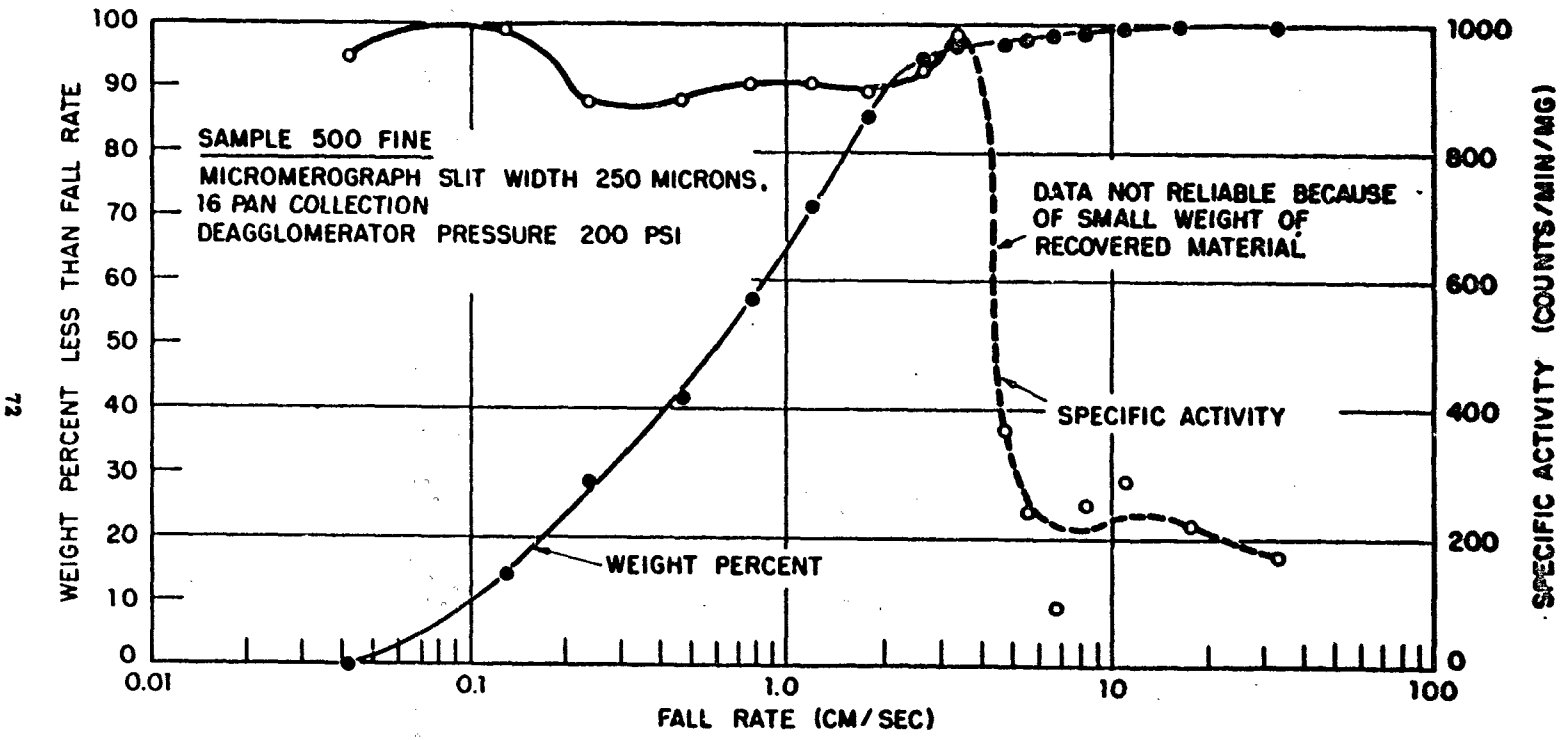

Figure C.7 Particle fall rate distribution and specific activity curves for cloud samples, Shot Koa: Sample 500, fine.

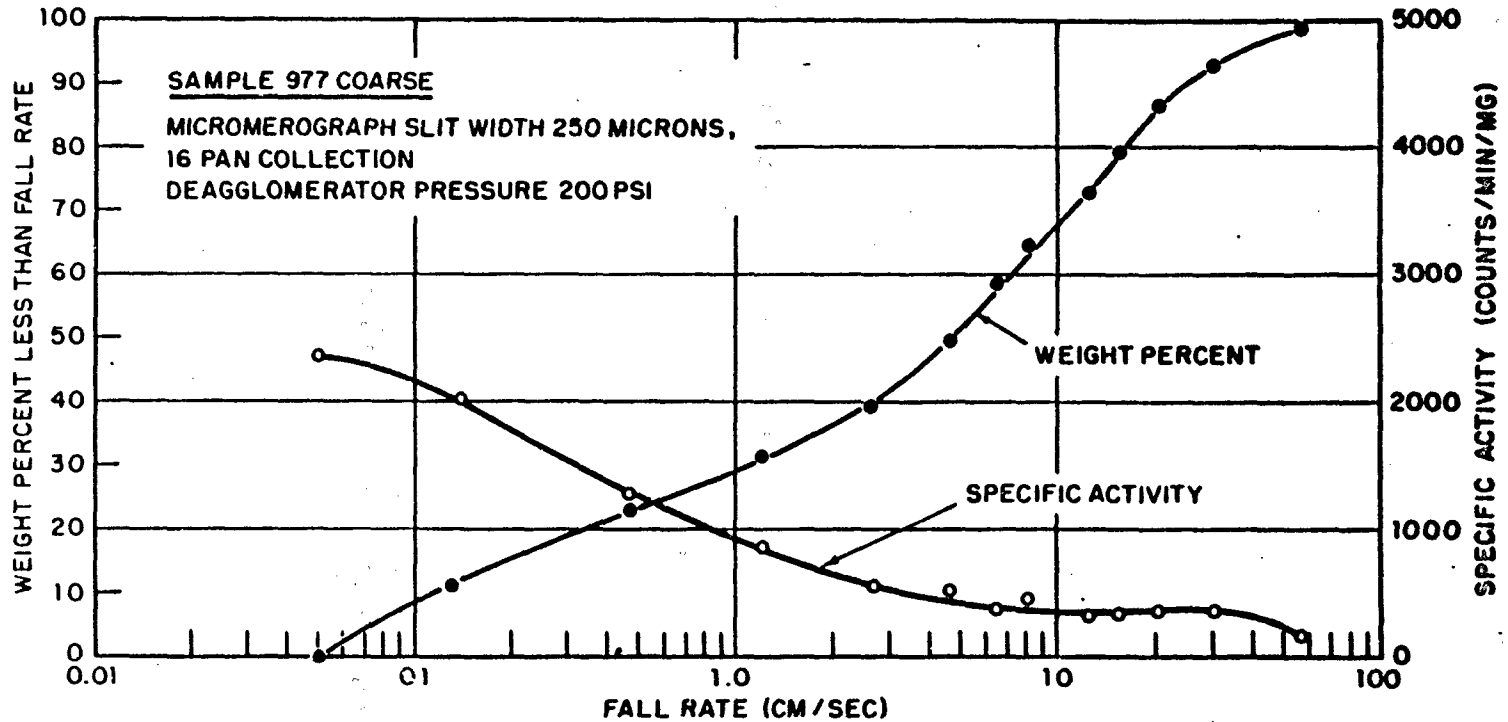

Figure C.8 Particle fall rate distribution and specific activity curves for cloud samples, Shot Koa: Sample 977, coarse.

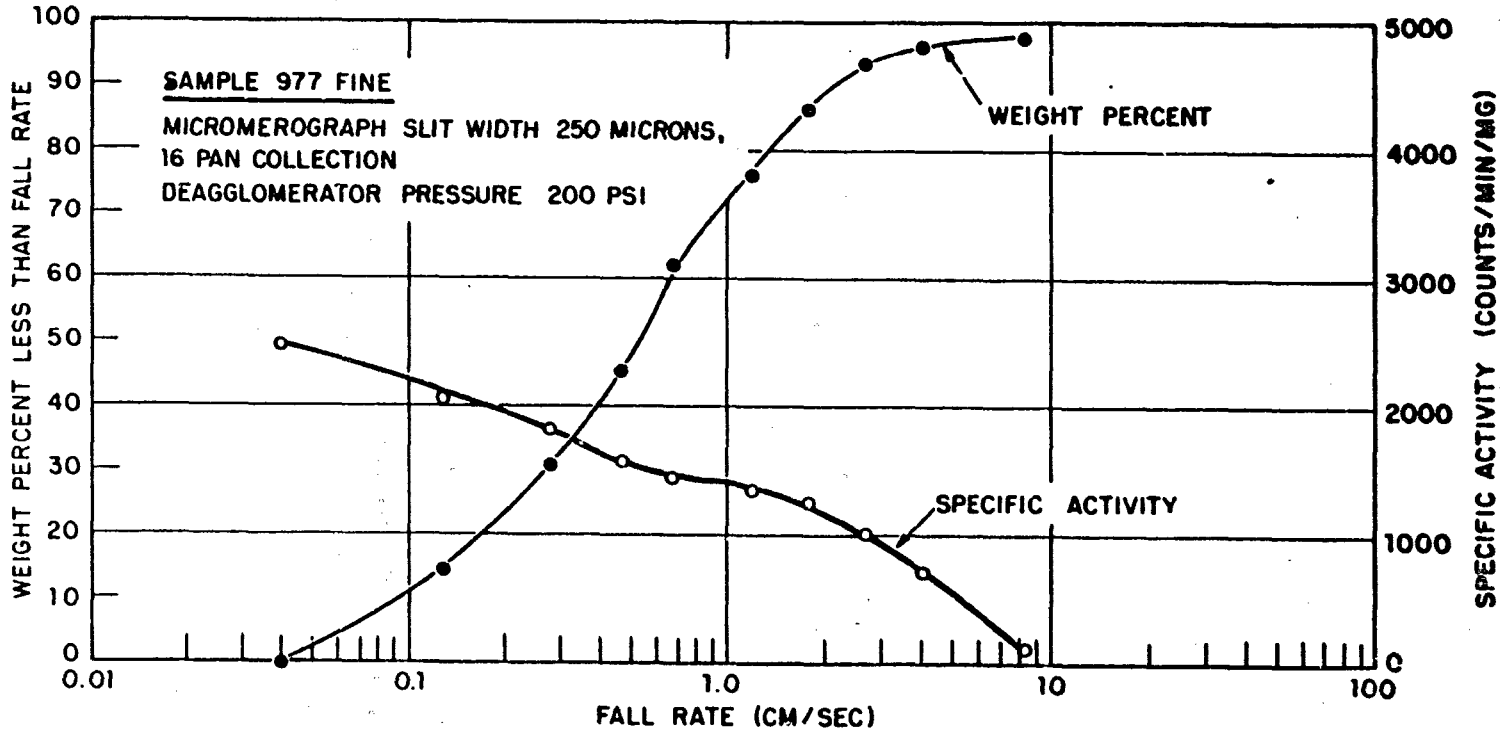

Figure C.9 Particle fall rate distribution and specific activity curves for cloud samples, Shot Koa: Sample 977, fine.

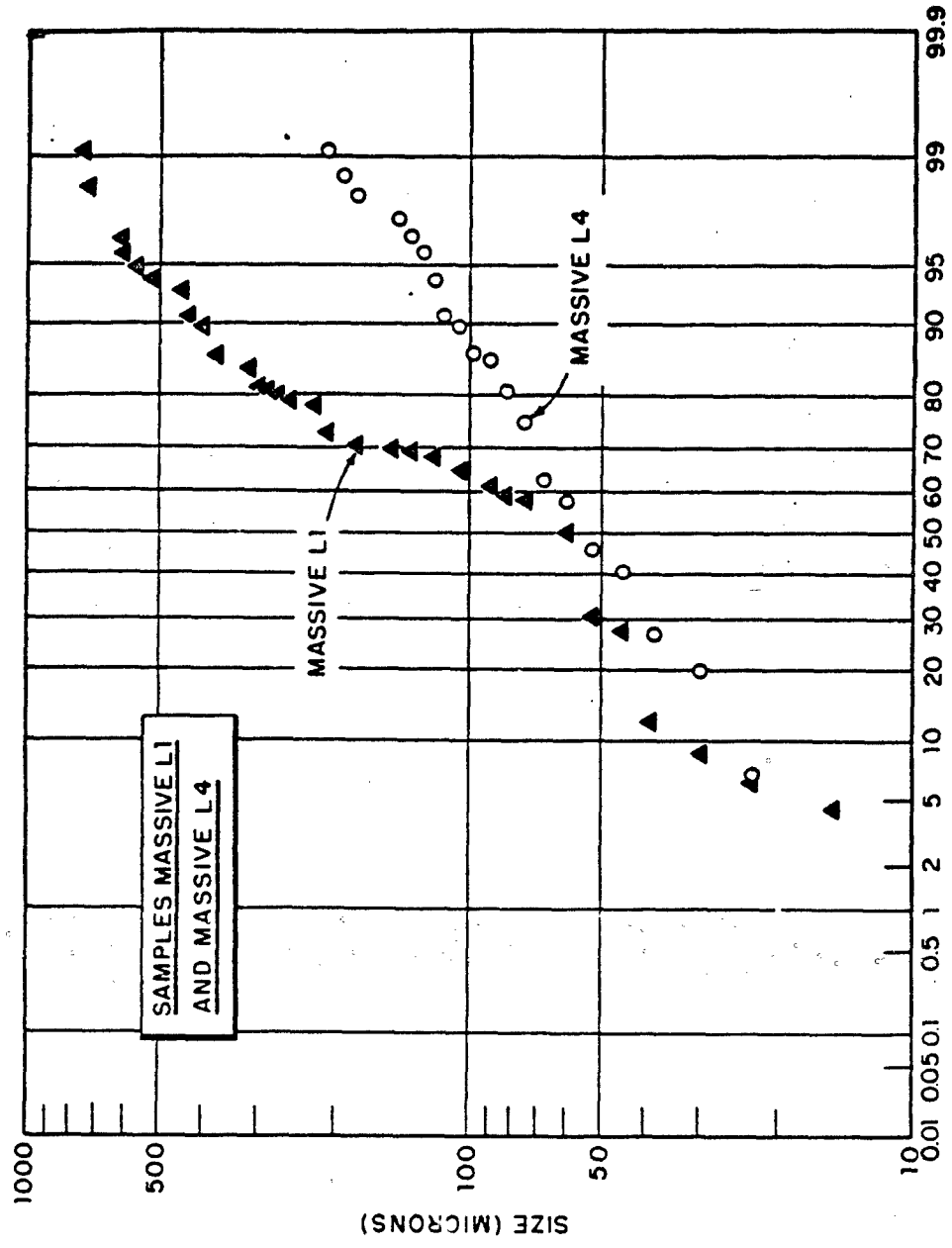

Figure C.10 Particle size distribution curves for height line samples, Shot Koa: Samples Massive L1 and Massive L4.

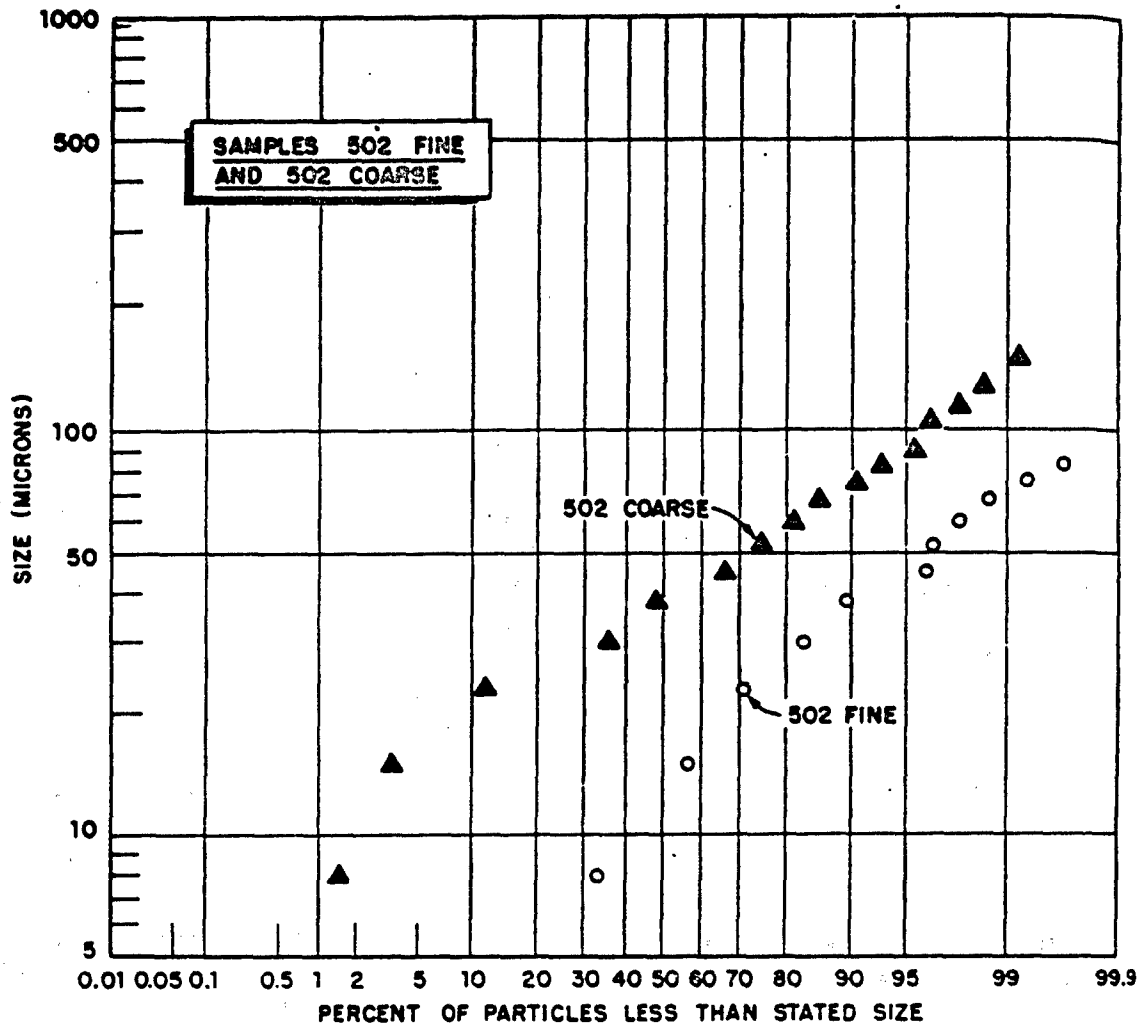

Figure C.11 Particle size distribution curves for cloud samples, Shot Koa: Samples 502, coarse, and 502, fine.

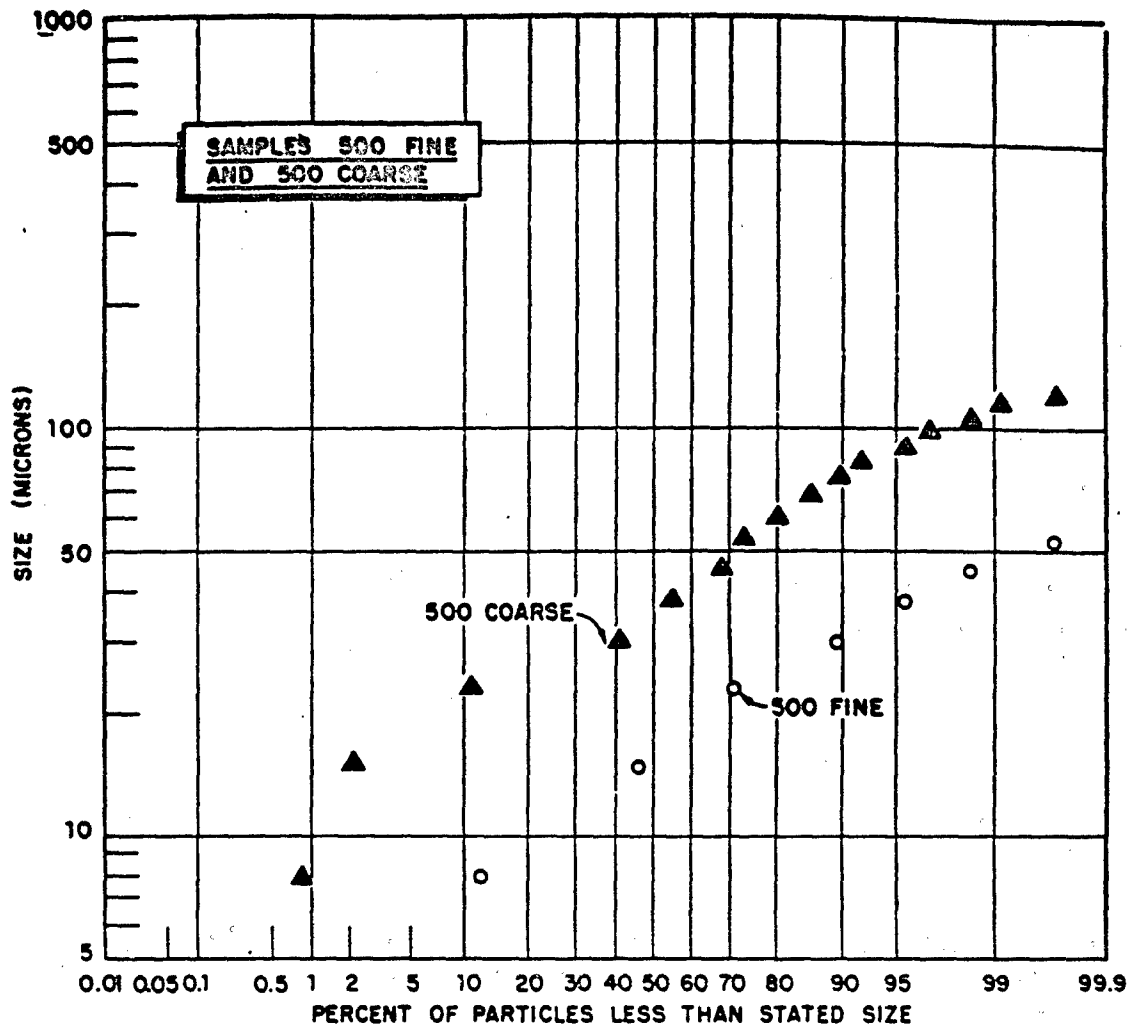

Figure C.12 Particle size distribution curves for cloud samples, Shot Koa: Samples 500, coarse, and 500, fine.

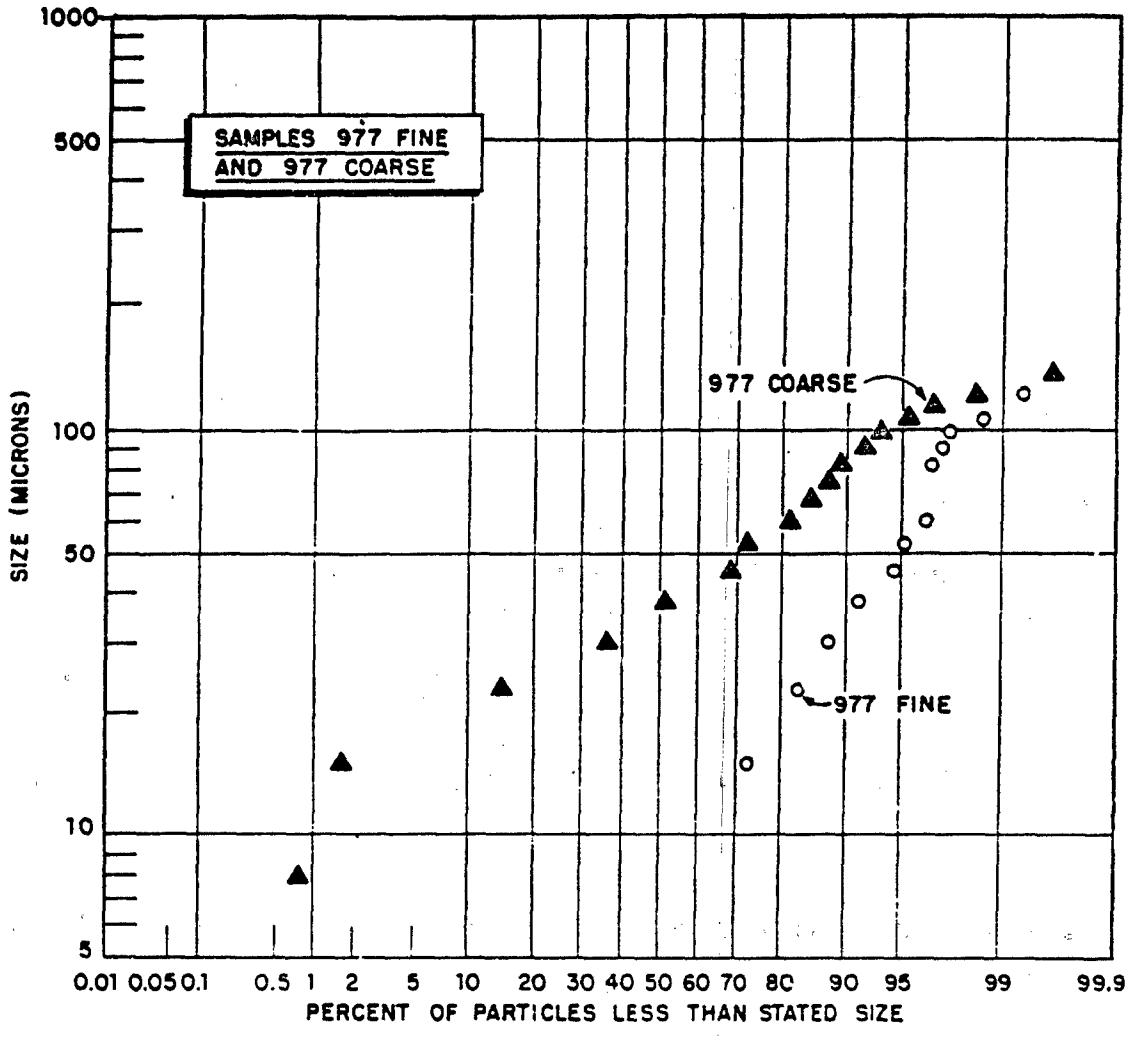

Figure C.13 Particle size distribution curves for cloud samples, Shot Koa: Samples 977, coarse, and 977, fine.

Appendix D

METEOROLOGICAL DATA TABLES

Meteorological data for the shot days of Koa, Walnut, and Oak are presented. Tables D.1 through D.3 give winds aloft, whereas Tables D.4 through D.6 give atmospheric temperature data.

TABLE D.1 WINDS ALOFT DATA, 13 AND 14 MAY 1958, SHOT KOA

W, wind bearing to nearest 10°; v, wind speed, knots.

Altitude	H − ½		H + 5½		H + 8½		H + 11½		H + 17½		H + 23½		H + 28½	
10^3 feet	w	v	w	v	w	v	w	v	w	v	w	v	w	v
1	07	025	08	028	09	023	08	023	08	023	06	021	07	021
2	07	027	07	033	09	030	08	025	09	024	06	023	08	023
3	08	028	07	032	09	030	08	026	09	026	08	023	08	021
4	08	031	08	025	09	030	09	027	09	027	08	022	09	017
5	09	029	08	025	09	026	10	023	09	025	09	024	09	016
6	10	025	09	020	09	022	11	023	09	022	09	027	09	020
7	10	027	10	016	08	019	10	023	09	021	09	023	10	021
8	10	027	10	017	09	016	08	015	09	019	09	015	10	014
9	09	022	10	017	09	010	09	017	09	012	09	012	10	009
10	09	022	12	016	10	022	09	012	09	008	05	009	10	005
12	10	025	13	017	09	015	12	011	09	006	02	004	29	003
14	11	022	15	012	12	009	12	004	09	004		004	25	002
16	12	012	14	012	11	008	19	010	–	–	33	004	30	003
18	11	010	14	012	15	009	18	004	33	007	21	004	31	008
20	07	007	13	004	15	008	22	008	27	010	24	010	28	004
23	20	008	18	016	16	014	18	014	24	009	27	013	29	006
25	27	012	16	016	16	019	12	012	22	012	28	017	30	016
30	25	021	24	018	15	020	25	019	22	018	25	014	27	015
35	19	027	17	027	17	025	17	018	20	024	24	016	25	020
40	22	025	19	025	22	020	23	027	22	023	24	022	23	030
45	24	035	26	045	25	039	24	034	25	023	29	021	26	025
50	29	03[illegible]	28	030	28	027	28	029	27	025	27	026	27	022
55	28	011	23	012	19	019	20	028	23	022	24	029	28	020
60	14	015	21	006	24	006	27	010	30	008	35	013	02	012
65	09	006	06	007	06	009	04	011	04	004	07	007	06	007
70	10	014	13	008	06	005	15	006	06	010	07	012	09	012
75	10	020	07	017	08	020	07	014	11	021	12	015	07	010
80	10	027	09	031	10	033	11	026	10	025	09	023	10	018
85	09	036	10	046	09	048	10	044	09	035	–	–	09	039
90	09	051	11	062	–	–	10	053	09	053	–	–	09	048

TABLE D.2 WINDS ALOFT DATA, 15 JUNE 1958, SHOT WALNUT

W, wind bearing to nearest 10°; v, wind speed, knots.

Altitude	H − ½		H + 2½		H + 5½		H + 8		H + 11½		H + 15½	
10^3 feet	w	v	w	v	w	v	w	v	w	v	w	v
1	07	010	09	020	10	015	04	004	06	016	07	018
2	08	019	08	019	08	017	07	021	07	018	06	022
3	07	019	09	019	10	017	06	018	06	018	09	022
4	09	019	11	019	10	017	09	018	09	018	10	022
5	09	017	11	019	10	016	10	017	09	021	10	022
6	09	013	11	018	11	018	11	017	09	023	10	020
7	09	013	11	017	11	018	11	018	09	022	10	020
8	09	013	11	014	11	015	10	015	10	017	10	020
9	10	013	11	014	11	012	11	012	10	014	10	019
10	10	013	11	014	10	013	12	012	12	015	10	017
12	09	010	11	011	12	009	10	011	09	010	11	013
14	11	015	09	009	11	007	12	007	11	006	12	006
16	11	020	10	013	13	010	10	008	11	008	14	011
18	11	020	11	016	12	018	12	010	12	013	12	010
20	11	018	13	011	13	017	13	014	12	012	10	011
23	15	016	14	008	11	006	13	012	13	012	10	012
25	20	011	17	006	12	006	12	016	14	016	11	016
30	18	025	15	012	16	013	16	020	17	021	13	016
35	16	021	19	019	16	025	18	018	18	019	17	014
40	21	023	18	025	16	024	18	014	17	024	17	[illegible]
45	18	014	18	015	16	023	16	024	17	039	17	[illegible]
50	19	014	18	024	15	026	15	023	18	038	21	021
55	11	008	14	014	17	005	19	025	05	013	13	016
60	08	017	00	013	08	015	14	004	09	017	09	015
65	10	023	–	–	11	026	–	–	–	–	07	019
70	09	025	–	–	09	024	–	–	08	029	09	021
75	09	042	–	–	09	034	–	–	–	–	10	040
80	09	050	–	–	09	046	–	–	09	015	10	039
85	09	050	–	–	09	050	–	–	–	–	09	038
90	09	054	–	–	10	055	–	–	08	047	09	035

TABLE D.3 WINDS ALOFT DATA, 29 JUNE 1958, SHOT OAK

W, wind bearing to nearest 10°; v, wind speed, knots.

Altitude	H − 1½		H + 1		H + 2½		H + 4½		H + 10½		H + 12½		H + 15½	
10^3 feet	w	v	w	v	w	v	w	v	w	v	w	v	w	v
1	09	019	09	018	08	020	08	015	09	021	09	022	10	011
2	09	015	10	021	09	019	08	019	10	026	09	027	10	023
3	10	015	10	021	09	019	08	019	10	024	09	026	10	023
4	11	015	10	021	10	019	09	017	10	022	09	026	10	022
5	11	018	11	019	10	018	10	017	11	017	10	020	10	025
6	10	018	11	017	10	015	11	015	10	014	10	023	09	025
7	10	016	12	017	11	013	12	015	10	016	11	019	09	023
8	11	016	12	017	13	010	13	015	10	017	11	017	10	019
9	11	016	13	016	14	011	13	015	10	015	11	018	10	014
10	11	016	14	015	15	013	13	015	10	011	11	015	10	015
12	11	014	15	014	19	013	13	016	11	014	12	011	10	011
14	11	013	13	016	15	015	15	019	13	010	08	009	09	007
16	12	016	13	015	15	019	15	017	13	006	07	005	09	013
18	12	015	13	015	15	016	15	017	13	006	08	006	08	013
20	13	019	13	016	–	–	16	017	16	014	20	004	08	011
23	14	020	14	015	–	–	16	023	17	010	16	007	08	013
25	13	019	14	019	16	019	15	020	17	010	16	006	10	010
30	16	018	14	014	14	014	14	017	19	008	16	007	17	003
35	14	015	13	014	13	010	14	014	16	009	14	005	14	008
40	13	013	12	017	12	022	11	014	10	014	11	014	13	008
45	07	015	09	020	07	019	09	016	08	015	07	013	09	007
50	10	015	09	011	12	010	16	018	14	007	15	005	09	003
55	13	006	15	006	14	005	07	007	04	010	05	010	09	010
60	10	029	11	010	–	–	08	027	08	026	07	028	09	004
65	08	026	–	–	–	–	09	029	10	030	09	028	10	010
70	10	034	–	–	–	–	09	037	09	036	09	034	09	035
75	10	053	–	–	–	–	09	049	09	047	08	045	10	050
80	10	064	–	–	–	–	10	058	10	058	–	–	09	058
85	10	072	–	–	–	–	10	061	09	068	–	–	09	066
90	10	076	–	–	–	–	09	063	09	073	–	–	–	–

TABLE D.4 ATMOSPHERIC TEMPERATURE DATA, 13 MAY 1958, SHOT KOA

Altitude	Temperature
feet	°C
Surface	27.8
310	26.8
2,231	21.5
4,950	17.2
7,874	11.5
10,310	09.5
14,450	2.5
16,929	−0.5
18,209	−2.5
19,095	−4.2
19,240	−4.2
19,554	−4.2
24,920	−14.2
26,903	−18.2
29,331	−23.5
31,070	−28.1
31,870	−30.2
36,036	−39.8
36,050	−40.2
40,930	−51.8
46,850	−65.2
51,810	−75.0
54,680	−77.7
56,859	−78.0
57,634	−75.0
60,621	−74.0
63,030	−77.0
64,482	−62.0
68,120	−63.8
73,656	−56.0
79,167	−57.0
82,540	−50.0
94,149	−45.0

TABLE D.5 ATMOSPHERIC TEMPERATURE DATA, 15 JUNE 1958, SHOT WALNUT

Altitude feet	Temperature °C
Surface	25.2
310	24.2
4,910	14.8
5,348	12.0
8,202	9.8
10,240	7.2
11,417	5.5
13,123	2.5
14,350	0.5
16,240	−2.8
19,080	−8.5
24,640	−19.2
31,440	−34.5
34,056	−40.2
35,550	−44.0
40,330	−57.0
46,140	−68.0
53,460	−79.0
53,900	−78.0
57,618	−76.0
60,555	−79.0
61,083	−68.0
64,680	−70.0
65,703	−66.0
67,270	−66.8
69,300	−67.0
70,257	−62.0
73,920	−63.0
76,197	−60.0
78,804	−62.0
79,629	−56.0
81,390	−54.0
96,947	−42.0

TABLE D.6 ATMOSPHERIC TEMPERATURE DATA, 29 JUNE 1958, SHOT OAK

Altitude feet	Temperature °C
Surface	25.5
280	25.2
3,900	16.8
4,890	15.5
10,210	7.2
14,320	−0.2
19,050	−7.2
24,640	−17.8
31,490	−32.8
31,560	−33.2
35,620	−42.2
40,420	−55.2
42,910	−62.0
46,240	−68.2
48,850	−74.0
49,740	−77.0
50,590	−71.0
56,050	−74.8
57,590	−78.0

Appendix E

DERIVATION OF FORMULA FOR PERCENT MOLYBDENUM LEFT IN CLOUD

The formula given in Chapter 3 for the percent Mo^{99} left in the cloud is based on a material balance for some nuclide, Y. It can be derived as follows:

Let Y_E = atoms Y formed in the explosion

Y_C = atoms Y left in cloud

Y_{FO} = atoms Y in fallout

Mo_E = atoms Mo^{99} formed in the explosion

Mo_C = atoms Mo^{99} left in the cloud

Mo_{FO} = atoms Mo^{99} in the fallout

y = fraction of Mo^{99} atoms left in cloud

k = the ratio atoms Y: atoms Mo^{99} formed in thermal neutron fission, a constant

$[R^{99}(Y)]_E$ = R-value for nuclide Y in explosion

$[R^{99}(Y)]_C$ = R-value for nuclide Y in cloud

$[R^{99}(Y)]_{FO}$ = R-value for nuclide Y in fallout

$$Y_E = Y_C + Y_{FO} \qquad \text{(E.1)}$$

$$= Mo_E\, Y_E/Mo_E$$

$$= Mo_E\, k\, [R^{99}(Y)]_E$$

since $[R^{99}(Y)]_E = [Y_E/Mo_E]/k$

$$Y_C = Mo_C\, Y_C/Mo_C$$

$$= Mo_C\, k\, [R^{99}(Y)]_C$$

since $[R^{99}(Y)]_C = [Y_C/Mo_C]/k$

$$Y_{FO} = Mo_{FO}\, Y_{FO}/Mo_{FO}$$

$$= Mo_{FO}\, k\, [R^{99}(Y)]_{FO}$$

since $[R^{99}(Y)]_{FO} = [Y_{FO}/Mo_{FO}]/k$

From Equation E.1 since $Mo_C = Mo_E y$ and $Mo_{FO} = Mo_E(1-y)$

$$Mo_E\, k\, [R^{99}(Y)]_E = Mo_E y\, k\, [R^{99}(Y)]_C + Mo_E(1-y)\, k\, [R^{99}(Y)]_{FO} \qquad (E.2)$$

dividing Equation E.2 by $Mo_E\, k$ and rearranging

$$y = \frac{[R^{99}(Y)]_E - [R^{99}(Y)]_{FO}}{[R^{99}(Y)]_C - [R^{99}(Y)]_{FO}}$$

REFERENCES

1. Fallout Project Planning Conference, Atomic Energy Commission, Washington, D.C., 10 June 1957.

2. Fallout Project Planning Conference, Headquarters, Armed Forces Special Weapons Project, Washington, D.C., 12 - 13 September 1957.

3. J. Frenkel; "Kinetic Theory of Liquids"; Oxford Press, London, 1946.

4. J.L. Magee; "Particle Size of Debris from the Atomic Bomb, Appendix II"; World Wide Effects of Atomic Weapons, Project Sunshine, R-251-AEC, 6 August 1953; The RAND Corporation, Santa Monica, California; Secret Restricted Data.

5. K. Stewart; "The Condensation of a Vapor to an Assembly of Droplets (with Particular Reference to Atomic Explosion Debris)"; Trans. Faraday Soc. 52, 161 - 73 (1956).

6. E.C. Freiling; "Recent Developments in the Study of Fractionation, I"; USNRDL Technical Memorandum No. 73, U.S. Naval Radiological Defense Laboratory, San Francisco, California; Confidential Restricted Data.

7. R.D. Evans; "The Atomic Nucleus"; McGraw-Hill Book Company, New York, New York, 1955.

8. "World Wide Effects of Atomic Weapons, Project Sunshine"; R-251-AEC, 6 August 1953; The RAND Corporation, Santa Monica, California; Secret Restricted Data.

9. C.E. Adams; "Fallout Particles from Shots Zuni and Tewa, Operation Redwing"; USNRDL-TR-133, 1957; U.S. Naval Radiological Defense Laboratory, San Francisco, California; Confidential.

10. R.C. Tompkins and D.W. Krey; "Mechanism of Fallout Particle Formation: I"; Technical Report CWLR 2059, 27 November 1956; Chemical Warfare Laboratories, Army Chemical Center, Maryland; Secret Restricted Data.

11. C.E. Adams, N.H. Farlow and W.R. Schell; "The Composition, Structures and Origin of Radioactive Fallout"; USNRDL-TR-209, 3 February 1958; U.S. Naval Radiological Defense Laboratory, San Francisco, California; Unclassified.

12. C.E. Adams and J.D. O'Connor; "The Nature of Radioactive Particles: VI, Fallout Particles from a Tower Shot, Operation Redwing"; USNRDL Report in Publication; U.S. Naval Radiological Defense Laboratory, San Francisco, California: Unclassified.

13. T. Triffet and P.D. LaRiviere; "Characterization of Fallout"; Project 2.63, Operation Redwing, WT-1317, March 15, 1961; U.S. Naval Radiological Defense Laboratory, San Francisco, California; Secret Restricted Data.

14. N.G. Stewart, R.N. Crooks and E.M.R. Fisher; "The Radiological Dose to Persons in the U.K. due to Debris from Nuclear Test Explosions prior to January 1956"; AERE HP/R-2017; Harwell, United Kingdom; Unclassified.

15. E.R. Tompkins and L.B. Werner; "Chemical, Physical and Radiochemical Characteristics of the Contaminant"; Project 2.6a, Operation Castle, WT-917, January 1956; U.S. Naval Radiological Defense Laboratory, San Francisco, California; Secret Restricted Data.

16. Private communication, Dr. G. Cowan, Los Alamos Scientific Laboratory, Los Alamos, New Mexico, June 1958.

17. S.M. Greenfield, W.W. Kellogg, F.J. Krieger and R.R. Rapp; "Transport and Early Deposition of Radioactive Debris from Atomic Explosions"; Project Aureole, R-265-AEC, 1 July 1954; The RAND Corporation, Santa Monica, California; Secret Restricted Data.

18. L. Machta; "Entrainment and the Maximum Height of the Atomic Cloud"; Bulletin Am. Meteor. Soc., 31, 215 (1950); Unclassified.

19. I.C. Cheeseman and D. Sams; "On the Rise of an Atomic Cloud"; AWRE Report E9/57, August 1957; Aldermaston, United Kingdom; Unclassified.

20. R.R. Soule and T.H. Shirasawa; "Rocket Determination of Activity Distribution Within the Stabilized Cloud"; Project 2.61, Operation Redwing, WT-1315, April 1960; U.S. Naval Radiological Defense Laboratory, San Francisco, California; Secret Restricted Data.

21. A.D. Anderson; "A Theory for Close-In Fallout"; USNRDL-TR-249, 23 July 1958; U.S. Naval Radiological Defense Laboratory, San Francisco, California; Unclassified.

22. E.A. Schuert; "A Fallout Forecasting Technique with Results Obtained At the Eniwetok Proving Ground"; USNRDL-TR-139, 3 April 1957; U.S. Naval Radiological Defense Laboratory, San Francisco, California; Unclassified.

23. J.M. Dallavalle; "Micromeritics"; Pittmann Publishing Corporation, New York, New York, 1948; Unclassified.

24. Hearings before the Special Subcommittee on Radiation of the Joint Committee on Atomic Energy, Congress of the United States, Eighty-fifth Congress; First Session on "The Nature of Radioactive Fallout and its Effects on Man"; Part 1, May 27, 28, 29 and June 3, 1957; U.S. Government Printing Office, Washington, D.C.; Unclassified.

25. A.K. Stebbins III et al., "Third Annual HASP Briefing"; DASA-531, 15 December 1959; Defense Atomic Support Agency, Washington 25, D.C.; Unclassified.

26. W.F. Libby; "Radioactive Fallout, Particularly from the Russian October Series"; Proc. Nat. Acad. Sci. of U.S.A. 45, 959, 1959.

27. Hearings before the Special Subcommittee on Radiation of the Joint Committee on Atomic Energy, Congress of the United States, Eighty-fifth Congress; First Session on "The Nature of Radioactive Fallout and its Effects on Man"; Part 2, June 4, 5, 6, and 7, 1957; U.S. Government Printing Office, Washington, D.C.; Unclassified.

28. L.B. Werner; "Percent of Weapon Debris Removed by Local Fallout"; Review and Lectures No. 39, USNRDL 28 August 1957; U.S. Naval Radiological Defense Laboratory, San Francisco, California; Secret Restricted Data.

29. RAND Fallout Symposium, AFSWP-1050, 1 April 1957; Armed Forces Special Weapons Project, Washington 25, D.C.; Secret Restricted Data.

30. N.M. Lulejian; "Radioactive Fallout from Atomic Bombs"; Report CS-36417, November 1953; Air Research and Development Command, Andrews Air Force Base, Washington, D.C.; Secret Restricted Data.

31. R.D. Cadle; "Effects of Soil, Yield, and Scaled Depth on Contamination from Atomic Bombs"; Cm. C. Contract DA-18-108-CML-3842, 29 June 1953; Stanford Research Institute, Menlo Park, California; Secret Restricted Data.

32. R.L. Stetson and others; "Distribution and Intensity of Fallout"; Project 2.5a, Operation Castle, WT-915, January 1956; U.S. Naval Radiological Defense Laboratory, San Francisco, California; Secret Restricted Data.

33. T.R. Folsom and L.B. Werner; "Distribution of Radioactive Fallout by Survey and Analyses of Contaminated Sea Water"; Project 2.7, Operation Castle, WT-933, April 1959; Scripps Institution of Oceanography, La Jolla, California and U.S. Naval Radiological Defense Laboratory, San Francisco, California; Secret Restricted Data.

34. D.C. Borg, L.D. Gates, T.A. Gibson, Jr., and R.W. Paine, Jr.; "Radioactive Fallout Hazards from Surface Bursts of Very High Yield Nuclear Weapons"; AFSWP-507; May 1954; Armed Forces Special Weapons Project, Washington 25, D.C.; Secret Restricted Data.

35. R.C. Tompkins; "Radiochemical Estimation of Total Activity Included Within Dose Rate Contours for Bravo Shot, Operation Castle"; CRLR 636, March 1956; Army Chemical Center, Maryland; Secret Restricted Data.

36. H.D. Levine and R.T. Graveson; "Radioactive Debris from Operation Castle, Aerial Survey of Open Sea Following Yankee-Nectar"; NYOO-4618, 20 December 1954; Health and Safety Laboratory, New York Operations Office, USAEC, New York, New York; Secret Restricted Data.

37. N.E. Ballou; "Radiochemical and Physical Chemical Properties of Products of a Deep Underwater Nuclear Detonation"; Project 2.3, Operation Wigwam, WT-1011, April 1957; U.S. Naval Radiological Defense Laboratory, San Francisco, California; Secret Restricted Data.

38. R.L. Stetson et al; "Distribution and Intensity of Fallout from the Underground Shot"; Project 2.5.2, Operation Teapot, WT-1154, March 1958; U.S. Naval Radiological Defense Laboratory, San Francisco, California; Unclassified.

39. V.A.J. Van Lint, L.E. Killion, J.A. Chiment and D.C. Campbell; "Fallout Studies during Operation Redwing"; Program 2 Summary, ITR-1354, October 1956; Field Command, Armed Forces Special Weapons Project, Albuquerque, New Mexico; Secret Restricted Data.

40. B.L. Tucker; "Fraction of Redwing Activity in Local Fallout"; 9 July 1957; The RAND Corporation, Santa Monica, California; Secret Restricted Data.

41. Hearings before the Special Subcommittee on Radiation of the Joint Committee on Atomic Energy, Congress of the United States, Eighty-sixth Congress, first session on Fallout from Nuclear Weapons Tests; 5, 6, 7, and 8 May 1959; Unclassified.

42. Adm. E. Parker; "Radioactive Fallout from Nuclear Explosions"; Statement before the Department of Defense Subcommittee of the Committee on Appropriations, House of Representatives, 23 March 1960.

43. W.F. Libby; "Current Research Findings on Radioactive Fallout"; Proc. Nat. Acad. Sci. 42, 945-964; December 1956; Unclassified.

44. A.G. Hoard, Merrill Eisenbud and J.H. Harley; " Annotated Bibliography on Fallout Resulting from Nuclear Explosions"; NYO-4753, September 1956; Health and Safety Laboratory, New York Operations Office, USAEC, New York, New York; Unclassified.

45. A.G. Hoard, Merrill Eisenbud and J.H. Harley; "Annotated Bibliography on Long Range Effects of Fallout from Nuclear Explosions"; NYO-4753, Supplement 1, November 1956; Health and Safety Laboratory, New York Operations Office, USAEC, New York, New York; Unclassified.

46. A.J. Breslin and M.E. Cassidy; "Radioactive Debris from Operation Castle, Islands of the Mid-Pacific"; NYO-4623, January 1955; Health and Safety Laboratory, New York Operations Office, USAEC, New York, New York; Secret Restricted Data.

47. C.T. Rainey and others; "Disbribution and Characteristics of Fallout at Distances Greater than Ten Miles from Ground Zero"; Project 27.1, Operation Upshot-Knothole, WT-811, February 1954; University of California, Los Angeles, California; Unclassified.

48. K.H. Larson; "Radio-Ecological Aspects of Nuclear Fallout"; Operation Plumbbob, Program 37; Department of Agriculture, Washington, D.C.; Unclassified.

49. J. Lockhart, R.A. Baus and J.H. Blifford; "Atmospheric Radioactivity along the 80th Meridian, 1956"; NRL Report 4965, July 23, 1957; Naval Research Laboratory, Washington, D.C.; Unclassified.

50. A.K. Stebbins III; "Progress Report on the High Altitude Sampling Program"; DASA-529, 1 July 1959; Defense Atomic Support Agency, Washington 25, D.C.; Unclassified.

51. A.K. Stebbins III; "HASP Special Report"; DASA-532b, 1 June 1960; Defense Atomic Support Agency, Washington 25, D.C.; Unclassified.

52. Summary Report, High Altitude Sampling Program (Technical Report Nr 1) March 1957-February 1958; Defense Atomic Support Agency, Washington 25, D.C.; Secret.

53. Summary Report, High Altitude Sampling Program (Technical Report Nr 2) March 1958-March 1959; Defense Atomic Support Agency, Washington 25, D.C.; Secret.

54. Summary Report, High Altitude Sampling Program (Technical Report Nr 3) (in press); Defense Atomic Support Agency, Washington 25, D.C.;

55. H.W. Feely; "Strontium-90 Content of the Stratosphere," "A Low Concentration of Strontium-90 In the Stratosphere Indicates a Short Stratospheric Residence Time," Science 131, 645 (1960).

56. J. Spar; "Strontium-90 in the Stratosphere," presented at the Strontium-90 Symposium, Bad Kreuznach, Germany, 28 October 1959.

57. W.F. Libby; "Radioactive Strontium in Fallout"; Proc. Nat. Acad. Sci. 42, No.6, pp. 365-390, June 1956; Unclassified.

58. R.D. Maxwell et al; "Evaluation of Radioactive Fallout"; AFSWP 978, 15 September 1955; Armed Forces Special Weapons Project, Washington 25, D.C., Secret Restricted Data.

59. L.F. Hubert, L. Machta and R.J. List; "A Meteorological Analysis of the Transport of Debris from Iperation Ivy"; U.S. Weather Bureau, NYO-4555, October 1953; Health and Safety Laboratory, New York Operations Office, USAEC, New York, New York; Secret Restricted Data.

60. L. Machta and R.J. List; "Analysis of Stratospheric Sr^{90} Measurements"; March 1959; U.S. Weather Bureau, Washington, D.C.; Unclassified.

61. N.E. Ballou and L.R. Bunney; "Nature and Distribution of Residual Contamination, II"; Project 2.6c-2, Operation Jangle, WT-397, June 1952; U.S. Naval Radiological Defense Laboratory, San Francisco, California; Secret Restricted Data.

62. Private communication, P.C. Stevenson; Chemistry Division, University of California Radiation Laboratory, Livermore, California.

63. Private communication, R.W. Spence and G.A. Cowan; Group J-11, Los Alamos Scientific Laboratory, Los Alamos, New Mexico.

64. Private communication, K. Street; Chemistry Division, University of California Radiation Laboratory, Livermore, California.

65. Philip Krey; "AFSWP Fallout Symposium"; AFSWP-895, January 1955; Armed Forces Special Weapons Project. Washington 25 D.C.; Secret Restricted Data.

66. L.R. Bunney and N.E. Ballou; "Bomb Fraction Measurement Techniques"; USNRDL-TR-176, 11 September 1957; U.S. Naval Radiological Defense Laboratory, San Francisco, California; Secret Restricted Data.

67. P.C. Stevenson, H.G. Hicks, W.E. Nervik and H.B. Levy; "Correlation of Fractionation Phenomena in Tewa Event, Operation Redwing"; UCRL 5027, 21 November 1957; University of California Radiation Laboratory, Livermore, California; Secret Restricted Data.

68. L.R. Bunney and E.C. Freiling; "Recent Developments in the Study of Fractionation, II"; USNRDL Technical Memorandum No. 81, 19 February 1958; U.S. Naval Radiological Defense Laboratory, San Francisco, California; Confidential Restricted Data.

69. A.W. Goodrich; "A Rocket System for Sampling Particulate Matter Contained in Nuclear Clouds"; Cooper Development Corporation, Monrovia, California, 31 January 1959; Unclassified.

70. Private communication, Dr. T. Triffet, November 1957, U.S. Naval Radiological Defense Laboratory, San Francisco, California.

71. Private communication, E.A. Schuert, November 1957, U.S. Naval Radiological Defense Laboratory, San Francisco, California.

72. C.W. Bastian, R. Robbiani and J. Hargrave; "X-Band Radar Determination of Nuclear Cloud Parameters"; U.S. Army Signal Research and Development Laboratory, Fort Monmouth, New Jersey, 13 October 1958; Secret Restricted Data.

73. L. Wish; "Quantitative Radiochemical Analysis by Ion Exchange; Anion Exchange Behaviour in Mixed Acid Solutions and Development of a Sequential Separation Scheme"; Anal. Chem. 31, 326, 1959.

74. E. Scadden; "Improved Molybdenum Separation Procedure"; Nucleonics 15, No. 4, 102, 1957.

75. L.R. Bunney, E.C. Freiling, L.D. McIsaac and E.H. Scadden; "Radiochemical Procedure for Individual Rare Earths"; Nucleonics 15, No. 2, 81-83, 1957.

76. L.E. Glendenin; "Determination of Strontium and Barium Activities in Fission"; Paper 236 in NNES, Div. IV, 9, 1460, edited by C.D. Coryell and N. Sugarman, McGraw-Hill Book Company, New York, New York., 1951.

77. E.J. Hoagland; "Note on the Determination of Strontium as the Carbonate"; Paper 237, Ibid.

78. J.B. Niday; "Radiochemical Procedure for Cesium"; UCRL-4377, p. 13, 10 August 1954; University of California Radiation Laboratory, Livermore, California.

79. J. Kleinberg (editor); "Collected Radiochemical Procedures"; LA-1721, Second edition, 18 August 1958; Los Alamos Scientific Laboratory, Los Alamos, New Mexico.